Final Report

Effects of Blast Furnace Slag Characteristics on Durability of Cementitious Systems for Florida Concrete Structures

FDOT Contract Number BDV25-977-28

Date: July 30, 2019

Submitted To: Dr. Harvey DeFord, Ph.D.

Structural Materials Research Specialist

Florida Department of Transportation

State Materials Office

5007 NE 39th Avenue

Gainesville, FL 32609

Phone: 352-955-6671

Email: Harvey.deford@dot.state.fl.us

Submitted By: Dr. Abla Zayed

Department of Civil and Environmental Engineering

University of South Florida

4202 E Fowler Avenue

Tampa, FL 33620

Phone: 813-974-5823

zayed@usf.edu

Disclaimer

The opinions, findings, and conclusions expressed in this publication are those of the authors and not necessarily those of the State of Florida Department of Transportation (FDOT) or the U.S. Department of Transportation (USDOT) or the Federal Highway Administration (FHWA).

Approximate Conversions to SI Units (from FHWA)				
Symbol	**When You Know**	**Multiply By**	**To Find**	**Symbol**
Length				
in	inches	25.4	millimeters	mm
ft	feet	0.305	meters	m
yd	yards	0.914	meters	m
mi	miles	1.61	kilometers	km
Area				
in^2	square inches	645.2	square millimeters	mm^2
ft^2	square feet	0.093	square meters	m^2
yd^2	square yard	0.836	square meters	m^2
mi^2	square miles	2.59	square kilometers	km^2
Volume				
fl oz	fluid ounces	29.57	milliliters	mL
gal	gallons	3.785	liters	L
ft^3	cubic feet	0.028	cubic meters	m^3
yd^3	cubic yards	0.765	cubic meters	m^3
NOTE: volumes greater than 1000 L shall be shown in m^3				
Mass				
oz	ounces	28.35	grams	g
lb	pounds	0.454	kilograms	kg
Temperature (exact degrees)				
°F	Fahrenheit	5 (F-32)/9 or (F-32)/1.8	Celsius	°C
Illumination				
fc	foot-candles	10.76	lux	lx
fl	foot-Lamberts	3.426	candela/m^2	cd/m^2
Force and Pressure or Stress				
lbf	pound-force	4.45	newtons	N
lbf/in^2	pound-force per square inch	6.89	kilopascals	kPa

Technical Report Documentation Page

1. Report No.	2. Government Accession No.	3. Recipient's Catalog No.

4. Title and Subtitle	5. Report Date
Effects of Blast Furnace Slag Characteristics on Durability of Cementitious Systems for Florida Concrete Structures	August 2019
	6. Performing Organization Code

7. Author(s)	8. Performing Organization Report No.
Abla Zayed, Kyle Riding, Yuri Stetsko, Natallia Shanahan, Ananya Markandeya, Farzaneh Nosouhian, Dhanushika Mapa, Mustafa Fincan	

9. Performing Organization Name and Address	10. Work Unit No. (TRAIS)
Department of Civil and Environmental Engineering University of South Florida 4202 E Fowler Avenue; ENB 118 Tampa, FL 33620-5350	11. Contract or Grant No. BDV25-977-28

12. Sponsoring Agency Name and Address	13. Type of Report and Period Covered
US Department of Transportation-Florida Department of Transportation 605 Suwannee St, MS 30 Tallahassee, FL 32399	Final Report April 2016-August 2019
	14. Sponsoring Agency Code

15. Supplementary Notes

16. Abstract

Four ordinary portland cements (OPC) and 8 ground-granulated blast furnace slags (GGBFS) were tested to assess the cracking potential and sulfate durability of slag-blended cementitious systems. The as-received materials were tested for their physical, chemical and mineralogical composition using Blaine fineness, particle size distribution, specific gravity, X-ray fluorescence, and X-ray diffraction coupled with Rietveld refinement. The variables in the selected cements included, tricalcium aluminate, tricalcium silicate, sulfates, alkali content, and fineness. The variables in the slag matrix included, alumina content, magnesia-to-alumina ratio, and Blaine fineness/mean particle size. Sulfate durability was assessed using ASTM C1012 at a constant w/cm ratio. Pastes and mortars were subjected to a battery of tests including phase assemblage studies using quantitative X-ray diffraction and thermodynamic modeling. Mercury intrusion porosimetry was conducted on selected samples to assess the pore size distribution prior to exposure to a sulfate environment; the paste was also examined by quantitative X-ray diffraction to assess the phase assemblage prior to sulfate exposure. Cracking indices were assessed using a rigid cracking frame. The cracking frame was operated under a temperature profile collected using semi-adiabatic calorimetry. The slag variables studied in those experiments included fineness and alumina and magnesia content, while for cements, only tricalcium aluminate, tricalcium silicate and sulfate content were varied. The findings of this study indicate the significance of GGBFS alumina content, alumina-to magnesia ratio, and fineness on slag-blended concrete cracking potential. Higher alumina content, higher slag fineness and higher alumina-to-magnesia ratio resulted in higher cracking potential indices. Additionally, increasing slag alumina content, alumina-to-magnesia ratio and fineness had negative effects on sulfate durability of the slag-blended cementitious systems.

17. Key Word	18. Distribution Statement

19. Security Classif. (of this report)	20. Security Classif. (of this page)	21. No. of Pages	22. Price
None	None	164	

Form DOT F 1700.7 (8-72) Reproduction of completed page authorized

Acknowledgement

This work has been sponsored by the Florida Department of Transportation (FDOT) and the Federal Highway Administration (FHWA). The Principal Investigator appreciates the valuable discussions with Dr. Harvey DeFord, Project Manager, and Mr. Michael Bergin, PE. The following students are acknowledged for participating in collecting data and experimental work: Andrew Williams, William Johnson and Jair Burgos.

Executive Summary

1.1 Background

Mineral admixtures (supplementary cementitious materials, SCMs) are used extensively in Florida structural concrete elements to enhance durability and service life. However, recent field data indicate higher maximum temperatures occurring in structural elements constructed from portland cement concrete blended with ground granulated blast furnace slag (GGBFS). Higher temperatures were occurring during the first 18-24 hours instead of typical 3-5 days in massive slag-concrete structural elements. Additionally, the current specifications are insufficient to prevent the use of portland cement-slag concrete mixes with inadequate resistance to sulfate expansion from being used in structural concrete exposed to extremely aggressive environments. Premature concrete degradation due to sulfate attack will shorten the service life and increase maintenance costs. This study emphasizes the materials characteristics of slag that affect the performance and durability of slag-blended concrete mixtures to minimize the risk of concrete degradation and extend the service life of structural concrete elements in the state of Florida.

1.2 Research Objectives

The objectives of this investigation are:

1. To investigate the effects of slag chemical and physical characteristics on sulfate durability of cementitious systems.
2. Establish limits on the identified characteristics to ensure durability of cementitious systems exposed to aggressive conditions during service.

Satisfying the objectives of this study will provide the Florida Department of Transportation (FDOT) with the scientific knowledge needed to change specifications pertaining to slag-containing structural concrete mixtures to ensure a sustainable and durable infrastructure in the state of Florida.

In addressing the objectives of this study, several slag sources were identified that had different chemical/physical characteristics. The as-received materials were characterized using X-ray fluorescence, quantitative X-ray diffraction coupled with Rietveld refinement, laser particle size distribution, Blaine fineness, and specific gravity. For sulfate durability studies, several

ordinary portland cements (OPC) were used at slag replacement levels of: 0, 30%, 50% and 70%. Strength evolution and expansion measurements were conducted for a period of 540 days or 18 months. In assessing the cracking indices of slag-blended concrete mixtures, two cements of variable tricalcium aluminate content and 8 slags of variable physical and chemical characteristics were prepared at a replacement level of 60%. Cracking indices were established using a rigid cracking frame and an imposed temperature profile collected under semi-adiabatic conditions.

1.3 Main Findings

The findings indicate that sulfate durability of slag-blended mixtures depends on the alumina content of the slag and the Blaine fineness/particle size distribution. Additionally, in a limited number of experiments, it was determined that the effectiveness of using calcium sulfate additions to improve the long-term durability of slags with high alumina contents is affected by the cement chemistry, an effect that needs further research. The findings also indicate that the cracking potential of slag-blended concrete is affected by the cement composition, slag alumina content, slag alumina-to-magnesia ratio and Blaine fineness/mean particle size of the slag.

1.4 Recommendations

Based on the findings of this study, the following recommendations can be made:

1. The Florida Department of Transportation should implement modifications to slag specifications to include Blaine fineness (BF) grade limits.
2. Slag Mill Certificate should identify if the slag is produced by blending granules and/or blending of slags produced from different blast furnaces. If GGBFS granules are blended, the source of the blends should not be changed without additional reapproval.
3. For applications where temperature rise of a structural element is of concern, cementitious content, cement fineness, slag alumina content and fineness must be considered. Adiabatic temperature rise should be determined experimentally using the same materials (including chemical admixtures) and proportions as used in the mixture design of the structural element. The measured adiabatic temperature must be used in the analysis performed to develop the thermal control plan for the

structural element. Testing for adiabatic temperature rise should be conducted in an approved laboratory facility.

4. The cementitious materials characteristics such as Blaine fineness, complete chemical oxide composition, mineralogy, limestone additions to slag, calcium sulfate additions to slag, and processing additions used in cement production must be attached to the testing results and should match what is proposed to be used in an approved mixture design. Variation of a cement source or a slag source should be accompanied by retesting and reapproval.
5. It is recommended that when a concrete mixture design is submitted to the State Materials Office for approval, where temperature rise or sulfate durability is of concern, the submitter should identify alternative cementitious materials sources in the event there is a shortage of supply in the cementitious materials submitted for mixture approval. In this event, the submitter must provide the same testing data for the alternative material as that used on the original mixture design.
6. It is recommended that the minimum amount of slag that can render a structural element durable should be used due to the higher shrinkage and higher carbonation in concrete elements prepared with high slag replacement levels (above 50%). The effect is more pronounced in thin reinforced sections.
7. For external sulfate durability, testing was conducted for a limited period of 18 months using ASTM C1012 while maintaining a constant w/cm ratio of 0.485 for control and slag-blended mortars. The following recommendations are provided for slag-blended cementitious systems with Type II(MH) OPC (ASTM C150-16) according to ACI 201.2R-16 class of exposure criteria:
    a. **Type II (MH)-Ground Granulated Blast Furnace Slag in Class S3 Exposure** (SO_4^{2-} > 10,000 ppm in water or water-soluble SO_4^{2-} > 20,000 ppm in soil):
        i. For slag cements with alumina contents ≤ 8%, the following are recommended:
            1) Alumina-to-magnesia ratio (A/M) ≤ 0.75,
            2) Blaine fineness of ≤ 640 m^2/kg, and
            3) Replacement of portland cement with 30% - 70% slag.

ii. For slag cements with alumina contents of greater than 8% and less than or equal to 11%, the following are recommended:
    1) A/M ≤ 0.95,
    2) Blaine fineness of ≤ 590 m^2/kg, and
    3) Replacement of portland cement with 70% slag.
iii. Slag cements with alumina contents greater than 11% must be tested according to ASTM C1012 using a constant w/cm ratio of 0.485. The expansion for the specific portland cement-slag cement combination must be less than 0.1% at 18 months to be used in a structural element subjected to S3 exposure conditions. If the expansion criterion is met, the approval for use is only for the specific combination of portland cement and slag cement at the specific replacement percentage used in the ASTM C1012 testing.

b. **Type II(MH) - Ground Granulated Blast Furnace Slag in Class S2 Exposure** (SO_4^{2-} content 1,500 - 10,000 ppm in water or water-soluble SO_4^{2-} content 2,000 - 20,000 ppm in soil):
    i. For slag cements with alumina contents ≤ 8%, the following are recommended:
        1) A/M ≤ 0.75,
        2) Blaine fineness of ≤ 640 m^2/kg, and
        3) Replacement of portland cement with 30% - 70% slag.
    ii. For slag cements with alumina contents of greater than 8% and less than or equal to 11%, the following are recommended:
        1) A/M ≤ 0.95,
        2) Blaine fineness of ≤ 590 m^2/kg, and
        3) Replacement of portland cement with 30% - 70% slag.
    iii. Slag cements with alumina contents greater than 11% must be tested according to ASTM C1012 using a constant w/cm ratio of 0.485. The expansion for the specific portland cement-slag cement combination must be less than 0.1% at 12 months to be used in a structural element subjected to S2 exposure conditions. If the

expansion criterion is met, the approval for use is only for the specific combination of portland cement and slag cement at the specific replacement percentage used in the ASTM C1012 testing.

8. For external sulfate durability, the following recommendations are provided for slag-blended cementitious systems with Type I (ASTM C150-16):
    a. **Type I - Ground Granulated Blast Furnace Slag in Class S3 Exposure**:
        i. For slag cements with alumina contents ≤ 8%, the following are recommended:
            1) A/M ≤ 0.75,
            2) Blaine fineness of ≤ 640 m^2/kg, and
            3) Replacement of portland cement with 50% - 70% slag.
        ii. For slags with alumina contents of 8% to 11%:
            1) A/M ≤ 0.95,
            2) Blaine fineness of ≤ 590 m^2/kg, and
            3) Replacement of portland cement with 70% slag.
        iii. Slag cements with alumina contents greater than 11% must be tested according to ASTM C1012 using a constant w/cm ratio of 0.485. The expansion for the specific portland cement-slag cement combination must be less than 0.1% at 18 months to be used in a structural element subjected to S3 exposure conditions. If the expansion criterion is met, the approval for use is only for the specific combination of portland cement and slag cement at the specific replacement percentage used in the ASTM C1012 testing.
    b. **Type I - Ground Granulated Blast Furnace Slag in Class S2 Exposure**:
        i. For slag cements with alumina contents of ≤ 8%, the following are recommended:
            1) A/M ≤ 0.75,
            2) Blaine fineness of ≤ 640 m^2/kg, and
            3) Replacement of portland cement with 30% to 70% slag.
        ii. For slag cements with alumina contents from 8% to 11% :

1) A/M ≤ 0.95,
2) Blaine fineness of ≤ 590 m^2/kg, and
3) Replacement of portland cement with 50% to 70% slag.

iii. Slag cements with alumina contents greater than 11% must be tested according to ASTM C1012 using a constant w/cm ratio of 0.485. The expansion for the specific portland cement-slag cement combination must be less than 0.1% at 12 months to be used in a structural element subjected to S2 exposure conditions. If the expansion criterion is met, the approval for use is only for the specific combination of portland cement and slag cement at the specific replacement percentage used in the ASTM C1012 testing.

It is recognized that the recommendations listed under item 7 and 8 can be modified if the GGBFS Blaine fineness is decreased or if calcium sulfate/limestone additions are blended with GGBFS. Since it is also recognized that performance of slag-blended cementitious systems is influenced by the cement source and not just the slag, approval should be only issued for specific cement-slag combinations. The GGBFS source should provide:

1) A detailed elemental oxide composition of the slag cement,
2) The Blaine fineness,
3) The amount and chemical composition of each calcium sulfate addition,
4) The amount and chemical composition (must show percent of $CaCO_3$) of limestone, if added,
5) Identify any blending of granules from different blast furnaces. If blended, the slag supplier should identify the granule source of each slag in the blend and immediately notify the State Materials Office of any changes to the blend,
6) Any changes to the types or quantities of additions to the slag cement, or to the granule proportions if blended, will require additional testing and reapproval.

It is also recognized that Blaine fineness of slag can affect the slag designated grade. The findings of the current study indicate that slags of similar chemical composition but ground to higher fineness have a negative effect on temperature rise, cracking indices and sulfate durability.

The construction industry and regulating agencies should consider emphasizing durability and strength when designing structural concrete elements rather than strength alone.

1.5 Recommendations for Future Study

Based on the findings of this study, the following is recommended;

1. Initiate a study on the effect of slag fineness and alumina content on the measured adiabatic temperature rise in slag-blended concrete.
2. Initiate a study to assess sulfate optimization of higher-alumina slags in blended cementitious systems and their effect on the slag-blended systems durability. This will help minimize any potential shortage in the availability of quality slag cement needed for durable structural concrete in the state of Florida.

TABLE OF CONTENTS

LIST OF FIGURES

LIST OF TABLES

Chapter 1 Literature Review

1.1 Introduction

Supplementary cementitious materials (SCMs) are used extensively in Florida structural concrete elements to enhance durability and service life. Portland cement concretes containing ground granulated blast furnace slag (GGBFS) are generally expected to have good resistance to sulfate attack and control of temperature rise. Recent field data from Central and South Florida [1] indicate temperatures at the center of structural elements that reached 80° to 82°C (176° to 180°F) during the first few days of hydration. The temperature rise was unusual in that its magnitude was higher and the timing of its occurrence was earlier than what was typically experienced by field engineers. In a recent study [2], a mixture containing GGBFS, similar in proportions to mixtures typically used in the field, showed worse performance compared to a plain control mixture when exposed to a sulfate medium.

The data indicate that GGBFS and all mixtures constituents used in the field or the lab study were in compliance with current standard specifications. The pressing issue now is if the current specifications governing the use or qualification of GGBFS in structural elements are adequate to sustain and maintain quality field performance of mixtures incorporating GGBFS. The current specifications for GGBFS have limited chemical and/or physical requirements that the Florida Department of Transportation can use to ensure adequate field performance. The current study was initiated in order to address the effects of chemical and physical characteristics of GGBFS on durability of cementitious systems. The focus of the study is to address the role of GGBFS characteristics on temperature rise, cracking potential, and external sulfate attack in cementitious systems.

Ground granulated blast furnace slag (GGBS), or slag cement, is a commonly used supplementary cementitious material (SCM). It is generally considered to improve workability and reduce concrete temperature rise during initial hydration [3]. The temperature rise of slag concrete and the resulting thermal cracking risk are a function of GGBFS reactivity. Sulfate durability is also affected by the rate of slag reaction as well as the hydration products formed. Therefore, it is important to understand the effects of GGBFS chemical composition and physical characteristics on its reactivity.

GGBFS is a by-product of iron ore refinement. Although it is predominantly composed of calcium aluminosilicate glass, its exact oxide composition varies depending on the oxide composition of the ore, fluxing agents, and coke used to make the iron [4], [5]. Commonly, limestone is used as a flux, but it can also be mixed with forsterite and dolomite [6]. The typical range of chemical compositions for different slags [7] is summarized in Table 1-1.

Table 1-1: Typical Global Slag Composition.

Analyte	**Content (weight %)**
CaO	30-50
SiO_2	28-38
Al_2O_3	8-24
MgO	1-18
Fe_2O_3	1-3
MnO	1-3
S	1-2.5
TiO_2	<4
Na_2O+K_2O	<2

In order for slag to be suitable for use in concrete, it needs to contain a large amount of amorphous material, between 90 and 100%, which is achieved by rapid cooling from 1400-1500˚C [6], [7]. Slow cooling results in a formation of large amounts of inert crystalline phases, which is undesirable because they do not contribute to the development of mechanical properties, and the reactivity of slag generally decreases with increasing the crystalline content [8]. However, Taylor [9] suggested that, in small amounts, their presence may be beneficial to "improve reactivity, as they provide nucleation sites." Snellings et al. [6] stated that in addition to providing nucleation sites, crystalline phases improve slag reactivity due to mechanical stress "introduced by the phase separation." After cooling, slags are ground to a fineness of about 350 m^2/kg, with values above 500 m^2/kg having been reported as well [3], [10]. As with ordinary portland cement (OPC),

increasing fineness increases slag reactivity. Recent work by the Japanese has introduced slags of lower Blaine fineness of 275 m^2/kg for mass concrete [11].

Slag is a latent hydraulic material, which means that it does not require an activator to react with water and develop cementing properties [3], [4], [10]. However, this reaction is very slow. In a mixture with ordinary portland cement (OPC), hydration of GGBFS is activated by the high pH of the pore solution resulting from cement hydration, and the presence of alkalis and sulfates [4], [10], [12]. Hydration of slag releases alkalis into the pore solution, resulting in continued hydration at later ages [3].

1.2 Slag Reactivity

Based on the review of the current literature, the reactivity of slag is affected by the following factors: the characteristics of the slag (chemical composition, fineness, amorphous content), characteristics of the activator (pH, alkali and sulfate content in the case of cement), and hydration temperature. ASTM C989 [13] specifies an activity index, which is based on comparing compressive strength of a 50/50 OPC-GGBFS blend to that of unblended reference cement, in order to determine slag reactivity. Therefore, compressive strength will also be included in this discussion as a measure of slag reactivity in addition to other methods, such as monitoring heat evolution using isothermal calorimetry.

1.2.1 Slag Characteristics

As mentioned previously, slag chemical composition particularly SiO_2, CaO, Al_2O_3, and MgO contents have been identified as having an effect on slag reactivity [6]. Ramezanianpour [14] stated that "the cause of the hydraulic activity and its relation to the physical state and chemical composition of a slag has not been determined yet." Several hydraulic moduli have been proposed based on the mass ratios of these oxides in order to assess slag reactivity. A review of these moduli can be found in [14]. However, the correlation between these moduli and properties of hydrated slags are generally poor [6], [14]–[16]. While the oxide ratios have not been successful in predicting slag performance, it is still important to understand their effect on slag reactivity.

As can be seen in Table 1-1, the majority of slag is composed of CaO and SiO_2. It is generally agreed that the CaO content has a positive effect on reactivity [15]. The presence of

alumina in the glass phase has been reported to improve GGBFS reactivity [6]. A number of studies have been conducted on OPC/GGBFS blends; however, in these cases it is often difficult to separate the reaction of slag from that of OPC. Whittaker [17] observed, based on isothermal calorimetry measurements, that the addition of slag accelerates the rate of alite hydration, which could be seen as an increase in the magnitude of the main hydration peak. This was attributed to the filler effect as the same increase was produced by slag with a different chemical composition and very similar particle size distribution. An increase in the aluminate peak with slag addition was observed as well, and the magnitude of the peak increased with increasing Al_2O_3 content of slag. This increase in the aluminate peak appears to suggest that some alumina present in the slag may be reacting as well. Wu et al. [18] noted an increase in the aluminate peak with increasing cement replacement level at temperatures of 27°C and above (slag Al_2O_3 of 9.56%). However, at 5°C, no differences were observed in the heat flow curves of pastes containing 40-65% slag. The authors concluded that slag reaction contributes to early-age heat flow at temperatures of 27°C and above. This view of early-age slag reactivity is also supported by Ballim and Graham [19], who concluded, based on adiabatic calorimetry measurements of concretes with 20 to 80% slag, that "the hydration of the GGBFS is contributing to the generation of heat in concrete, even at these relatively early ages" (up to the maturity of 20 hours). However, Kocaba [15] states that the increase in the aluminate peak in the presence of slag is solely due to the filler effect. In support of this opinion, the author references a study [20] where a similar increase in the aluminate peak was observed for 10% cement replacement with rutile as well as corundum.

Wang et al. [21] investigated reactivity of various slags in terms of heat evolution measured by isothermal calorimetry and compressive strength. Isothermal calorimetry measurements were performed on slags mixed with 2N caustic soda solution, while compressive strength measurements were performed on slags mixed with ground clinker and anhydrite, with slag comprising 75% of the mixture. The authors observed that heat evolution increased with increasing Al_2O_3 content in the slag. The Al_2O_3 content range reported for heat measurements was approximately between 6 and 15%. Additionally, an interaction between Al_2O_3 and CaO contents was also observed. Wang et al. [21] stated that in order to maximize the reactivity (heat release), CaO content in the slag should be maintained above 40%. Similar results were obtained for compressive strength (Al_2O_3 range of 6-19.5%), except a decline in compressive strength was observed after the age 2 days when Al_2O_3 was increased above 15% with a corresponding CaO

decrease from 39.1 to 32.2%. In a high-lime slag, a continuous increase in strength was observed at all ages with increase in Al_2O_3. This was attributed to a change in Al coordination, as observed by nuclear magnetic resonance (NMR), from tetrahedrally coordinated below 15% to forming a "tricluster." The tricluster arrangement results in a closer packing and increased charge neutrality of the glass fraction of slag; however, the authors speculated that increasing CaO compensates for the increased packing induced by tricluster formation through the increase of non-bridging oxygen atoms. Therefore, Wang et al. [21] concluded that slag reactivity, in terms of total heat evolution and compressive strength up to 28 days, can be improved by maintaining "Al_2O_3 over 10.5% and CaO over 40%."

However, Ben Haha et al. [22] did not observe a change in Al coordination for slag Al_2O_3 contents of 7-16.7%. This implies that increasing Al_2O_3 content does not affect packing and therefore reactivity of the glassy phase. The authors investigated the effect of Al_2O_3 content on hydration of 3 GGBFSs activated with NaOH and water glass. The selected slags had similar fineness (approximately 500 m^2/kg), CaO content (about 35-39%) and MgO content (6.4-7.2%). The authors stated that "for a given age, no significant difference in compressive strength" was observed with increasing Al_2O_3 content regardless of the activator used. However, increasing Al_2O_3 content in the presence of NaOH activator resulted in increased heat evolution during the first 2 days, at which time a cross-over in the cumulative heat evolution curves was observed, with the low-Al_2O_3 slag generating the most heat beyond 2 days. In the presence of water glass, cumulative heat was always higher for the low-Al_2O_3 slag. Ben Haha et al. [22] suggested that increasing the amount of aluminum ions in the pore solution may have decreased the dissolution of the amorphous silica in the slag, as has been observed in other systems at high pH [23], [24].

Ben Haha et al. [22] also investigated the effect of MgO content on hydration of alkali-activated GGBFS using 3 slags of similar fineness (approximately 500 m^2/kg), CaO content (about 36-38%) and Al_2O_3 content (11.3-12.0%). MgO content of the slags varied from 7.7 to 13.2%. Although Moranville-Regourd [25] states the Mg^+ can act as a network modifier thereby disrupting the close packing on the silicate network of the amorphous phase, Ben Haha et al. [22] did not observe any changes in the ^{29}Si NMR spectra with increasing MgO content. However, both compressive strength and the total heat evolution increased with increasing MgO content. Similar systematic studies are needed for OPC-GGBFS systems.

Binici et al. [26] investigated the effect of fineness on heat release and strength development of cement blended with slag. The authors prepared blends of clinker, gypsum, GGBFS, and ground basaltic pumice where the percentages of these materials were fixed at 66, 4, 20, and 20%, respectively. The authors report that each material was ground separately to obtain three Blaine fineness values of 250, 400 and 550 m^2/kg. The blends are reported to have the same fineness values, so it is assumed that blends were produced by combining materials of the same fineness. Binici et al. [26] observed an increase in the total heat as measured by isothermal calorimetry with an increase in fineness. A similar trend was observed in the unblended clinker+gypsum samples; heat release increased with increasing clinker fineness, which is a well-documented phenomenon [27], [28]. The slag selected for this study contained 13.7% Al_2O_3 and only 28.2% CaO, which, based on the preceding discussion of the study by Wang et al. [21], would point to a possible low reactivity of this slag. An increase in the compressive and flexural strengths with increasing fineness was observed as well. The effect of slag fineness remains unclear, since it appears that the finenesses of clinker, GGBFS, and pumice was varied simultaneously in this study.

In contrast to the study by Binici et al. [26], where grinding time was varied for each material in order to achieve the specified fineness, Kumar et al. [29] used fixed grinding times for cement-GGBFS blends to assess the effect of fineness on slag reactivity. GGBFS used in this study had a high Al_2O_3 content of 21.6% and a CaO content of 33.0%. Slag and cement were interground together as well as ground separately. Oner [30] pointed out that slag is more difficult to grind compared to clinker, so fixed grinding times for slag and clinker would produce a slag that is coarser than clinker. Unfortunately, fineness of the ground cement and slag was not measured by the authors [29] prior to recombining them into a 50/50 blend, but particle size of this blend was reported to be somewhat smaller than for the interground 50/50 cement-GGBFS blend. Particle sizes for both of these blends were significantly smaller than those of the commercial slag cement. Based on compressive strength measurements up to 28 days as well as SEM measurements, where smaller slag particles were observed for the separately ground blend, the authors concluded that increasing slag fineness increases its reactivity. However, it should be noted that for both the interground and separately ground blends, cement fineness was increased as well, and the filler effect of slag on cement hydration was not considered.

Oner [30] employed separate grinding procedures to evaluate the effect of slag fineness on reactivity assessed in terms of compressive strength. Only one slag was used in this study with CaO and Al_2O_3 contents of 37.35 and 10.56% respectively. GGBFS fineness was varied from 300 to 600 m^2/kg, while clinker+gypsum fineness remained constant at 300 m^2/kg. Oner [30] stated that "compressive strength values increase with increasing fineness of slag"; however, this increase only becomes notable at 28 days. At 2 days, compressive strengths appear to be the same regardless of fineness, and at 7 days the increase is only marginal. It is interesting to note that fineness had no effect on flexural strength between the ages of 2-28 days. Although this study isolated the effect of slag fineness by maintaining cement fineness constant, only one slag was examined, which raises the question of whether this conclusion can be applied to slags in general. It is clear from the above literature review that additional research is needed into the effect of fineness and slag chemical composition on reactivity, especially for the OPC-GGBFS systems.

1.2.2 Activator Characteristics

Although a number of activators can be used to accelerate GGBFS hydration, the focus of this literature review is on the OPC-GGBFS systems. Therefore, cement will be the only activator considered here.

1.2.3 Cement Composition

Slags are activated by calcium hydroxide (CH) released during cement hydration, and the alkalis and sulfates from the as-received cement [4], [31]. However, there have been no systematic studies on the effects of cement composition and reactivity and currently, there is no clear agreement in the literature regarding the effects of these parameters on hydration of OPC-GGBFS blends. Whittaker [16] compared the total heat evolution for OPC/GGBFS blends prepared with 2 different cements and concluded that "clinker composition had no apparent effect on the hydration kinetics of the slag." It should be noted that the cements studied by Whittaker [16] had similar C_3S (61.0 and 58.7 %) and C_3A (7.5 and 8.0%) contents, which are the phases producing notable calorimetric peaks on hydration. Alkali equivalent content of these cements was very similar at 0.69 and 0.61%, and so was their anhydrite content. One cement had a slightly higher amount of hemihydrate at 1.5% compared to 0.6% in the other. Their particle size distributions were also very similar. The main difference between cements was in their content of C_2S (11.9

and 21.6%) and C_4AF (8.3 and 2.9%) phases which are known for their low rates of reaction. On the other hand, Kocaba [15] showed that the effect of slag on OPC hydration depends on the mineralogical composition of the cement. She reported acceleration of the C_3S reaction, based on the isothermal calorimetry results, with addition of 40% slag for one cement (Cement A), and retardation of the C_3S reaction for two other cements (Cements B and C). No explanation was offered for this phenomenon. C_3S content for cement A was 68%, while for Cements B and C it was 49 and 65%, respectively. Cement A also had the lowest C_3A content compared to the other cements, the lowest equivalent alkali, and the lowest sulfate content. Additionally, Cement A had the highest fineness (d_{50} = 9 μm), and Cement C had the lowest fineness (d_{50} = 20 μm). The d_{50} for Cement B was 14 μm. It appears that for cements with high reactivity (high C_3S, high fineness) addition of slag may result in further acceleration of hydration reactions.

In 1995, De Schutter and Taerwe [32], who modeled hydration of OPC and of slag cements, proposed that hydration of OPC/slag blends is comprised of two separate reactions, OPC hydration and slag hydration. Observations by Whittaker [16] are consistent with this hypothesis; however, a greater range of cement and slag compositions would have to be tested to conclusively state that slag hydration is not affected by cement mineralogy.

It is clear that there is a general agreement in the literature that addition of slag accelerates cement hydration. However, there still appears to be a disagreement on the explanation for this phenomenon. While some researchers attribute the increased heat flow rate per gram of cement merely to the filler effect, others suggest that a reaction of slag is a contributing factor as well. Although this may seem to be a purely academic debate, identifying the exact mechanism of acceleration will have important engineering implications. Slag is frequently used in mass concrete, where temperature rise and thermal gradients are determined by the heat generation of the cementitious components of the concrete mixture. If acceleration is only due to the filler effect, temperature rise could potentially be controlled by adjusting slag fineness. However, if slag participates in the early hydration stages of the cementitious system then the chemical composition of slag will need to be considered.

1.3 Hydration Products

As for the effect of slag on hydration products, cement replacement with GGBFS results in a decrease in the C/S ratio of C-S-H and an increase in Al incorporation into C-S-H [12]. Whittaker [16] demonstrated that Al uptake by C-S-H is dependent on the Al_2O_3 content of slag, with the Al/Si ratio of C-S-H in hydrated samples increasing with increasing Al_2O_3 content of slag. Increased Al incorporation into C-S-H was observed by [22] as well. Ben Haha et al. [22] also reported that "Al incorporation in C–S–H decreases with increasing MgO content." The authors did not observe any Ca substitution by Mg. Jackson et al. [33] reported aluminum incorporation in the tobermorite structure resulted in a significant increase in bulk modulus.

In addition to C-S-H, hydration products predicted by thermodynamic modeling for OPC/slag blends include CH, hydrotalcite, ettringite, calcite, monocarboaluminate and, at cement replacement levels above 70%, stratlingite [12], [34]. Increasing MgO content of the slag results in an increased formation of hydrotalcite in alkali-actvated slags [22]. This increased formation of hydrotalcite was used to explain a decrease in the coarse capillary porosity during the first 28 days with increasing MgO content as measured by backscattered electron microscopy.

A possible change in ettringite morphology with slag addition has been suggested [35]. Experimental measurements revealed that hydration phase assemblage is affected not only by the cement replacement levels as predicted by [12], but also by chemical composition of the slag. Whittaker [16] reported that increasing Al_2O_3 content of slag reduces CH, while increasing formation of Aluminate-Ferrite-Monosubstituent (AFm) phases, in the form of mono- and hemicarboaluminate, as well as monosulfoaluminate.

1.4 Effect of Slag on Temperature Rise and Thermal Cracking

Cement hydration is an exothermic process, which releases 150 to 350 joules per gram of cement during the early stages of hydration [36] depending on the cement mineralogical composition, fineness, w/c ratio, and temperature. At complete hydration, 400 to 500 joules are released per gram of cement, which would result in a 60 to 80°C concrete temperature rise under adiabatic conditions [37]. Cement replacement with slag is a commonly used strategy to decrease concrete temperature rise [3], [10], [38]. However, since isothermal calorimetry measurements showed an increase in aluminate peak magnitude with increasing Al_2O_3 content of GGBFS [17],

[18], further research is needed to determine the effectiveness of cement replacement with high-alumina slags for temperature control in mass concrete.

Bamforth [39] demonstrated that the effectiveness of slag in reducing concrete temperature rise is dependent on the lift height of placed concrete; as the lift height increases, so does the maximum concrete temperature. While greater temperature reduction was achieved with higher volumes of cement replacement by slag at all lift heights, this reduction is minimized when lift height is increased above 2 m. Increase in lift height decreases heat dissipation, so conditions for thicker elements begin to approach adiabatic. Reactivity of slag has been shown to increase with increasing temperature [8], [18], [40], and slag has been reported to have a higher temperature sensitivity compared to OPC [41], [42], which explains the decrease in temperature rise reduction with increasing lift height. Unfortunately, no information was provided on concrete mixtures used to make these conclusions [39], so it is unclear if there were any differences in slag composition.

Bamforth [39] also compared field performance of 75% GGBFS concrete to that of OPC in terms of temperature rise in mass concrete. Cement-rich concrete mixtures were selected for this study with cementitious content of 400 kg/m^3; w/cm ratio was slightly lower for the GGBFS concrete at 0.41 compared to the OPC concrete at 0.45. The author observed that replacing 75% of cement with high-alumina slag (13.62% Al_2O_3) produced only marginal improvement of 15% in terms of reducing the temperature rise of mass concrete (lift height of 4.5 m). Additionally, thermal tensile strains recorded in the 75% GGBFS concrete exceeded those observed in OPC concrete and cracking of GGBFS concrete was detected as well in spite of lower maximum concrete temperature and lower thermal gradients experienced by GGBFS concrete. The cracking indicates tensile stresses exceeded concrete tensile strength. Tensile stress can be calculated using Equation 1-1:

$$\sigma_t = K_r \frac{E}{1+\varphi} \alpha \Delta T \qquad \text{Equation 1-1}$$

where σ_t is the tensile stress, K_r is the degree of restraint, E is the elastic modulus, α is the coefficient of thermal expansion, ΔT is the temperature change, and ϕ is the creep coefficient [10]. Bamforth [39] calculated the coefficient of thermal movement based on the collected field strain and temperature data, which was higher for GGBFS than for OPC concrete. An increase in α results in an increase in tensile stresses, as can be seen from Equation 1-1.

Additionally, further laboratory investigation revealed that addition of slag increased the elastic modulus (*E*) of concrete at a given compressive strength and significantly reduced creep (by approximately 70% at 75% cement replacement level). Improvement in later-age elastic modulus with slag incorporation has been reported by others [43], [44]; however, at early ages of 3-28 days Darquennes et al. [44] concluded that *E* was unaffected by the level of cement replacement with GGBFS. The lack of consensus on the effect of slag on the elastic modulus has been highlighted by Özbay et al. [45] in their review of the current literature. The disagreement between the results reported by Darquennes et al. [44] and Bamforth [39] can be explained by different curing conditions of the concrete specimens in these studies. Concrete cylinders tested by Darquennes et al. [44] were cured at 20°C, while concrete specimens examined by Bamforth [39] were subjected to the same temperature conditions as those recorded for field concrete.

An increase in *E* as reported by Bamforth [39] would lead to an increase in tensile stresses according to Equation 1-1. It also implies a reduction in tensile strength and a reduced ability of concrete to resist tensile stresses, which were shown to be higher in GGBFS concrete. Aly and Sanjayan [35] reported lower elastic moduli and lower tensile strengths for OPC-GGBFS concrete at the ages of 7-11 days compared to OPC concrete. On the contrary, Berndt [46] observed that cement replacement with GGBFS improved the 28-day splitting tensile strength of concrete at 50% cement replacement level. No significant difference was observed between tensile strength of the control sample and 70% GGBFS concrete at 28 days. Due to elevated temperatures experienced by concretes in the study by Bamforth [39], samples tested by Berndt [46] may be of more comparable maturity than those of Aly and Sanjayan [35]. Saito et al. [47] observed that the degree of reaction of slag increases with increasing curing temperature in the studied temperature range of 5 to 40°C, so the degree of hydration of concrete in [35] is expected to be significantly lower than in [39]. The contradictory results of [39] and [46] can again be attributed to the difference in the curing temperatures as all concretes examined by Berndt [46] were cured at 23°C. It appears that curing temperature has a significant effect on the elastic modulus and tensile strength development of slag concrete.

There is no agreement in the current literature regarding the effect of GGBFS on creep as well [45], although curing temperature appears to have a similar effect on creep as on elastic modulus and tensile strength. While creep is reduced under high temperature conditions [39], under drying conditions and ambient temperature, as may be experienced by concrete during the

steady-state stage of hydration, creep has been reported to increase with increasing slag content [48]. Although the mechanism responsible for the creep behavior of concrete is not well understood, it is generally believed to be a response of C-S-H to the applied stress that results in redistribution of water from C-S-H to the capillary pores [31]. It would therefore appear that an increase in curing temperature of OPC-GGBFS concrete, which can occur under mass concrete conditions, may have a significant effect on the developed microstructure.

Harada et al. [49] reported that when concrete temperature exceeds 40°C, ettringite transforms into monosulfoaluminate. This phase transformation has been shown to increase capillary porosity [50], and can therefore have significant implications on cracking potential and durability of concrete mixtures. Williams et al. [51] also reported an increased in the 3-100 nm pores, as measured by nitrogen adsorption, that was attributed to the ettringite-to-monosulfoaluminate transformation in the 10% metakaolin concrete. Ettringite stability is also affected by the pH of the pore solution; if the pH falls below 11.5, ettringite will decompose to gypsum [52], although it is unclear what effect this transformation has on porosity.

Tensile strength is predominantly affected by capillary porosity [3], [31], [53], [54], and an increase in capillary porosity due to phase transformation of ettringite at higher temperatures may, therefore, result in a decrease in tensile strength and an increase in cracking potential.

An increase in capillary porosity with GGBFS addition has been observed for concretes cured at ambient temperature as well, which has been attributed to its lower degree of hydration at early ages compared to plain OPC mixtures [3]. As a result, an increase in both drying and autogenous shrinkage with GGBFS addition has been reported in the literature [3], [48], [49], [55], although Hooton [41] states that “drying shrinkage should be similar regardless of the presence of slag.” Aly and Sanjayan [35] point out that shrinkage testing according to ASTM C157 may be inadequate to predict shrinkage cracking performance of structural concrete containing slag as “tensile creep, tensile elastic modulus and tensile strength of concretes with slag-blended cements also have significant influence on cracking potential and can vary between OPC and slag concretes.”

1.5 External Sulfate Attack

Sulfate attack is another durability issue that is of major concern in Florida. Sulfate attack can occur when concrete is exposed to sulfate concentrations above 0.1% and is manifested by expansion and/or loss of strength and cohesion [3]. Expansion is typically attributed to secondary ettringite formation from the reaction of monosulfoaluminate present in concrete with the sulfate ions from the environment and possibly gypsum formation from the reaction of CH with sulfates, although the expansive nature of secondary gypsum formation is still debated in the literature [56]–[62]. Loss of strength and cohesion is due to decalcification of C-S-H [31]; secondary gypsum formation has been suggested to play a role as well [61]. Typical preventative measures include reducing C_3A content of cement in order to reduce secondary ettringite formation and decreasing permeability of the concrete mixture [31], although reduction of C_3S content in order to reduce CH and secondary ettringite formation has been suggested as well [63], [64].

Gollop and Taylor compared deterioration processes during sulfate attack on OPC-slag blends to those occurring in plain OPC mixtures [65] and concluded that these processes were generally similar, except low quantities of gypsum were formed in the OPC-slag blends. This was explained by the lower CH content and lower Ca/Si ratio of C-S-H in mixtures containing slag.

Cement replacement by GGBFS is generally reported to improve concrete performance in sodium sulfate environments through reduction of the C_3A content of the cementitious materials, consumption of CH during slag hydration, and decrease in permeability [13], [45]. However, ASTM C989 [13] cautions that sulfate resistance of OPC-slag blends may be dependent on the Al_2O_3 content of the slag. While the standard comments on the effect of low-alumina (11% Al_2O_3) and high-alumina (18% Al_2O_3) slags on sulfate durability, there is no comment on the effect of the slags with Al_2O_3 content of 11-18%.

1.5.1 Role of Alumina

As stated in ASTM C989 [13], cement replacement by slags containing less than 11% Al_2O_3 appears to improve sulfate resistance regardless of cement characteristics or cements replacement level. Hooton [41] demonstrated that expansion in sodium sulfate solution decreased with increasing cement replacement by GGBFS for a slag with Al_2O_3 content of 8.4%.

A relationship between expansion and Al_2O_3 content of slag was observed by Hooton and Emery [66], who reported that expansion increased with increasing Al_2O_3 content from 8.4 to 11.4% at a constant cement replacement level of 50%. Slags used in this study had comparable Blaine fineness and similar contents of other oxides. Higgins [67] examined performance of two slags with Al_2O_3 contents of 11.8 and 12.5% exposed to 1.5 and 1.3% sodium sulfate solutions respectively. The author reported that although initially replacing cement with these slags at a 60% level dramatically improved performance, where virtually no expansion was recorded, an inflection point in the expansion curves was observed at 30 months for the 11.8% Al_2O_3 slag and at 12 months for the 12.5% Al_2O_3 slag, after which the rate of expansion increased dramatically and rapid expansion was recorded. However, this phenomenon was not observed when cement replacement level was increased to 70% for each slag.

Increase in deterioration with increasing Al_2O_3 content of GGBFS was observed by other researchers as well. Gollop and Taylor [68] compared sulfate resistance of concrete prepared with 3 different slags, X, Y and Z, at 69% cement replacement level. Al_2O_3 content of the slags was 11.2, 13.4, and 16.0%, respectively. The authors observed, visually and under a scanning electron microscope (SEM), an increase in deterioration with increasing Al_2O_3 content. For samples prepared with slags Y (13.4% Al_2O_3) and Z (16.0% Al_2O_3), the deterioration was more extensive than in OPC samples, while samples with slag X (11.2% Al_2O_3) performed better than OPC concrete, although not as well as the samples prepared with sulfate-resistant portland cement (68% C_3S, 2% C_3A based on oxide chemical composition provided in [69]). It appears that there may be a threshold, in the slag Al_2O_3 content for a given cement replacement level, above which slag addition does not provide any improvement in sulfate resistance. The least amount of damage was observed in concrete prepared with 92% of slag Y. This suggests that perhaps an overall cementitious Al_2O_3 content should be considered, especially since C_3A content of cement has been identified as one of the factors affecting sulfate durability of OPC-GGBFS blends [38].

Whittaker [16] evaluated sulfate resistance of 3 slags with Al_2O_3 contents of 11.6, 7.36, and 12.33% A visual assessment of deterioration was made and expansion in sodium sulfate solution was measured. Although minimal expansion was recorded for all OPC-GGBFS concretes at 40% cement replacement levels, the highest amount of cracking was observed in the samples prepared with 12.33% Al_2O_3 slag, and decalcification was detected in all slag samples using scanning electron microscopy (SEM). It appears that expansion measurements alone may not be

sufficient to evaluate deterioration of OPC-BFS blends. Yu et al. [70] make an important point that "slag blends may not show expansion within the period of the tests, even though loss of materials from the surface of the specimen may be quite significant."

There are several reasons why increasing the slag Al_2O_3 content may be problematic in terms of sulfate resistance. First, Whittaker [16] observed increased formation of monosulfoaluminate with increasing Al_2O_3 content. Formation of monosulfoaluminate prior to sulfate exposure was also reported by Zayed et al. [2] in the 52% GGBFS mortar prisms prepared with 14.25% Al_2O_3 slag. Increase in monosulfoaluminate content would lead to increased formation of secondary ettringite and consequently increased expansion. Second, increased heat release may lead to an increase in field concrete temperature above 40°C causing decomposition of ettringite to monosulfoaluminate [49] and its reformation at a later age.

Increase in Al_2O_3 content also results in an increased uptake of Al by C-S-H. It is not clear what effect, if any, this may have on sulfate resistance. It has been established that Al incorporated in to C-S-H (C-A-S-H) does not participate in secondary ettringite formation [68]. Jackson et al. [33] speculated that increased Al/Si observed in the tobermorite of the ancient Roman concrete may be beneficial for improving durability.

1.5.2 Effect of Calcium Sulfate Addition on Sulfate Resistance

There is no agreement in the literature regarding the effect of calcium sulfate addition on sulfate resistance of OPC-GGBFS blends. Gollop and Taylor [68] observed improved sulfate resistance with addition of gypsum to concrete containing 65% of slag Y (13.4% Al_2O_3). SEM examination of cubes stored in sodium sulfate solution revealed that addition of 5% gypsum reduced the depth of decalcification of C-S-H from the cube surfaces compared to the mixture containing 69% of slag Y without the addition of gypsum. Addition of gypsum also resulted in formation of ettringite in addition to monosulfoaluminate, which was observed in the 69% slag Y sample. The authors concluded that addition of gypsum to a blend of OPC with high-alumina slag improves sulfate resistance due to formation of ettringite during initial hydration.

Improvement of sulfate resistance with addition of 3% anhydrite to OPC-GGBFS concrete was reported by Whittaker [16]. However, addition of anhydrite resulted in an increase in total

heat evolution during the first 7 days and increased chemical shrinkage and lowered compressive strengths at all ages.

Yu et al. [70] reported that addition of 1.7% gypsum improved the performance of 70% GGBFS mortar bars prepared with 15.85% Al_2O_3 slag in terms of delaying the onset of expansion and failure of the mortar bars exposed to the sodium sulfate solution. Addition of gypsum shifted the onset of rapid expansion from approximately 180 days for the 70% GGBFS sample to 360 days for the 70% GGBFS+gypsum specimens. Contrary to Gollop and Taylor [68], Yu et al. [70] concluded that addition of gypsum does not have a significant effect on sulfate resistance of OPC-slag blends.

1.5.3 Effect of Slag on Permeability

Although a number of sources state that slag incorporation in concrete mixtures decreases permeability and porosity [13], [31], [45], contradictory reports can be found in the literature. Whittaker [16] reported higher porosity in the OPC-GGBFS blends at early ages (after 1 day) compared to plain OPC as measured by backscatter scanning electron microscopy (BSE SEM). Increase in total nitrogen-accessible porosity at an age of 7 days was reported with 52% cement replacement with slag [71]. This trend was maintained up to the age of 28 days, after which the differences in porosity between the OPC-GGBFS systems and the plain OPC samples began to decrease and eventually became comparable at later ages [16]. Canut [72] reported porosity refinement with slag incorporation after the age of 28 days as measured by mercury intrusion porosimetry.

Attari et al. [73] followed the porosity evolution of OPC-BFS blends at 0, 30, 50 and 70% cement replacement during the first 24 weeks using BSE SEM. No consistent trend was observed. This may be because the w/cm ratios were varied in the range of 0.5-0.56, although the authors did not specify which w/cm corresponded to what mixture. Berndt [46] observed that cement replacement with 50 and 70% GGBFS only had a slight effect on concrete permeability at the age of 84 days; coefficient of permeability increased from 1.0×10^{-10} cm/s for the control mix to 1.4×10^{-10} cm/s for the 70% GGBFS concrete.

The increase in the early-age porosity can be attributed to the slower reaction of slag compared to OPC, which would result in reduced filling of capillary pores with hydration products.

Although porosity at later ages may be improved by continued slag hydration, concrete structures in the field are exposed to sulfates shortly after casting. However, this does not appear to have a detrimental effect on field performance of GGBFS concrete at high replacement levels. Stroh et al. [74] compared the field performance of concrete samples containing 80% slag to those of plain OPC after exposure to sulfate-bearing soils for a period of 19 years. The slag used in this study had an Al_2O_3 content of 13.30%, but was relatively coarse, with a Blaine fineness of 268 m^2/kg. Cement used in this study contained 8.5% C_3A and had a Blaine fineness of 326 m^2/kg. The w/cm ratio for both mixtures was 0.53. The 80% slag sample exhibited lower degradation in the sulfate environment compared to OPC concrete. This was attributed to improvement in the pore structure with slag addition, as sulfate penetration depths were lower in the slag concrete.

1.5.4 Role of Fineness

The effect of slag fineness on sulfate resistance has not received much attention in the literature. Wee et al. [75] reported that, at 65% cement replacement level, there was no clear trend between GGBFS fineness and sulfate resistance. Locher [76] studied the effect of increasing slag fineness from 300 to 500 m^2/kg using 3 clinkers of tricalcium aluminate of 0%, 8% and 11% and 2 granulated blast furnace slags with alumina contents of 11.0% and 17.7%. The gypsum content was 5% and several replacement levels were studied. The findings indicate that increasing slag fineness had a negative effect on sulfate durability. A replacement level above 65% is indicated for slags of higher fineness (500 m^2/kg) to improve sulfate resistance.

1.6 Conclusion

The above review indicates the importance of considering the effect of GGBFS composition and fineness on the reactivity of slag. It also indicates that the hydration temperature might reveal different behavior for slag in terms of increasing its reactivity and therefore the potential of a mixture for excessive temperature rise, especially if a concrete mixture is used in massive structural elements where placement is not limited to low ambient temperature. In summary, there are a number of open questions in the literature regarding the effect of the physical and chemical characteristics of ground granulated blast furnace slag on the cracking potential and sulfate resistance of concrete mixtures. In both cases, Al_2O_3 content of slag appears to be of major importance. Slag fineness and C_3A content of cement appear to be of significance as well.

1.7 References

[1] "Internal Communication," Florida Department of Transportation State Materials Office, 2016.

[2] A. Zayed, N. Shanahan, V. Tran, A. Markandeya, A. Williams, and A. Elnihum, "Effects of Chemical and Mineral Admixtures on Performance of Florida Structural Concrete," University of South Florida, Tampa, FL, 2016.

[3] A. M. Neville, *Properties of Concrete*, 4th ed. Harlow, England: Pearson Education Limited, 2006.

[4] R. Siddique and M. I. Khan, *Supplementary Cementing Materials*. Springer Science {&} Business Media.

[5] P. C. Hewlett, Ed., *Lea's Chemistry of Cement and Concrete*, 4th ed. New York, NY: Arnold, 1998.

[6] R. Snellings, G. Mertens, and J. Elsen, "Supplementary cementitious materials," *Rev. Mineral. Geochemistry*, vol. 74, no. 1, pp. 211–278, Dec. 2012.

[7] M. Morantville-Regourd, "Cements made from blastfurnace slag," in *Lea's Chemistry of Cement and Concrete*, 4th ed., P. C. Hewlett, Ed. New York, NY: Arnold, 1998, pp. 633–674.

[8] J. . Escalante, L. . Gómez, K. . Johal, G. Mendoza, H. Mancha, and J. Méndez, "Reactivity of blast-furnace slag in Portland cement blends hydrated under different conditions," *Cem. Concr. Res.*, vol. 31, no. 10, pp. 1403–1409, Oct. 2001.

[9] H. F. W. Taylor, *Cement Chemistry*, 2nd ed. London, UK: Thomas Telford Publishing, 1997.

[10] P. K. Mehta and P. J. M. Monteiro, *Concrete: Microstructure, Properties and Materials*, 3rd ed. New York, NY: McGraw-Hill, 2006.

[11] Y. Maeda, "Slag Cement-related Products Which Utilized a Property of the Ground Granulated Blast Furnace Slag," Nippon Steel & Sumikin Blast Furnace Slag Cement Co., Ltd, 2015.

[12] B. Lothenbach, K. Scrivener, and R. D. Hooton, "Supplementary cementitious materials," *Cem. Concr. Res.*, vol. 41, no. 12, pp. 1244–1256, 2011.

[13] ASTM C989 / C989M-17, "Standard Specification for Slag Cement for Use in Concrete and Mortars," West Conshohocken, PA: ASTM International, 2017.

[14] A. A. Ramezanianpour, *Cement Replacement Materials*. Berlin, Germany: Springer Berlin Heidelberg, 2014.

[15] V. Kocaba, "Development and Evaluation of Methods to Follow Microstructural Development of Cementitious Systems Including Slags," École Polytechnique Fédérale de Lausanne, 2009.

[16] M. J. Whittaker, "The Impact of Slag Composition on the Microstructure of Composite Slag Cements Exposed to Sulfate Attack," The University of Leeds, 2014.

[17] M. Whittaker, M. Zajac, M. Ben Haha, F. Bullerjahn, and L. Black, "The role of the alumina content of slag, plus the presence of additional sulfate on the hydration and microstructure of Portland cement-slag blends," *Cem. Concr. Res.*, vol. 66, pp. 91–101, Dec. 2014.

[18] X. Wu, D. Roy, and C. Langton, "Early stage hydration of slag-cement," *Cem. Concr. Res.*, vol. 13, no. 2, pp. 277–286, 1983.

[19] Y. Ballim and P. C. Graham, "The effects of supplementary cementing materials in modifying the heat of hydration of concrete," *Mater. Struct.*, vol. 42, no. 6, pp. 803–811, Jul. 2009.

[20] G. Le Saoût and K. L. Scrivener, "Early hydration of Portland cement with corundum addition," in *Proceedings of the 16th Internationale Baustofftatung*, 2006, pp. 409–416.

[21] P. Z. Wang, R. Trettin, V. Rudert, and T. Spaniol, "Influence of Al2O3 content on hydraulic reactivity of granulated blast-furnace slag, and the interaction between Al2O3 and CaO," *Adv. Cem. Res.*, vol. 16, no. 1, pp. 1–7, 2004.

[22] M. Ben Haha, B. Lothenbach, G. Le Saout, and F. Winnefeld, "Influence of slag chemistry on the hydration of alkali-activated blast-furnace slag — Part I: Effect of MgO," *Cem. Concr. Res.*, vol. 41, no. 9, pp. 955–963, 2011.

[23] T. Chappex, "The role of aluminium from supplementary cementitious materials in controlling alkali-silica reaction," Ecole Polytechnique Federale De Lausanne, 2012.

[24] B. R. Bickmore, K. L. Nagy, A. K. Gray, and a. R. Brinkerhoff, "The effect of Al(OH)4− on the dissolution rate of quartz," *Geochim. Cosmochim. Acta*, vol. 70, no. 2, pp. 290–305, Jan. 2006.

[25] M. Moranville-Regourd, "Cements made from blastfurnace slag," in *Lea's Chemistry of Cement and Concrete*, 4th ed., P. C. Hewlett, Ed. Arnold, 1998, pp. 633–674.

[26] H. Binici, H. Temiz, and M. M. Kose, "The effect of fineness on the properties of the

blended cements incorporating ground granulated blast furnace slag and ground basaltic pumice," *Constr. Build. Mater.*, vol. 21, no. 5, pp. 1122–1128, 2007.

[27] A. Sedaghat, N. Shanahan, and A. Zayed, "Predicting One-Day, Three-Day, and Seven-Day Heat of Hydration of Portland Cement," *J. Mater. Civ. Eng.*, vol. 27, no. 9, p. 04014257, 2015.

[28] A. Zayed, A. Sedaghat, A. J. Bien-Aime, and N. Shanahan, "Effects of portland cement particle size on heat of hydration," University of South Florida, Tampa, FL, 2013.

[29] S. Kumar, a. Bandopadhyay, V. Rajinikanth, T. C. Alex, and R. Kumar, "Improved processing of blended slag cement through mechanical activation," *J. Mater. Sci.*, vol. 39, pp. 3449–3452, 2004.

[30] M. Öner, "Study of intergrinding and separate grinding of blast furnace slag cement," *Cem. Concr. Res.*, vol. 30, no. 3, pp. 473–480, 2000.

[31] S. Mindess, F. J. Young, and D. Darwin, *Concrete*. Upper Saddle River, NJ: Pearson Education, Inc., 2003.

[32] G. De Schutter and L. Taerwe, "General hydration model for portland cement and blast furnace slag cement," *Cem. Concr. Res.*, vol. 25, no. 3, pp. 593–604, 1995.

[33] M. Jackson *et al.*, "Material and Elastic Properties of Al-Tobermorite in Ancient Roman Seawater Concrete," *J. Am. Ceram. Soc.*, vol. 96, no. 8, pp. 2598–2606, 2013.

[34] I. G. Richardson and G. W. Groves, "Microstructure and microanalysis of hardened cement pastes involving ground granulated blast-furnace slag," *J. Mater. Sci.*, vol. 27, no. 22, pp. 6204–6212, 1992.

[35] T. Aly and J. G. Sanjayan, "Factors contributing to early age shrinkage cracking of slag concretes subjected to 7-days moist curing," *Mater. Struct. Constr.*, vol. 41, no. 4, pp. 633–642, 2008.

[36] F. De Larrard, P. Acker, and R. Le Roy, "Shrinkage Creep and Thermal Properties," in *High Performance Concrete: Properties and Applications*, S. Shah and S. Ahmad, Eds. New York, NY: McGraw Hill, 1994, pp. 65–114.

[37] H. Gotfredsen and G. Idorn, "Curing technology at the Faroe Bridge, Denmark," in *Properties of Concrete at Early Ages*, J. F. Young, Ed. Detroit, MI: American Concrete Institute, 1986, pp. 17–32.

[38] G. J. Osborne, "Durability of Portland blast-furnace slag cement concrete," *Cem. Concr.*

Compos., vol. 21, no. 1, pp. 11–21, 1999.

[39] P. B. Bamforth, “In situ measurement of the effect of partial Portland cement replacement using either fly ash or ground granulated blast-furnace slag on the performance of mass concrete,” *Proc. Instn Civ. Engrs*, vol. 69, pp. 777–800, 1980.

[40] M. T. Palou, E. Kuzielová, M. Žemlička, M. Boháč, and R. Novotný, “The effect of curing temperature on the hydration of binary Portland cement,” *J. Therm. Anal. Calorim.*, 2016.

[41] R. D. Hooton, “Canadian use of ground granulated blast-furnace slag as a supplementary cementing material for enhanced performance of concrete,” *Can. J. Civ. Eng.*, vol. 27, no. 4, pp. 754–760, 2000.

[42] C. C. Castellano, V. L. Bonavetti, H. A. Donza, and E. F. Irassar, “The effect of w/b and temperature on the hydration and strength of blastfurnace slag cements,” *Constr. Build. Mater.*, vol. 111, pp. 679–688, 2016.

[43] J. M. Khatib and J. J. Hibbert, “Selected engineering properties of concrete incorporating slag and metakaolin,” *Constr. Build. Mater.*, vol. 19, no. 6, pp. 460–472, 2005.

[44] A. Darquennes, S. Staquet, M.-P. Delplancke-Ogletree, and B. Espion, “Effect of autogenous deformation on the cracking risk of slag cement concretes,” *Cem. Concr. Compos.*, vol. 33, no. 3, pp. 368–379, Mar. 2011.

[45] E. Özbay, M. Erdemir, and H. I. Durmuş, “Utilization and efficiency of ground granulated blast furnace slag on concrete properties - A review,” *Constr. Build. Mater.*, vol. 105, pp. 423–434, 2016.

[46] M. L. Berndt, “Properties of sustainable concrete containing fly ash, slag and recycled concrete aggregate,” *Constr. Build. Mater.*, vol. 23, no. 7, pp. 2606–2613, 2009.

[47] T. Saito, T. Uchida, Y. S. Lee, and N. Otsuki, “The Influence of Curing Temperature on Hydrated Products of Blast Furnace Slag Cement and Its Porosity at the Early Stage of Hydration,” *J. Soc. Mater. Sci. Japan*, vol. 58, no. 8, pp. 715–720, 2009.

[48] M. Shariq, J. Prasad, and H. Abbas, “Creep and drying shrinkage of concrete containing GGBFS,” *Cem. Concr. Compos.*, vol. 68, no. 1, pp. 35–45, 2016.

[49] K. Harada and H. Matsushita, “Effect of Gypsum Content in Cement on the Autogenous Shrinkage of Low-Heat Portland Blast Furnace Slag Cement,” *Memoris Fac. Eng. Univ.*, vol. 63, no. March 2003, pp. 51–66, 2003.

[50] B. Lothenbach, T. Matschei, G. Möschner, and F. P. Glasser, “Thermodynamic modelling

of the effect of temperature on the hydration and porosity of Portland cement," *Cem. Concr. Res.*, vol. 38, no. 1, pp. 1–18, 2008.

[51] A. Williams, A. Markandeya, Y. Stetsko, K. Riding, and A. Zayed, "Cracking potential and temperature sensitivity of metakaolin concrete," *Constr. Build. Mater.*, vol. 120, no. 2016, pp. 172–180, 2016.

[52] A. Neville, "The confused world of sulfate attack on concrete," *Cem. Concr. Res.*, vol. 34, no. 8, pp. 1275–1296, 2004.

[53] P. Sereda, R. Feldman, and V. Ramachandran, "Influence of Admixtures on the Structure and Strength Development," in *7th International Congress on the Chemistry of Cement*, 1980, vol. I, no. 979.

[54] J. Young, R. Berger, and F. Lawrence, "Studies on the hydration of tricalcium silicate pastes III. Influence of admixtures on hydration and strength development," *Cem. Concr. Res.*, vol. 3, no. 6, pp. 689–700, 1973.

[55] S. N. Lim and T. H. Wee, "Autogenous Shrinkage of Ground-Granulated Blast- Furnace Slag Concrete," *ACI Mater. J.*, no. 97, pp. 587–593, 2001.

[56] C. Yu, W. Sun, and K. Scrivener, "Mechanism of expansion of mortars immersed in sodium sulfate solutions," *Cem. Concr. Res.*, vol. 43, pp. 105–111, 2013.

[57] M. Gonzalez and E. Irassar, "Ettringite Formation in Low C3A Portland Cement Exposed to Sodium Sulfate Solution," *Cem. Concr. Res.*, vol. 27, no. 7, pp. 1061–1072, 1997.

[58] B. Tian and M. D. Cohen, "Does gypsum formation during sulfate attack on concrete lead to expansion," *Cem. Concr. Res.*, vol. 30, no. 1, pp. 117–123, 2000.

[59] M. Santhanam, M. D. Cohen, and J. Olek, "Effects of gypsum formation on the performance of cement mortars during external sulfate attack," *Cem. Concr. Res.*, vol. 33, no. 3, pp. 325–332, Mar. 2003.

[60] N. Shanahan and A. Zayed, "Role of tricalcium silicate in sulfate resistance," *Adv. Cem. Res.*, vol. 27, no. 7, pp. 409–416, 2015.

[61] M. D. Cohen and B. Mather, "Sulfate Attack on Concrete - Research Needs," *ACI Mater. J.*, vol. 88, no. 1, pp. 62–69, 1991.

[62] R. S. Gollop and H. F. W. Taylor, "Microstructural and microanalytical studies of sulfate attack. I. Ordinary portland cement paste," *Cem. Concr. Res.*, vol. 22, no. 6, pp. 1027–1038, 1992.

[63] N. G. Shanahan, “Influence of C3S content of cement on concrete sulfate durability,” University of South Florida, 2003.

[64] N. Shanahan and A. Zayed, “Cement composition and sulfate attack,” *Cem. Concr. Res.*, vol. 37, no. 4, pp. 618–623, Apr. 2007.

[65] R. S. Gollop and H. F. W. Taylor, “Microstructural and microanalytical studies of sulfate attack. IV. Reactions of a slag cement paste with sodium and magnesium sulfate solutions,” *Cem. Concr. Res.*, vol. 26, no. 7, pp. 1013–1028, 1996.

[66] R. D. Hooton and J. Emery, “Sulfate Resistance of a Candian slag cement,” *ACI Mater. J.*, no. 87, pp. 547–555, 1990.

[67] D. D. Higgins, “Increased sulfate resistance of ggbs concrete in the presence of carbonate,” *Cem. Concr. Compos.*, vol. 25, no. 8, pp. 913–919, 2003.

[68] R. Gollop and H. Taylor, “Microstructural and microanalytical studies of sulfate attack, V, comparison of different slag blends,” *Cem. Concr. Res.*, vol. 27, no. 7, pp. 1029–1044, 1996.

[69] R. S. Gollop and H. F. W. Taylor, “Microstructural and microanalytical studies of sulfate attack. II. Sulfate-resisting portland cement: Ferrite composition and hydration chemistry,” *Cem. Concr. Res.*, vol. 24, no. 7, pp. 1347–1358, 1994.

[70] C. Yu, W. Sun, and K. Scrivener, “Degradation mechanism of slag blended mortars immersed in sodium sulfate solution,” *Cem. Concr. Res.*, vol. 72, no. 1, pp. 37–47, 2015.

[71] N. Shanahan, A. Markandeya, A. Elnihum, Y. P. Stetsko, and A. Zayed, “Multi-technique investigation of metakaolin and slag blended portland cement pastes,” *Appl. Clay Sci.*, 2016.

[72] M. M. C. Canut, “Pore structure in blended cement pastes,” Technical University of Denmark, 2011.

[73] A. Attari, C. McNally, and M. G. Richardson, “A combined SEM - Calorimetric approach for assessing hydration and porosity development in GGBS concrete,” *Cem. Concr. Compos.*, vol. 68, pp. 46–56, 2016.

[74] J. Stroh, M.-C. Schlegel, E. F. Irassar, B. Meng, and F. Emmerling, “Applying high resolution SyXRD analysis on sulfate attacked concrete field samples,” *Cem. Concr. Res.*, vol. 66, pp. 19–26, 2014.

[75] T. H. Wee, A. K. Suryavanshi, S. F. Wong, and A. K. M. A. Rahman, “Sulfate Resistance of Concrete Containing Mineral Admixtures,” *Aci Mater. J.*, vol. 97, no. 5, pp. 536–549, 2000.

[76] F. W. Locher, “The Problems of the Sulfate Resistance of Slag Cements,” *Zement-Kalk-Gips*, vol. 19, no. 9, pp. 395–401, 1966.

Chapter 2 Chemical, Mineralogical and Physical Characterization of As-Received Cementitious Materials

2.1 Introduction

The goal of this study is to assess the effect of ground granulated blast furnace slag chemical and physical characteristics on the durability and performance of slag-blended cementitious systems. Two cements and three slags were initially selected for this study. The matrix design was subsequently expanded to include 4 cements and 8 slags to better assess the blended systems' performance. The cements were selected, based on their mill certificates, to have variable equivalent-alkali (Na_2O_{eq}) content and C_3A but similar Blaine fineness and C_3S content. C_3A was selected as a variable in this study because ASTM C989 [1] states that durability performance of slag may be affected by the C_3A content of the cement and the slag chemical composition. ASTM C150 [2] specifies a maximum of 8% C_3A for Type II cements, while for Type I cements there is no limit on the C_3A content. The cements were selected to have C_3A contents at the mid- and high-end levels of the Type I and Type II cements available on the market. One cement was selected to have a C_3A content that meets ASTM specifications for Type II cement, while the other cement was selected to have the C_3A content in excess of the 8% limit. Two more cements (Type I and Type III) were subsequently added to the matrix to study the effect of higher alkali content and fineness on the performance of these blended systems.

Slag selection was primarily based on the Al_2O_3 content. While there is no limit on the slag Al_2O_3 content in ASTM C989 [1], the standard points out that low-alumina slags (Al_2O_3 < 11%) are expected to improve sulfate durability of cement-slag blends, while high-alumina slags (Al_2O_3 > 18%) are expected to decrease it. However, there is no guidance on the effect of mid-range alumina slags (11% to 18%) on durability. Therefore, three slags were selected with alumina contents below the 11% limit, at the 11% limit, and between 11 and 18%. Subsequently, three additional slags were added to the matrix to assess the effect of slag fineness on durability of the blended system. Two slags, at low and moderate alumina contents, were collected from the suppliers at two different finenesses. The slag with the highest alumina content was ground in the laboratory. This chapter discusses the laboratory experiments performed to characterize the as-received materials. Two more slags were added, for a limited number of experiments, with a

variable sulfate content to assess the significance of sulfate optimization on the blended system performance. In this chapter, the chemical, mineralogical and physical characteristics of the as-received materials will be presented.

2.2 Elemental Oxide Composition of As-Received Cements and Slags

The elemental oxide compositions of the as-received cements (A, B, C and D) and slags (S8, S8F, S11c, S11f, S14, S14(S) and S16) used in this study were determined using x-ray fluorescence spectroscopy (XRF) according to ASTM C114 [3] and are listed in Table 2-1 and Table 2-3, respectively. For the as-received cements, the potential compound composition was calculated following ASTM C150 [2], and the results are depicted in Table 2-2. Cements for this study were selected based on their mill certificates to have a similar C_3S content and a variable C_3A content, as C_3A content has been indicated by ASTM C989 [4] to have a significant effect on durability of cement-slag blends. Additionally, Cements A and B were selected to have similar alkali content but lower than Cements C and D, since alkalis are known to affect cement reactivity [5], [6].

Slags were selected to obtain a range of Al_2O_3 contents, as Al_2O_3 content has been reported to have a significant effect on slag reactivity [7] as well as durability of slag-blended cementitious systems [4]. Table 2-3 shows that the Al_2O_3 content of slags varied from approximately 8% (S8) to 16% (S16). Slag reactivity has also been reported to increase with increasing CaO and MgO content [7]–[9]. The CaO content was similar for all the slags, while MgO content was highest for S8, S8F, and S11c and lowest for S14. Typical US slags can have higher MgO contents compared to Asian slags, which have an upper limit in their MgO content of 10%.

ASTM C989 [4] allows slags to be interground with gypsum, which would be reflected in the SO_3 content determined by XRF. However, this technique cannot distinguish between sulfur present in the form of sulfate and sulfur present as sulfide. The sulfide is formed within the molten slag and is present in the slag granules, whereas the sulfate is intentionally added during the grinding process. Therefore, sulfide content of all the slags was determined in accordance with ASTM C114 [3], and the total SO_3 content obtained from XRF was corrected to account for the presence of sulfide. The sulfide content, the total SO_3 content as determined by XRF, and the corrected SO_3 content are reported in Table 2-3. The results showed that the sulfur in all the slag

is predominantly present in the form of sulfide, indicating that these slags have not been interground with gypsum or other forms of calcium sulfate except for S14S.

Table 2-1: Oxide Chemical Composition of As-Received Cements

Analyte	**Cement A Type II(MH) (wt %)**	**Cement B Type I (wt %)**	**Cement C Type I (wt %)**	**Cement D Type III (wt %)**
SiO_2	21.2	20.1	19	18.8
Al_2O_3	5.15	5.6	5.9	5.7
Fe_2O_3	3.61	2	2.8	2.5
CaO	63.91	64.4	60.8	61
MgO	0.7	0.9	2.5	2.7
SO_3	2.59	3.6	4	4.2
Na_2O	0.14	0.08	0.32	0.3
K_2O	0.31	0.47	1.1	1.02
TiO_2	0.29	0.18	0.26	0.25
P_2O_5	0.15	0.33	0.26	0.25
Mn_2O_3	0.03	0.03	0.11	0.09
SrO	0.06	0.07	0.28	0.27
Cr_2O_3	0.02	0.01	0.01	0.01
ZnO	0.06	0.03	0.07	0.06
L.O.I. (950°C)	1.66	1.8	2.4	2.9
Total	99.89	99.56	99.82	100
Na_2O_{eq}	0.35	0.39	1.05	0.97
SO_3/Al_2O_3	0.5	0.64	0.68	0.74

Table 2-2: Bogue-Calculated Potential Compound Content for As-Received Cements

Phase	**Cement A**	**Cement B**	**Cement C**	**Cement D**
C_3S	52	59	48	52
C_2S	22	13	18	15
C_3A	8	11	11	11
C_4AF	11	6	9	8
C_4AF+2C_3A	26	29	30	29
$C_3S+4.75C_3A$	88	113	100	103

Table 2-3: Oxide Chemical Composition of As-Received Slags

Analyte	Slags						
	S8	**S8F**	**S11c**	**S11f**	**S14**	**S14(S)**	**S16**
SiO_2	38.59	38.61	36.15	35.67	35.44	33.7	32.86
Al_2O_3	8.09	7.73	10.71	10.82	14.25	13.67	16.29
Fe_2O_3	0.51	0.58	0.7	0.54	0.45	0.69	0.36
CaO	38.11	39.52	37.41	41.93	41.06	41.48	37.98
MgO	10.83	10.40	11.27	7.9	5.25	5.33	8.88
Total SO_3 (includes sulfur as sulfide and sulfate)	2.21	2.25	2.33	1.91	1.99	3.02	2.61
Sulfide Sulfur (S)	0.89	0.946	-	0.68	0.67	0.635	0.952
Sulfate Sulfur (as SO_3)	-0.02	-0.12	0.24	0.22	0.31	1.43	0.23
Na_2O	0.3	0.33	0.26	0.2	0.2	0.25	0.37
K_2O	0.38	0.26	0.37	0.37	0.3	0.26	0.44
TiO_2	0.37	0.36	0.47	0.59	0.5	0.54	1.21
P_2O_5	<0.01	<0.01	<0.01	<0.01	0.01	0.02	<0.01
Mn_2O_3	0.59	0.63	0.23	0.25	0.22	0.26	0.25
SrO	0.05	0.05	0.04	0.08	0.05	0.06	0.1
Cr_2O_3	<0.01	<0.01	<0.01	<0.01	<0.01	<0.01	<0.01
ZnO	<0.01	<0.01	<0.01	<0.01	<0.01	<0.01	<0.01
BaO	0.03	0.04	0.03	0.08	0.07	0.07	0.08
L.O.I (950˚C)	-0.17	-0.72	0.1	-0.48	0.05	0.42	-1.03
Corrected L.O.I (950˚C)	1.15	-	-	0.53	1.06	1.37	0.4
Total	99.89	100.04	100.09	99.85	99.84	99.77	100.41
Na_2O_{eq}	0.55	0.51	0.51	0.44	0.4	0.42	0.66

2.3 Mineralogical Analysis

Mineralogical compositions of the as-received cements and slags were determined using x-ray diffraction (XRD) measurements conducted in accordance with ASTM C1365 [10]. Prior to XRD measurements, each cement was wet-ground in ethanol in a McCrone micronizing mill to a particle size between 1 and 10 µm. The wet grinding method was used to minimize temperature increases during grinding to avoid dehydration of gypsum to hemihydrate or anhydrite. The samples were then dried in an oven at 40°C.

For as-received cements, selective dissolutions (extractions) were performed to aid the identification of the minor phases as well as the C_3S and C_3A crystal structures. Salicylic

acid/methanol (SAM) extraction was performed to dissolve the silicates and free lime, and isolate a concentrated residue of aluminates, ferrites, and minor phases, such as periclase, carbonates, alkali sulfates, and double alkali sulfates [11], [12]. Potassium hydroxide/sucrose extraction was used to dissolve aluminates and ferrites and obtain a residue of C_3S, C_2S, alkali sulfates, and MgO [11].

XRD scans were collected using the Phillips X'Pert PW3040 Pro diffractometer equipped with the X'Celerator Scientific detector and a Cu-Kα x-ray source. Tension and current were set to 45 kV and 40 mA respectively, and 5-mm divergence and anti-scatter slits were used in the automatic mode. Scans were collected for the 7-70˚ 2θ angular range. The back-loading technique was used to load samples into the sample holder in order to minimize preferred orientation. The sample was rotated at 30 rpm during data collection to improve counting statistics [13]. Three samples were prepared for each as-received material, and the average values are reported here.

Phase quantification was performed using the Rietveld refinement functionality of the Panalytical HighScore Plus 4.5 software. An external standard method was used to calculate the amorphous content of the as-received cements and slags [14]–[17]. Corundum (Standard Reference Material (SRM 676a)) obtained from the National Institute of Standards and Technology (NIST) was used as an external standard in this study. The mass absorption coefficient (MAC) of corundum, calculated using the MAC calculator functionality in the Panalytical HighScore Plus 4.5 software, was equal to 30.91 cm^2/g. MAC values for cements and slags were calculated based on their respective elemental oxide compositions listed in Table 2-1 and Table 2-3. Loss on ignition content was attributed to carbonate decomposition and release of CO_2.

Table 2-1, Table 2-4 and Table 2-5 list the values for each major phase determined from Bogue calculations and from X-ray diffraction for all as-received cements. The values of the main cement phases obtained through Rietveld refinement were lower than those calculated according to ASTM C150 [2] (Table 2-2). This was not surprising, as this discrepancy has been well-established in the literature [6], [11], [18]. It is noted from XRD analyses that cements had similar C_3S content except Cement B which has a higher value. Also noted is that cement A has the lowest C_3A content (5.5%) while Cements B, C, and D have the same C_3A content of 8%.

Table 2-5 lists the average values for each phase together with their corresponding standard deviations (σ) for slags. XRD analysis showed that all slags were predominantly amorphous, with

only a few weight percent of crystalline phases. Amorphous content has the most significant effect on slag reactivity as crystalline phases are not reactive and do not contribute to mechanical property development [6], [19].

Table 2-4: Cement Phase Content Using XRD

Phase	Cement A (wt %)	σ	Cement B (wt %)	σ	Cement C (wt %)	σ	Cement D (wt %)	σ
C_3S	48.1	0.1	54	0.5	48.1	0.9	49.5	0.3
C_2S	23.1	0.2	17.3	0.4	15.6	0.1	13.4	0.6
C_3A	5.5	0.2	8.4	0.1	8.3	0.1	8.1	0
Ferrite	9.9	0.1	5.6	0	7.6	0.1	6.8	0.2
Gypsum	2.6	0.2	4.3	0.1	3.8	0.2	2.2	0.1
Hemihydrate	1.5	0.1	1.4	0.1	1.7	0	3	0.1
Anhydrite	0	-	0.1	0	0	0	0	0
Calcite	1.2	0.2	0.3	0.1	1.6	0.1	1.8	0
Portlandite	-	-	0.2	0	0.2	0.1	0.2	0.1
Syngenite	0.7	0.1	0.4	0	0.9	0.1	0.7	0
Quartz	0.1	0	0.1	0	0.2	0	0.3	0
Aphthitalite	-	-	0.2	0	0.5	0.5	0.4	0
Amorphous/ unidentified	7.2	0.4	7.8	0.4	9.1	0.7	10.5	1

Table 2-5: Slag Phase Content Using XRD

Phase	Slag S8 (wt %)	σ	Slag 8F (wt %)	σ	Slag S11c (wt %)	σ	Slag S11f (wt %)	σ	Slag S14 (wt %)	σ	Slag S14(S) (wt %)	σ	Slag S16 (wt %)	σ
Calcite	0.7	0.1	0.4	0.1	0.5	0	0.3	0	0.6	0.1	0.6	0.1	0.3	0
Melilite	0.5	0.1	0.2	0	0.4	0.1	0.2	0	0.5	0	0.5	0.1	0.7	0
Merwinite	-	-	0.8	0.1	0.7	0	0.7	0	-	-	-	-	-	-
Quartz	-	-	-		0.1	0	-	-	1.5	0	0.1	0	-	-
Gypsum	-	-	-		-	-	-	-	0.4	0	1.1	0	-	-
Amorphous/ unidentified	98.9	0.2	98.6	0.1	98.3	0.2	98.8	0.1	97	0.1	97	0	99	0
Hemihydrate	-	-	-	-	-	-	-	-	-	-	0.7	0	-	-

2.4 Physical Characteristics

The physical characteristics of the as-received materials determined in this study were density, fineness, and particle size distribution. Density was determined in accordance with ASTM

C188 [20] and the results are listed in Table 2-6 and Table 2-7 for cements and slags, respectively. The measurements were performed in triplicate, and the standard deviation was within the limit specified by ASTM C188 [20]. Fineness was measured using the Blaine method as described in ASTM C204 [21]. Particle size distribution was determined using the LA-950 laser scattering particle size analyzer manufactured by HORIBA Instruments using the wet method. The as-received materials were measured in reagent-grade ethanol, and one drop of superplasticizer was added to improve particle dispersion. The obtained differential and cumulative particle size distributions are plotted in Figure 2-1 through Figure 2-4. The measurements were performed in triplicate and the average values are reported here.

Fineness has a significant effect on reactivity of cements as well as slags, with increase in fineness corresponding to an increase in reactivity [22]–[24]. Traditionally, the Blaine test is used to determine the fineness of both cements and slags. This is an indirect method of determining fineness as the test actually measures the flow of air through a compacted bed of cement or another powdered material. First, air permeability is measured for a calibration material, typically SRM114q obtained from NIST, with a known Blaine fineness. The fineness of all subsequently analyzed materials is calculated based on the values obtained for SRM114q. While this test is rapid and simple to perform, there are several drawbacks that have to be taken into account, especially when the Blaine test is used to measure fineness of materials other than cement. Arvaniti et al. [25] point out that the "reference material must have similar shape, particle size distribution, and surface properties to the material of interest or it cannot be a valid comparison." In another study, Arvaniti et al. [26] also pointed out that for SCMs, it is particularly difficult "to form a good compacted bed of specific porosity." Additionally, for materials other than cement, ASTM C204 [21] specifies that a b-value has to be determined before the actual fineness measurement. This b-value is then used for fineness calculation, and for cement is taken to be equal to 0.9. A recent discussion at the slag subcommittee meeting at the ASTM C204 December 2016 meeting revealed that slag producers consider experimentally-determined b-values for slag to be unreliable and use the b-value of 0.9 in their Blaine fineness calculation for slag. Subsequently, ASTM C989-18 indicates using a b value of 0.9 in determining slag Blaine fineness. In this investigation, Blaine fineness was determined for the as-received cements as well as slags using a b value of 0.9. As can be seen in Table 2-6, cement fineness was very similar with cement D showng the highest

fineness among the cements studied here. For slags, Table 2-7 indicates that the Blaine fineness for S8F and S11f were highest while S16 was the coarsest among the slags studied here.

Table 2-6: Cement Particle Size Analysis, Blaine Fineness and Density

Physical Properties	**Cement A**	**Cement B**	**Cement C**	**Cement D**
D_{10} (µm)	2	2.73	2.69	2.05
D_{50} (µm)	10	11.46	12.59	9.14
D_{90} (µm)	24.96	27.56	35.28	19.62
Mean size (MPS) (µm)	12.26	13.81	16.50	10.32
Blaine Fineness (m^2/kg)	485	474	436	522
Density (g/cm^3)	3.15	3.15	3.15	3.13

Table 2-7: Slag Particle Size Analysis, Blaine Fineness and Density

Physical Properties	**S8**	**S8F**	**S11c**	**S11f**	**S14**	**S14(S)**	**S16**
D_{10} (µm)	1.04	1.17	1.32	0.77	1.49	1.93	1.57
D_{50} (µm)	7.8	6.98	9.33	7.34	9.88	10.33	10.04
D_{90} (µm)	18.81	16.10	22.09	16.94	22.29	24.82	23.68
Mean size (MPS) (µm)	9.16	8.03	10.86	8.36	11.15	12.34	11.8
Blaine Fineness (m^2/kg)	642	698	589	680	574	595	466
Density (g/cm^3)	2.87	2.90	2.89	2.86	2.89	2.90	2.90

An alternative method of measuring fineness, and one that has been shown to have a better correlation with heat of hydration of cements [23], is laser particle size analysis. The main concern with laser diffraction particle size analysis is adequate sampling and dispersion of the particles as the presence of agglomerates can lead to incorrect results [25], [26]. The results of laser particle size analysis are presented in Table 2-6 and Table 2-7 as well as Figure 2-1 through Figure 2-4. Particle size distribution results were in general agreement with Blaine fineness. S8F had the smallest mean particle size (MPS) followed by S11f, while S16 MPS had the highest value.

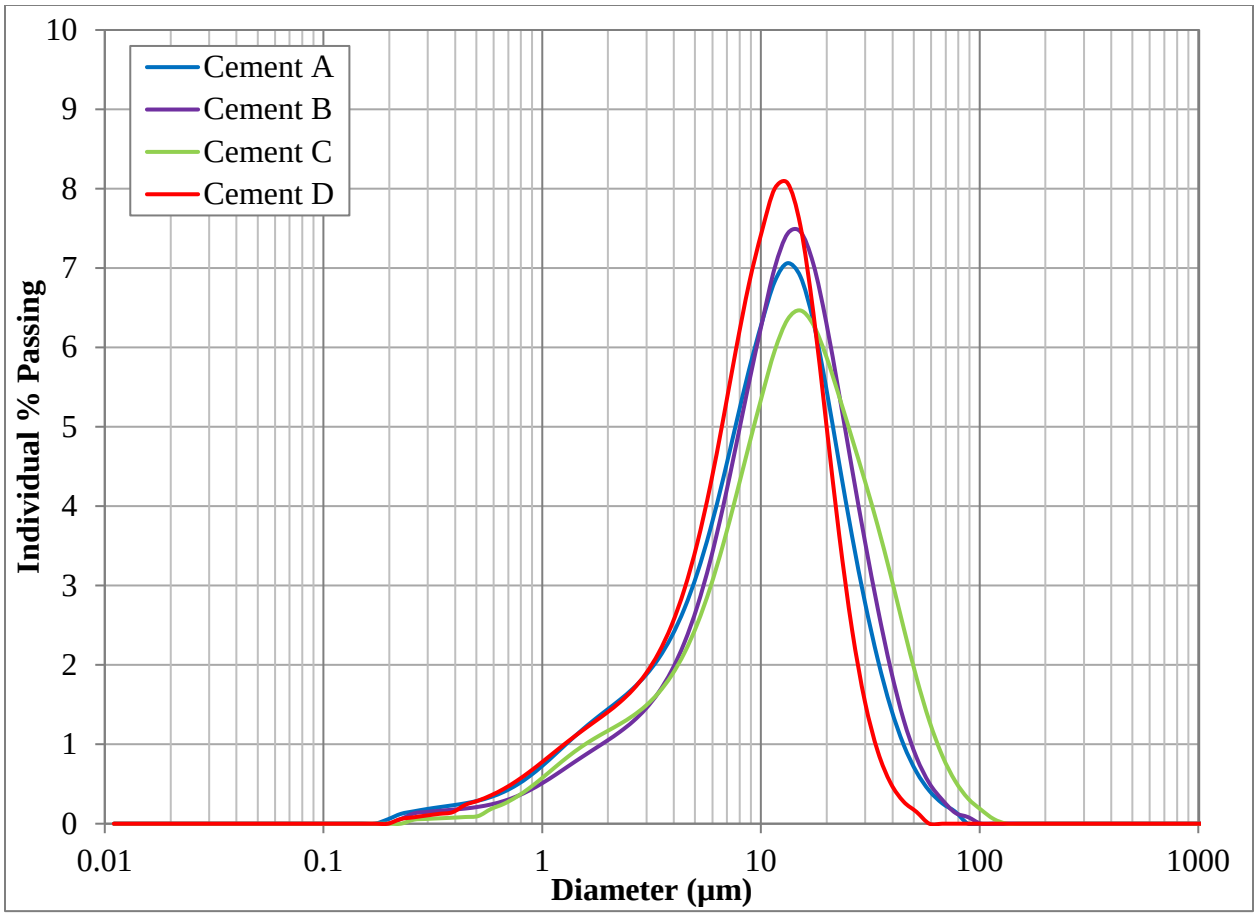

Figure 2-1: Differential Particle Size Distribution for Cements

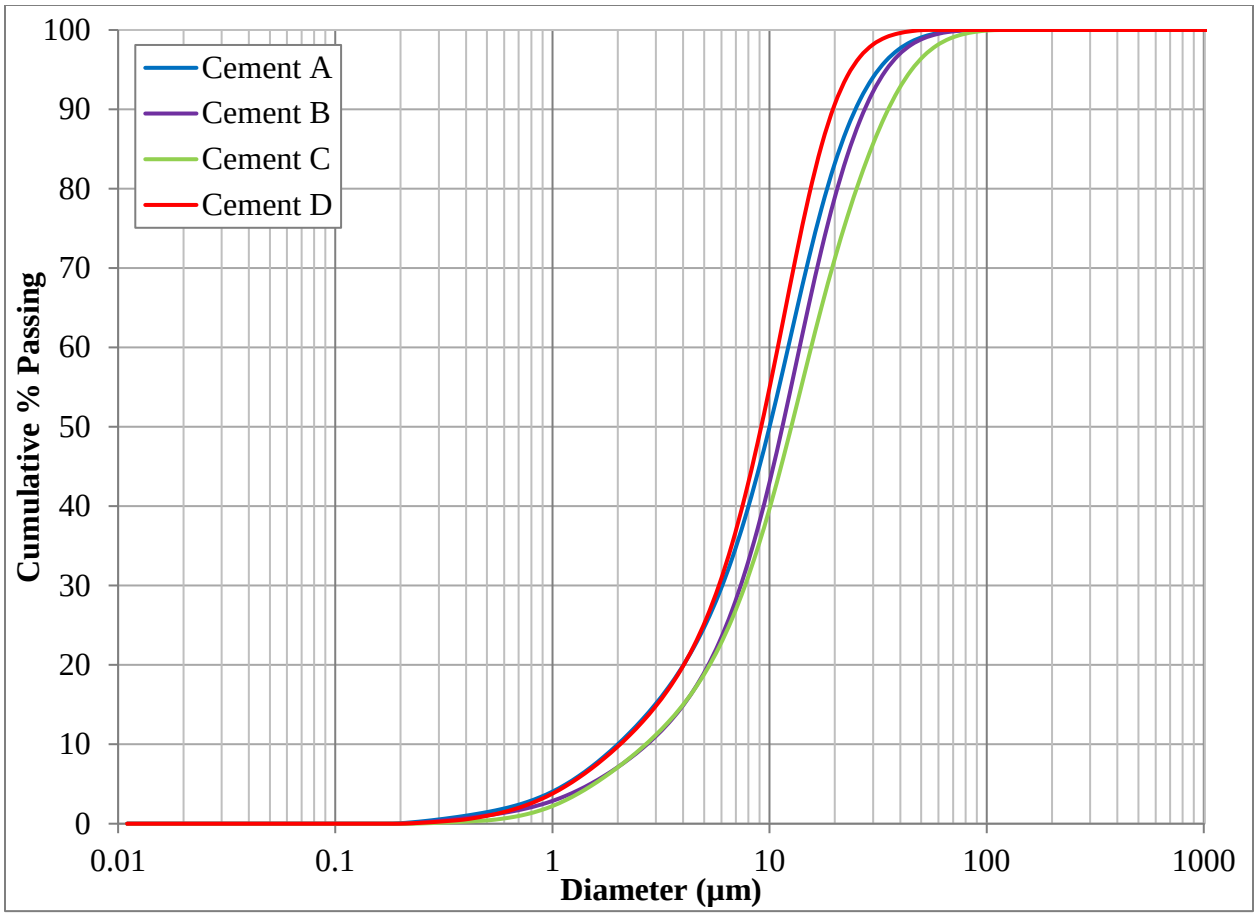

Figure 2-2: Cumulative Particle Size Distribution for Cements

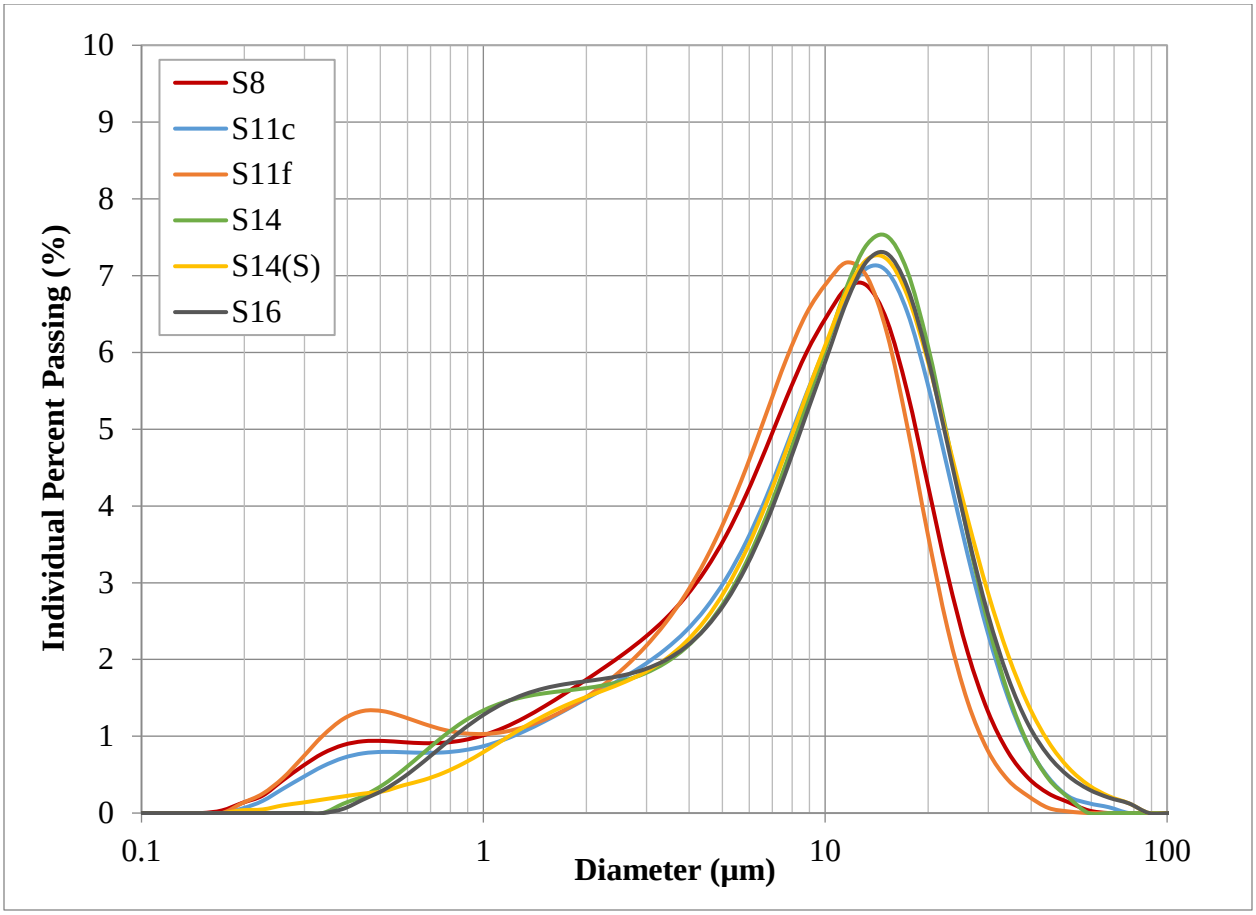

Figure 2-3: Differential Particle Size Distribution for Slags

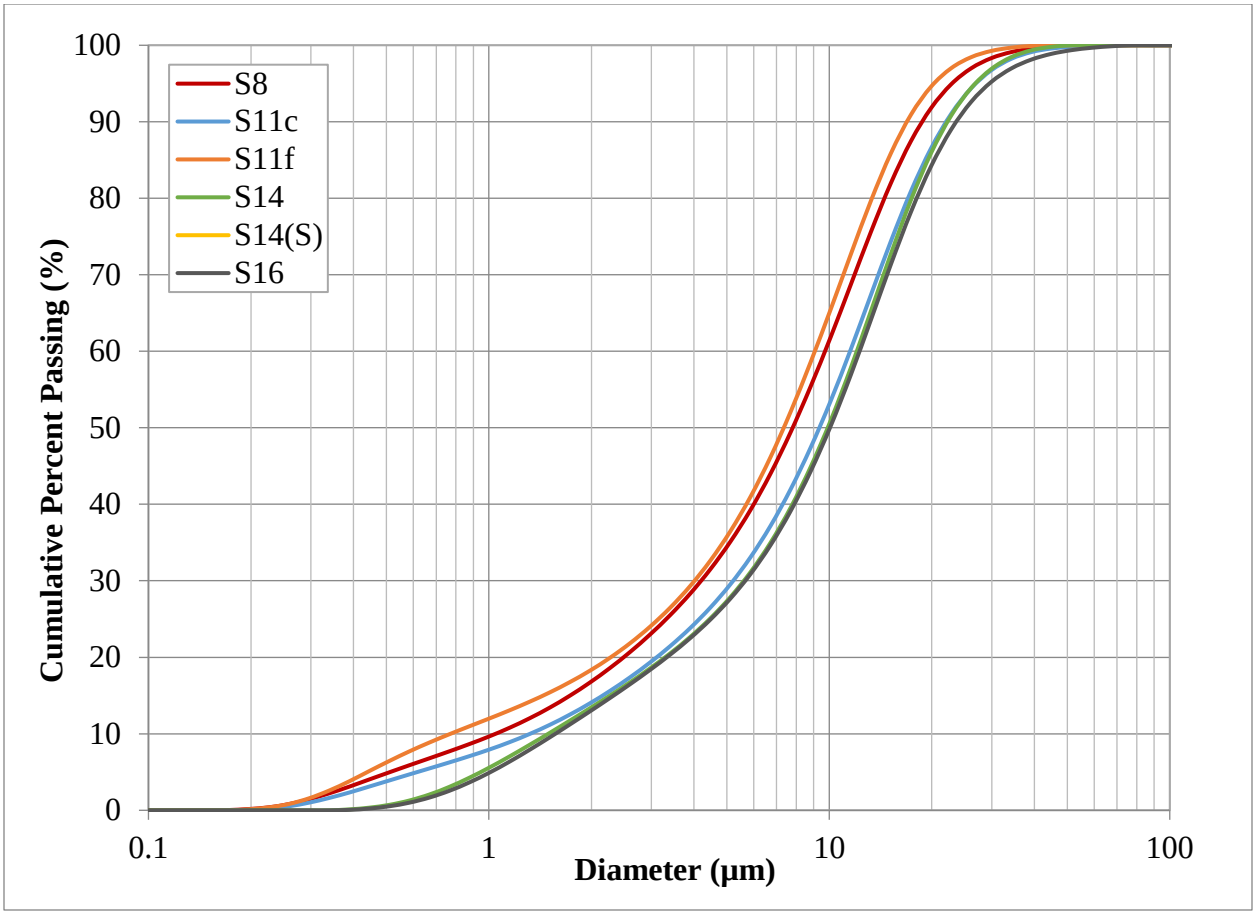

Figure 2-4: Cumulative Particle Size Distribution for Slags

2.5 Conclusions

As-received cements and slags were characterized in terms of their chemical and mineralogical compositions as well as their physical properties. Comparing all cements, Cement B had the highest C_3S content. Cement B also had a higher C_3A content than cement A, but a content similar to Cement C and D. Cement C had the highest alkali content, similar to Cement D; however, the latter had the highest Blaine fineness and therefore the smallest mean particle size. It is also noted that cements with the highest alkali contents had the highest sulfate demands, as shown by Cements C and D. According to the characterization tests performed here, it is therefore to be expected that Cement A will have the best performance in terms of durability and concrete temperature rise.

Slag properties, however, varied not only in terms of their alumina content, but also in terms of their fineness and magnesia-to-alumina ratio (M/A). S16 slag had the highest Al_2O_3 content, but also the lowest fineness, while the highest fineness was observed for the S11f slag. While slag reactivity is expected to increase with increasing Al_2O_3, it also increases with increasing fineness. Therefore, alumina content and fineness are expected to have a competing effect on early-age reactivity and concrete temperature rise. Reactivities of S11f and S16 are expected to be similar and higher than that of S8 due to the higher alumina contents (S16) and higher fineness (S11f).

2.6 References

[1] ASTM C989/C989M-14, “Standard Specification for Slag Cement for Use in Concrete and Mortars,” West Conshohocken, PA: ASTM International, 2014.

[2] ASTM C150/C150M-16, “Standard Specification for Portland Cement,” West Conshohocken, PA: ASTM International, 2016.

[3] ASTM C114-13, “Standard Test Method for Chemical Analysis of Hydraulic Cement,” West Conshohocken, PA: ASTM International, 2013.

[4] ASTM C989 / C989M-17, “Standard Specification for Slag Cement for Use in Concrete and Mortars,” West Conshohocken, PA: ASTM International, 2017.

[5] I. Odler, “Hydration, Setting and Hardening of Portland Cement,” in *Lea’s Chemistry of Cement and Concrete*, 4th ed., P. C. Hewlett, Ed. New York, NY, NY: Arnold, 1998, pp. 241–297.

[6] H. F. W. Taylor, *Cement Chemistry*, 2nd ed. London, UK: Thomas Telford Publishing, 1997.

[7] R. Snellings, G. Mertens, and J. Elsen, “Supplementary cementitious materials,” *Rev. Mineral. Geochemistry*, vol. 74, no. 1, pp. 211–278, Dec. 2012.

[8] A. A. Ramezanianpour, *Cement Replacement Materials*. Berlin, Germany: Springer Berlin Heidelberg, 2014.

[9] V. Kocaba, “Development and Evaluation of Methods to Follow Microstructural Development of Cementitious Systems Including Slags,” École Polytechnique Fédérale de Lausanne, 2009.

[10] ASTM C1365-06, “Standard Test Method for Determination of the Proportion of Phases in Portland Cement and Portland-Cement Clinker Using X-Ray Powder Diffraction Analysis,” West Conshohocken, PA: ASTM International, 2016.

[11] P. E. Stutzman, “Guide for X-Ray Powder Diffraction Analysis of Portland Cement and Clinker,” Gaithersburg, MD, 1996.

[12] W. A. Gutteridge, “On the Dissolution of the Interstitial Phases in Portland Cement,” *Cem. Concr. Res.*, vol. 9, no. 3, pp. 319–324, 1979.

[13] D. Bish and R. J. Reynolds, “Sample Preparation for X-Ray Diffraction,” in *Modern Powder Diffraction*, D. Bish and J. Post, Eds. Washington, DC: The Mineralogical Society of America, 1989, pp. 73–99.

[14] B. H. O'Connor and M. D. Raven, "Application of the Rietveld Refinement Procedure in Assaying Powdered Mixtures," *Powder Diffr.*, vol. 3, no. 01, pp. 2–6, Jan. 1988.

[15] D. Jansen, C. Stabler, F. Goetz-Neunhoeffer, S. Dittrich, and J. Neubauer, "Does Ordinary Portland Cement Contain Amorphous Phase? A Quantitative Study Using an External Standard Method," *Powder Diffr.*, vol. 26, no. 1, pp. 31–38, Mar. 2011.

[16] M. A. G. Aranda, A. G. De la Torre, and L. Leon-Reina, "Rietveld Quantitative Phase Analysis of OPC Clinkers, Cements and Hydration Products," *Reviews in Mineralogy and Geochemistry*, vol. 74, no. 1. pp. 169–209, 2012.

[17] I. C. Madsen, N. V. Y. Scarlett, and A. Kern, "Description and survey of methodologies for the determination of amorphous content via X-ray powder diffraction," *Zeitschrift für Krist.*, vol. 226, no. 12, pp. 944–955, Dec. 2011.

[18] P. Stutzman, "Powder diffraction analysis of hydraulic cements: ASTM Rietveld round-robin results on precision," *Powder Diffr.*, vol. 20, no. 02, pp. 97–100, Jun. 2005.

[19] J. Escalante, L. Gómez, K. Johal, G. Mendoza, H. Mancha, and J. Méndez, "Reactivity of blast-furnace slag in Portland cement blends hydrated under different conditions," *Cem. Concr. Res.*, vol. 31, no. 10, pp. 1403–1409, Oct. 2001.

[20] ASTM C188-15, "Standard Test Method for Density of Hydraulic Cement," West Conshohocken, PA: ASTM International, 2015.

[21] ASTM C204-16, "Standard Test Method for Fineness of Hydraulic Cement by Air Permeability Apparatus," West Conshohocken, PA: ASTM International, 2016.

[22] H. Binici, H. Temiz, and M. M. Kose, "The effect of fineness on the properties of the blended cements incorporating ground granulated blast furnace slag and ground basaltic pumice," *Constr. Build. Mater.*, vol. 21, no. 5, pp. 1122–1128, 2007.

[23] A. Sedaghat, N. Shanahan, and A. Zayed, "Predicting One-Day, Three-Day, and Seven-Day Heat of Hydration of Portland Cement," *J. Mater. Civ. Eng.*, vol. 27, no. 9, p. 04014257, 2015.

[24] A. Zayed, A. Sedaghat, A. J. Bien-Aime, and N. Shanahan, "Effects of portland cement particle size on heat of hydration," University of South Florida, Tampa, FL, 2013.

[25] E. C. Arvaniti, M. C. G. Juenger, S. A. Bernal, J. Duchesne, L. Courard, S. Leroy, J. L. Provis, A. Klemm, and N. De Belie, "Physical characterization methods for supplementary cementitious materials," *Mater. Struct.*, vol. 48, no. 11, pp. 3675–3686, 2015.

[26] E. C. Arvaniti, M. C. G. Juenger, S. A. Bernal, J. Duchesne, L. Courard, S. Leroy, J. L. Provis, A. Klemm, and N. De Belie, “Determination of particle size, surface area, and shape of supplementary cementitious materials by different techniques,” *Mater. Struct.*, vol. 48, no. 11, pp. 3687–3701, 2014.

Chapter 3 Effects of Slag Properties on Strength Evolution of Cementitious Mixtures

3.1 Introduction

Sulfate attack is a common durability issue for structural concrete in Florida. Sulfates can be present in groundwater, soil, and marine environments. Three mechanisms have been proposed to explain concrete deterioration during sulfate attack: 1) conversion of monosulfoaluminate ($C_4A\bar{S}H_{12}$) to ettringite ($C_6A\bar{S}_3H_{32}$), 2) reaction of CH with sulfate ions to form gypsum, and 3) decalcification of C-S-H. Cements with C_3A contents above 5% will form monosulfoaluminate during initial hydration due to the lack of sulfate ions [1]. When external sulfates penetrate the concrete, monosulfoaluminate reacts with this new source of sulfates and is converted to ettringite. This reaction is accompanied by an increase in solid volume causing expansion [2]–[5]. At later ages, sulfate ions react with CH to form gypsum, which has also been shown to result in expansion [6]–[8]. Formation of gypsum may result in a decrease in the pH of the pore solution, depending on the cation associated with the external sulfate ions. In the case of sodium sulfate, sodium hydroxide forms as the other product, in addition to gypsum, of the reaction of sulfate with CH. $Na(OH)_2$ is readily soluble, which maintains the high pH in the pore solution. However, when CH reacts with magnesium hydroxide, the resultant $Mg(OH)_2$ is not soluble, which decreases the pH of the pore solution. The decrease in alkalinity causes decalcification of C-S-H leading to loss in strength and cohesion [1].

Ground granulated blast furnace slag (slag) is frequently used in concretes exposed to sulfate environments to improve their resistance to sulfate attack. Cement replacement with slag can improve sulfate resistance by reducing the C_3A and C_3S content, through cement dilution, and through pore structure refinement. However, even though slag addition decreases C_3A, the total cementitious Al_2O_3 content may increase depending on the Al_2O_3 content of the slag, although Whittaker et al. [9] argued that alumina coming from slag is not readily available to form monosulfoaluminate and ettringite. Slags used in their study had relatively low Al_2O_3 contents of 7.3 and 12.3%. According to ASTM C989 [10], slags with low alumina (11%) offer increased resistance to sulfate attack whereas slags with high alumina content (18%) negatively affect concrete sulfate durability. However, the standard does not provide any information regarding slags with an alumina content in the range of 11 to 18%.

As stated earlier in Chapter 1, sulfate attack can occur when concrete is exposed to sulfate concentrations above 0.1% and is manifested by expansion and/or loss of strength and cohesion. Loss of strength and cohesion is due to decalcification of C-S-H. This chapter will evaluate compressive strength development of OPC-slag mortar in saturated lime solution at different cement replacement levels as well as in sodium sulfate solution in order to determine the effect of slag chemistry and physical characteristics on loss of cohesion.

3.2 Experimental Methods

In order to evaluate the effect of slag composition on compressive strength development, mortar mixtures were prepared with Cements A and B and slags S8, S11c, and S16 at 0, 30, 50, and 70% cement replacement levels. Mortars were prepared in accordance to ASTM C109 [11] and ASTM C305 [12], with the exception of the water-to-cementitious materials (w/cm) ratio. For mortars containing cementitious materials other than portland cement, ASTM C109 [11] specifies that the amount of mixing water should be adjusted to maintain constant flow of 110 ± 5. However, w/cm is a major factor affecting compressive strength, permeability, and consequently sulfate resistance [2]. Since the objective of this study was to compare compressive strength development of mortars prepared with different slags in lime and sulfate environments, the w/cm ratio was maintained constant at 0.485 in order to eliminate it as a variable.

After demolding, mortar cubes were cured in saturated lime and exposed to 5% sodium sulfate solutions. The saturated lime solution was prepared by adding 3 grams of calcium hydroxide per liter of deionized (DI) water. The sulfate solution was prepared following ASTM C1012 [13] and changed at the intervals specified in this standard in order to match the schedule for the expansion bars. Mortar cubes were tested at the ages 7, 28, 91, 180, 360 and 540 days. Some mixtures did not have their 540-day strength data available at the time this report was written.

Additionally, heat flow of Control A and Control B mortars was measured at 23˚C using a TAM Air 3-channel isothermal calorimeter manufactured by TA Instruments. Isothermal calorimetry was performed in accordance with ASTM C1702 [14], Method B, external mixing. The mixing procedure outlined in ASTM C305 [12] was used for isothermal calorimetry as well.

3.3 Results and Discussion

Sulfate resistance of cement-slag mixtures was evaluated with two cements, A and B. Before comparing the performance of slags with these cements, it was important to examine the behavior of these cements alone in lime and sulfate environments. Figure 3-1 shows that compressive strengths of Control A and Control B mortars in lime solution were very similar up to 180 days. For cement mortars with constant w/c ratio and curing temperature, and similar cement fineness, early-age compressive strength was primarily a function of the C_3S content of the cement. It is not surprising, therefore, that the compressive strengths of Control A and B mortars were similar. Cements A and B had similar Blaine fineness (485 and 474 m^2/kg respectively), and a slightly higher C_3S content for Cement B (54%) compared to that of Cement A (48%), which was reflected in slightly higher strengths of the Control B mixture.

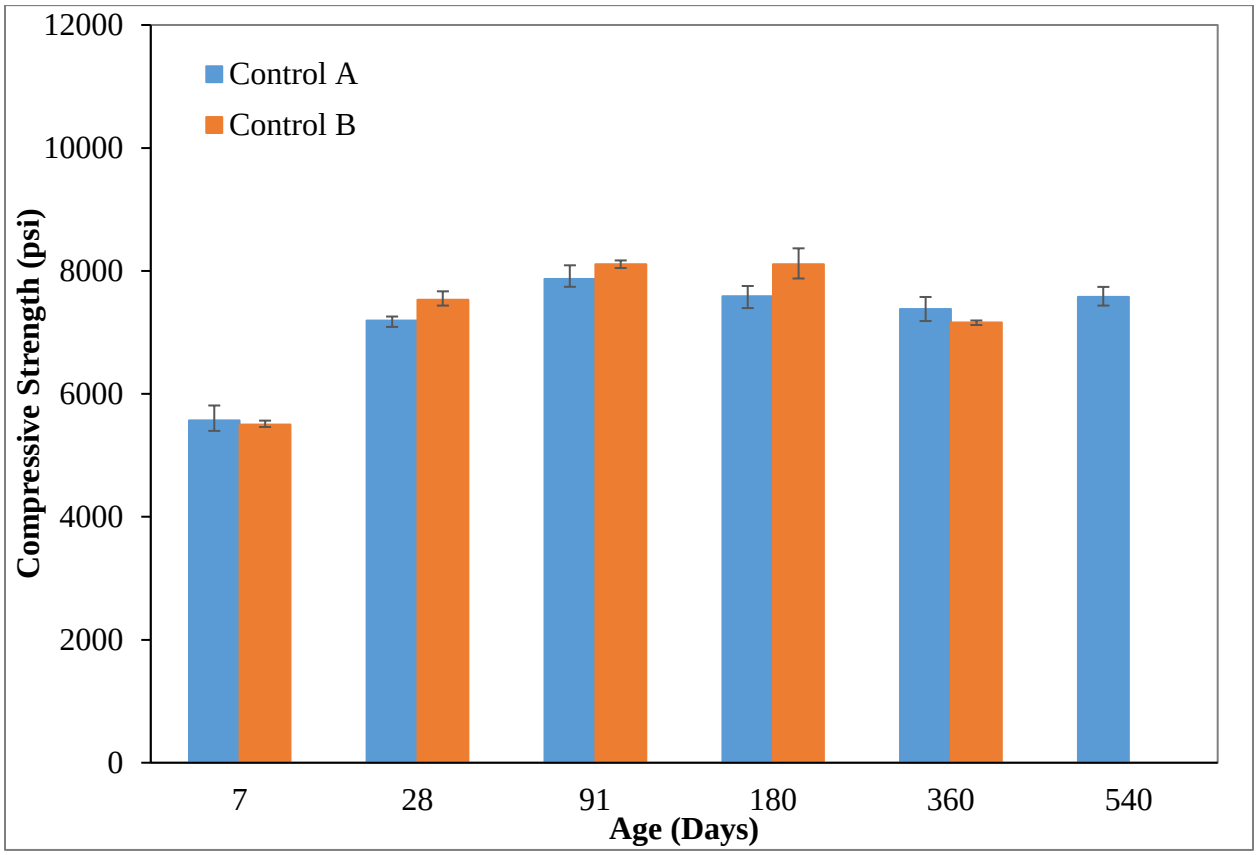

Figure 3-1: Compressive strength development of Control A and Control B mortars in saturated lime solution

In sulfate solution (Figure 3-2), strengths were similar at 7 and 28 days, after which compressive strength of Control BS mortar began to decrease. At 91 days, Control BS strength decreased by 10% compared to its 28-day value, and at 180 days the drop was approximately 25%. For Control AS, the drop in strength was observed after 91 days. At 180 days, Control AS strength decreased by 17% compared to its 28-day strength and by 19% compared to the 91-day strength. At 540 days, mixture BS completely disintegrated while AS mixture showed a strength ratio of 29% compared to its 28-day strength. The faster deterioration of Control BS mortar is not surprising, as Cement B has a higher C_3A content (8.4% determined by Rietveld refinement and 11% based on the Bogue calculations) compared to Cement A (5.5% determined by Rietveld refinement and 8% based on the Bogue calculations). The negative effect of C_3A on cement sulfate resistance has been well-established in the literature [1], [2]. ASTM C150 [15] limits the C_3A content of portland cements to a maximum of 5% for high sulfate resistance and 8% for moderate sulfate resistance. Therefore, Cement B could not be considered sulfate resistant, while Cement A would be expected to provide moderate resistance to sulfate attack. In addition to C_3A, increase in C_3S has also been reported to have a negative effect on sulfate durability [5], [7], [8], [16]–[18] and could have possibly contributed to lower compressive strengths of Control BS.

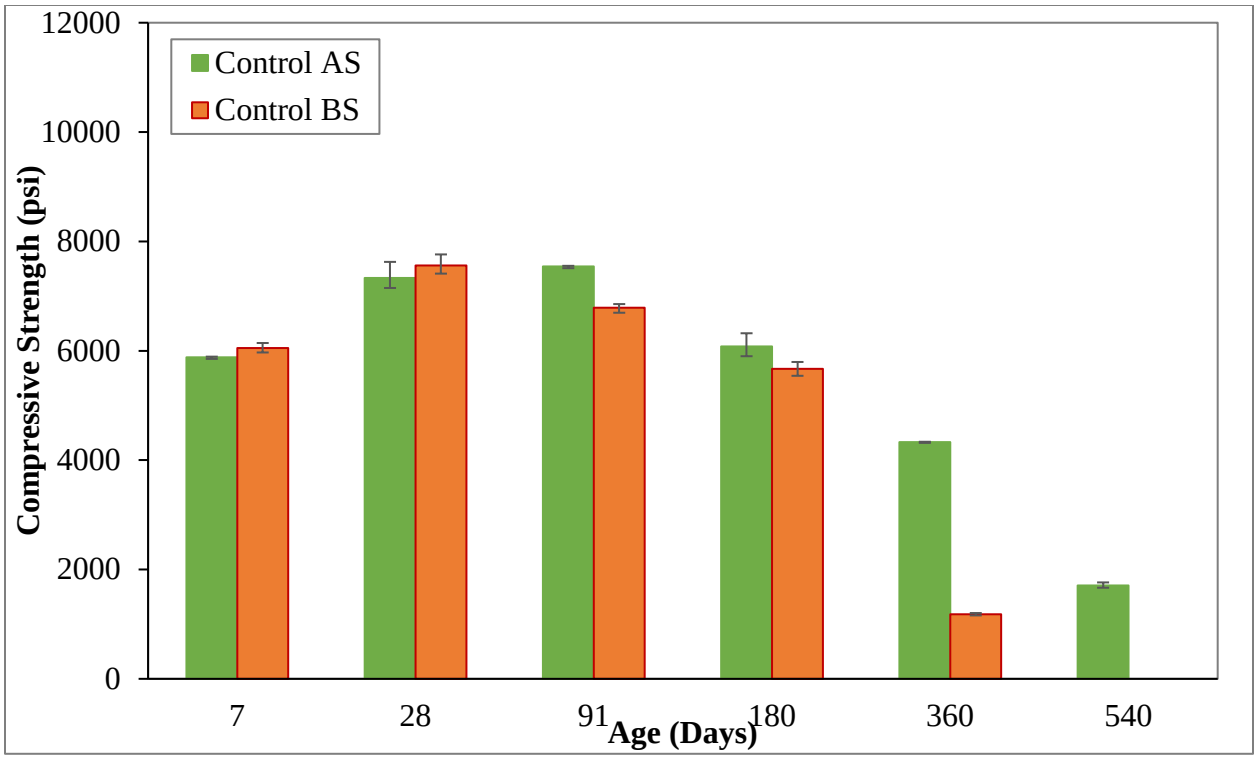

Figure 3-2: Compressive strength development of Control A and Control B mortars in 5% sodium sulfate solution

As can be seen in Figure 3-3, all 30% cement replacements with slag and that were cured in a saturated lime solution had higher compressive strengths compared to Control A at 180 days. At 28 days, 30S16-A exceeded Control A by more than 600 psi. This is attributed to the higher alumina content S16 resulting in higher early-reactivity. However, only modest strength increases were observed for S16 after 28 days, while 30S8-A had the highest rates of strength gain after 28 days. This is likely due to a higher later-age reactivity of this slag. Ben Haha et al. [19] showed that although early-age reactivity of low-Al_2O_3 slags is lower, their cumulative heat evolution is higher at later ages compared to the high-Al_2O_3 slags, indicating a higher later-age reactivity. In another study, Ben Haha et al. [20] also reported higher later-age heat evolution for slags with higher MgO content. Slags studied by Ben Haha et al. [20] were ground to similar fineness (500 ± 100 m^2/kg) and had similar Al_2O_3 contents (11.3-12%). Although the heat evolution of cement-slag mixtures was not measured in this study, Bentz et al. [21] showed that compressive strength of mortar mixtures prepared at different w/cm ratios is a linear function of the heat of hydration normalized by the amount of water present in the mixture. Oey et al. [22] applied this concept to OPC+SCM mixtures containing accelerator. All the mixtures in the current study had the same

w/cm ratio; therefore, compressive strength development of the cement-slag mixtures can be assumed to be indicative of their heat evolution and consequently reactivity. Slag S8 had the lowest Al_2O_3 and the highest MgO contents of all the slags in this study. Therefore, its high rate of strength gain with Cement A at later ages is not surprising.

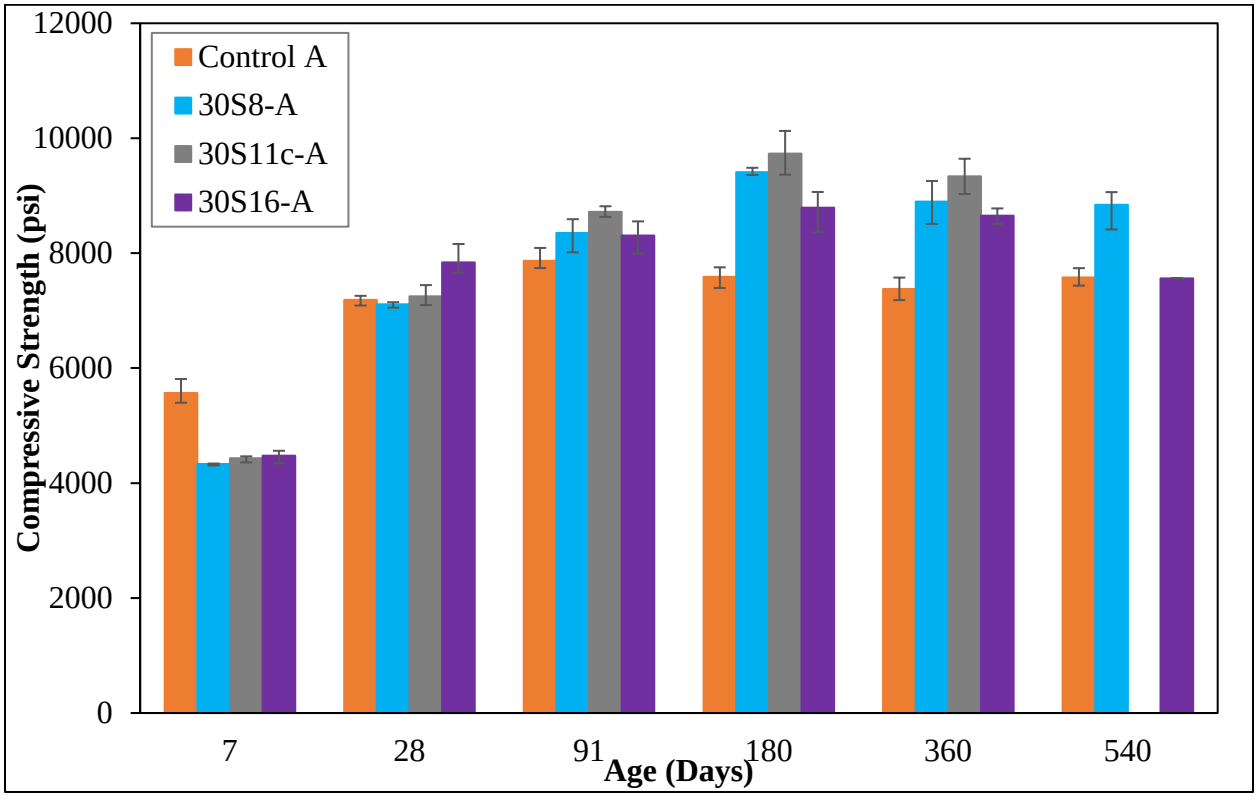

Figure 3-3: Compressive strength development of Cement A-30% slag mortars stored in saturated lime solution

Figure 3-4 shows the strength development of the 30% slag mortars with Cement B. At 28 days, only 30S16-B mortars had compressive strengths comparable to that of Control B, which is similar to the trends observed with Cement A. However, leveling off in strength evolution was observed for all mixtures incorporating Cement B at 91 days, indicating higher reactivity of Cement B. Cement B had higher C_3S and C_3A contents compared to Cement A, and would therefore be expected to have a faster rate of reaction at early ages. This is confirmed by isothermal calorimetry results (Figure 3-5), which show higher heat evolution for Cement B during the first 7 days, confirming its higher reactivity.

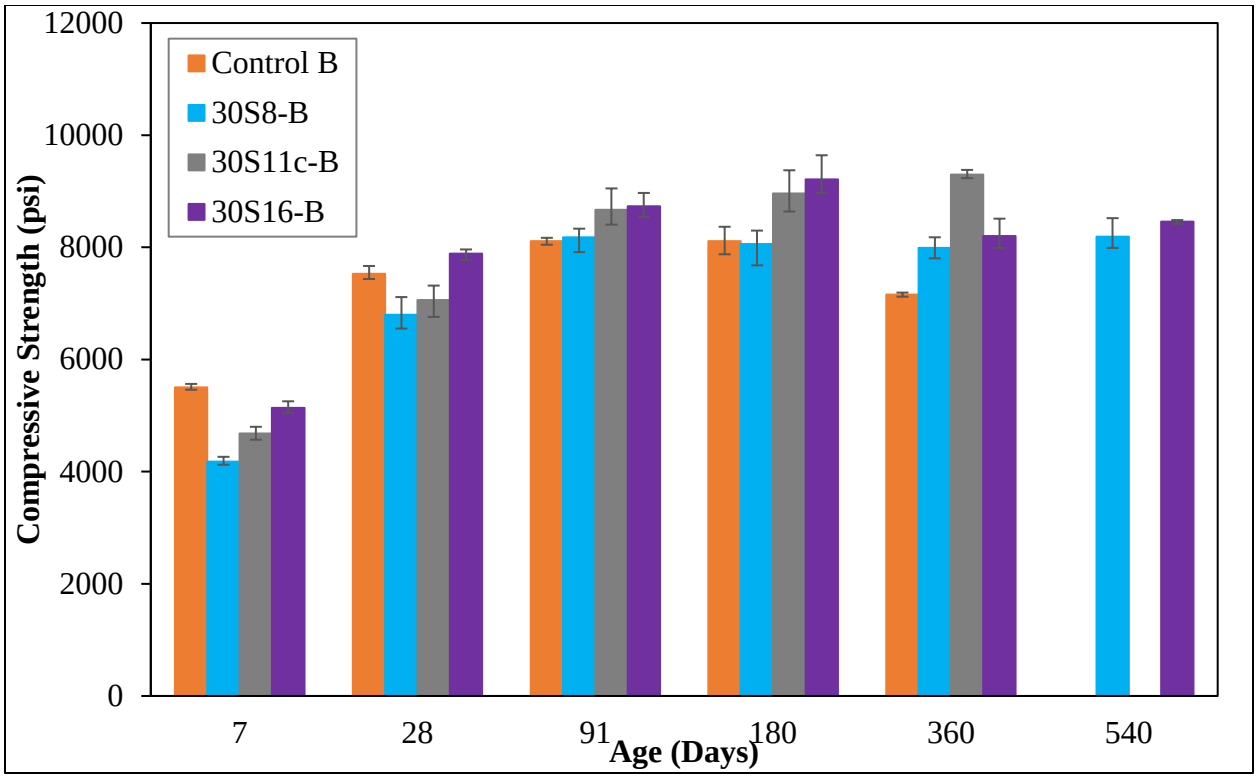

Figure 3-4: Compressive strength development of Cement B-30% slag mortars stored in saturated lime solution

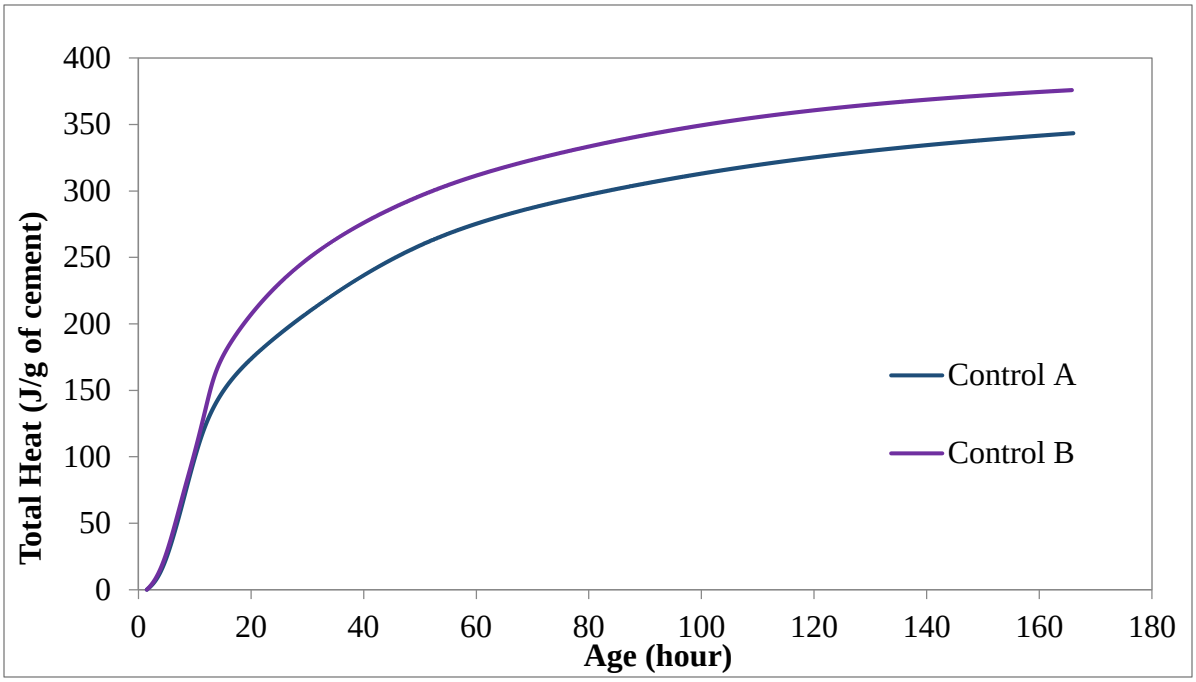

Figure 3-5: Heat evolution of Control A and Control B mortars measured by isothermal calorimetry at 23˚C

At 50% cement replacement with slag, 30S16-A again had the highest strengths of all the Cement A-slag mortars at 7 days. At 28 days, all the slag mixtures exceeded the strength of Control A. At 180 and 360 days, compressive strengths of all the slag mortars was significantly higher than that of Control A. Interestingly, the low-alumina slag (S8) had the highest strength.

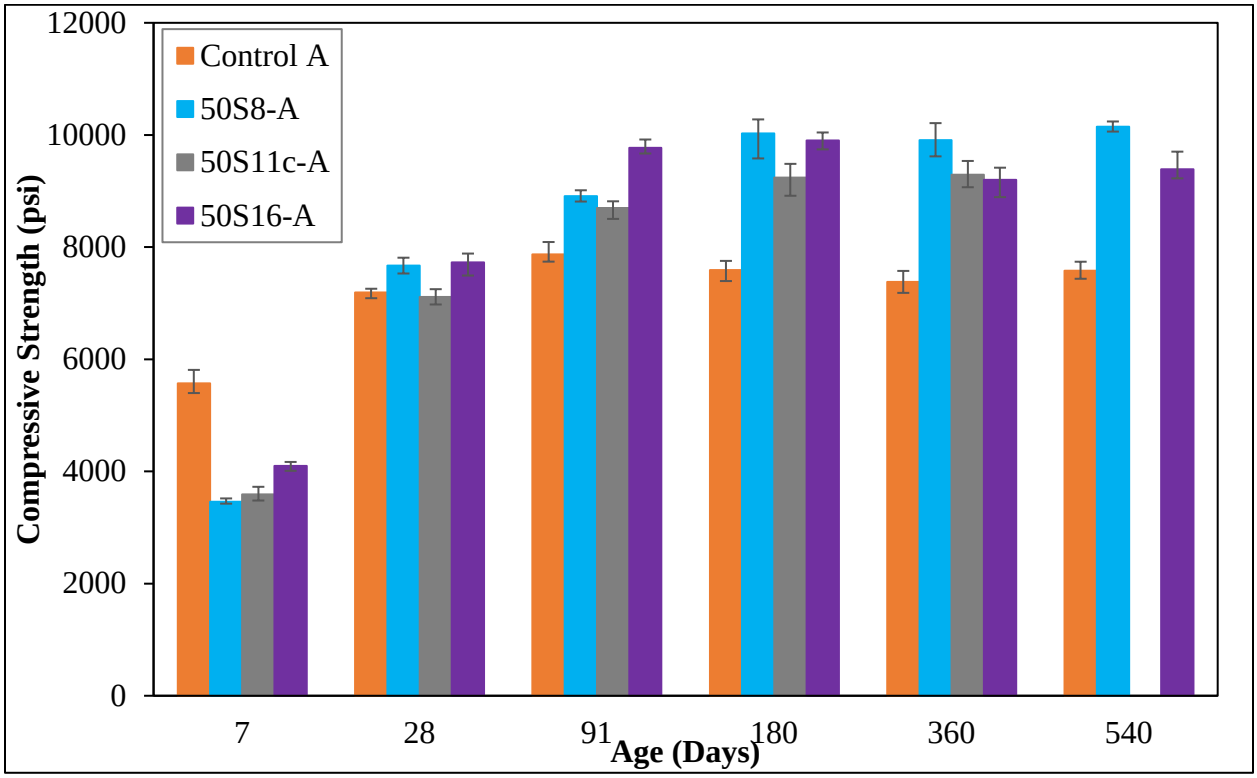

Figure 3-6: Compressive strength development of Cement A-50% slag mortars stored in saturated lime solution

For Cement B at 50% cement replacement with slag, the highest compressive strength was observed for 50S16-B starting at 28 days (Figure 3-7). After 28 days, compressive strength of the slag mortars appeared to increase with increasing Al_2O_3 content of the slag. By 360 days, the effect of the slag alumina content (8% to 16%) did not generate any differences in the observed strength trends in the slag-blended mixtures. However, at 540 days, the lower-alumina slag showed slightly higher strength.

With Cement A, a similar trend was observed at 70% cement replacement as at 30% replacement (Figure 3-8). Increasing slag alumina content increased strength. However, by 540 days, no significant strength differences were noted in slag-blended mixtures of variable alumina content.

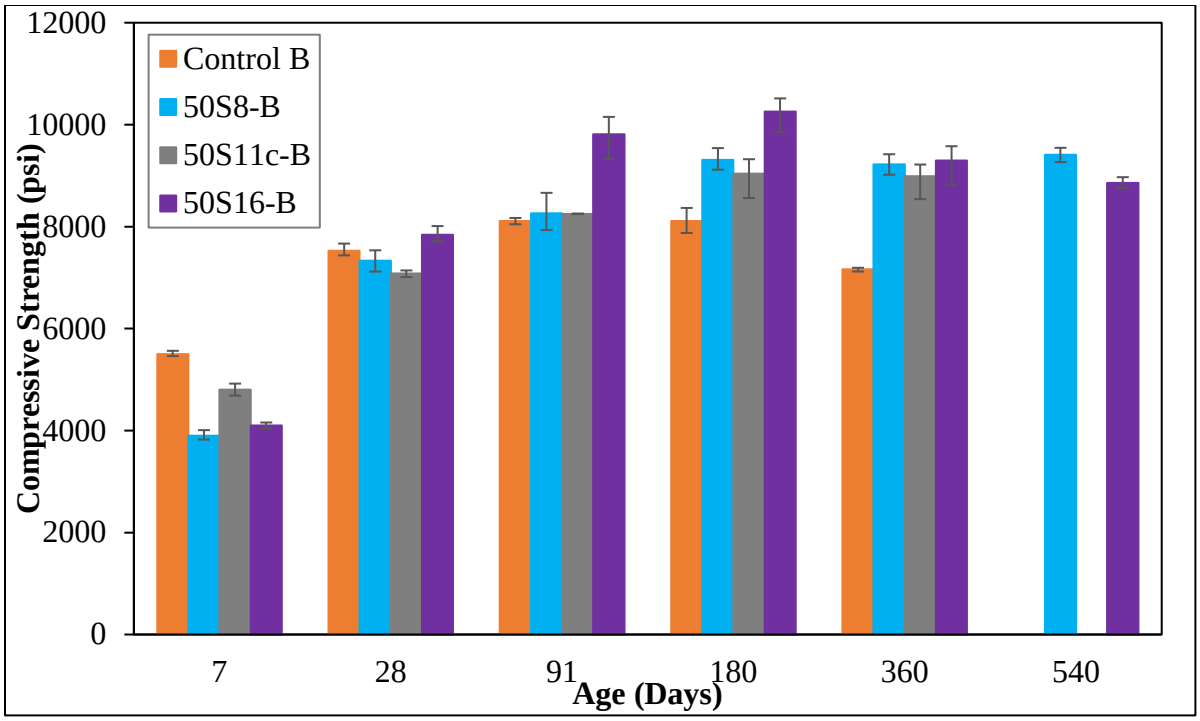

Figure 3-7: Compressive strength development of Cement B-50% slag mortars stored in saturated lime solution

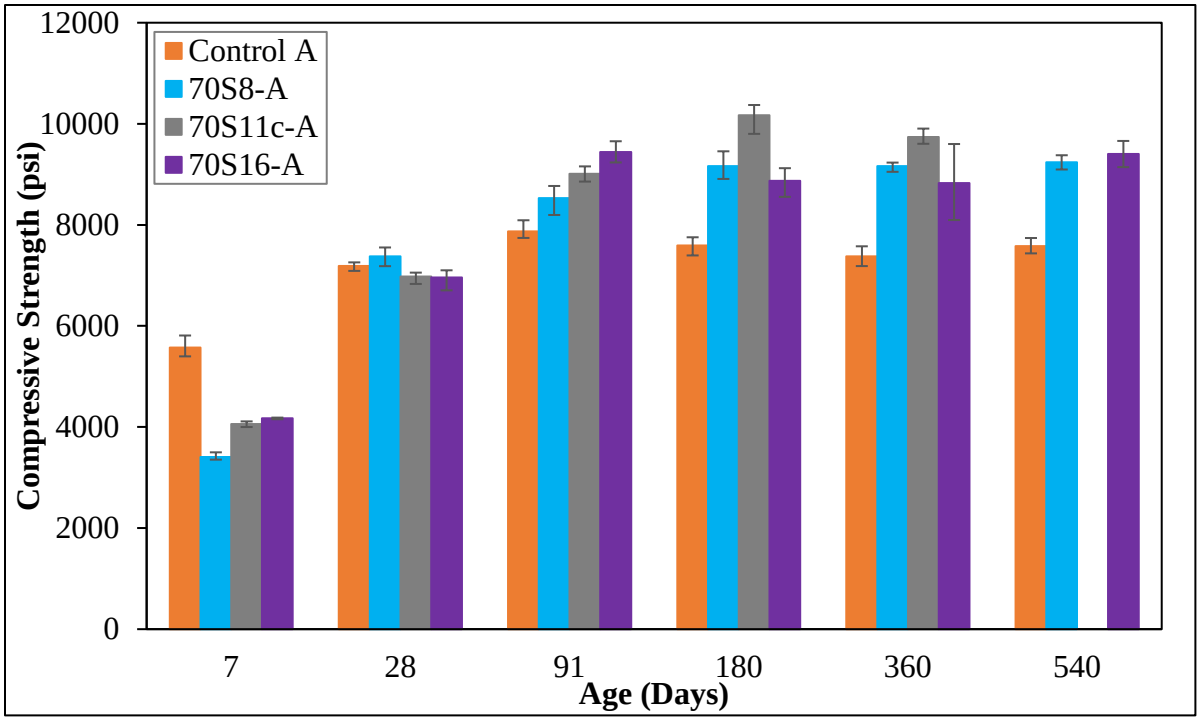

Figure 3-8: Compressive strength development of Cement A-70% slag mortars stored in saturated lime solution

Similarly, Cement B slag-blended mortars showed lower strength than the control at 7 days. By 180 days, all slag-blended mixtures showed higher strength than the control (Figure 3-9). At 540 days, the strength of all the slag-blended mixtures did not show any significant differences related to the alumina content of the slags.

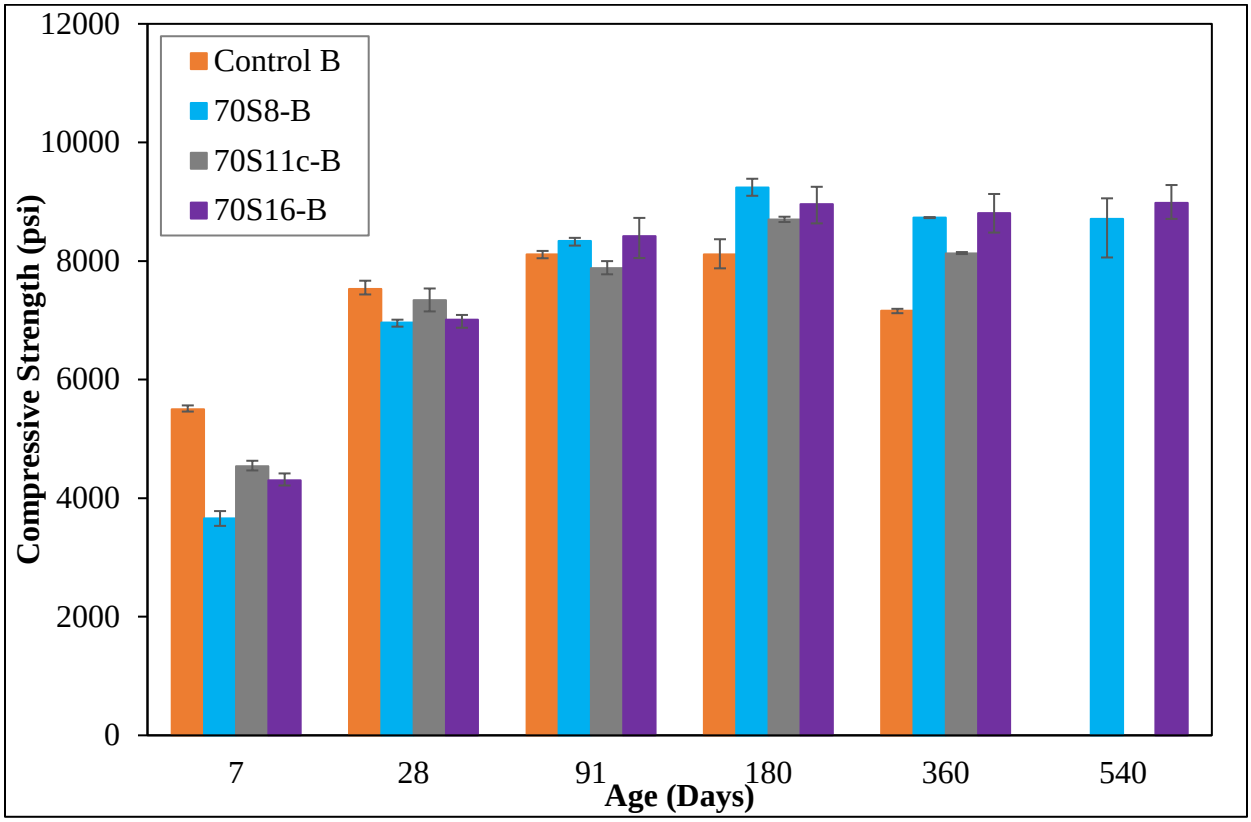

Figure 3-9: Compressive strength development of Cement B-70% slag mortars stored in saturate lime solution

Generally, the highest compressive strengths at 540 days for cement-slag mixtures in lime solution were obtained at 50% cement replacement level. A decrease in compressive strength with increasing slag content above an optimum value has been reported in the literature [23]–[26]. Oner and Akyuz [23] suggested that the optimal replacement level is approximately 55-59% of the total amount of binder material, while others proposed a 40% cement replacement level [24], [25] to maximize compressive strength. A more accurate determination of the optimal slag content may depend on the desired testing age. In this study, 50% slag content appears to be optimal for the ages reported here.

Additionally, it was observed in this study that for most slag mixtures, the 28-day compressive strengths of the 30% and 50% slag mortars were similar, while compressive strength of the 70% mortar was lower. This is not surprising as slag reacts slower than portland cement [2].

Figure 3-10 through Figure 3-15 show compressive strength evolution of cement-slag mortar mixtures exposed to 5% sodium sulfate solution. It was observed that cement replacement with 30-70% slag improved strength evolution in a sulfate environment, indicating higher sulfate resistance, during 540 days of exposure regardless of cement or slag composition, except for 30S16.

Figure 3-10 shows that the trends for the Cement A-slag mortars in sulfate solution were very similar to those observed in lime solution (Figure 3-3), except the 30S11c-AS mixture had the highest compressive strength at 360 days.

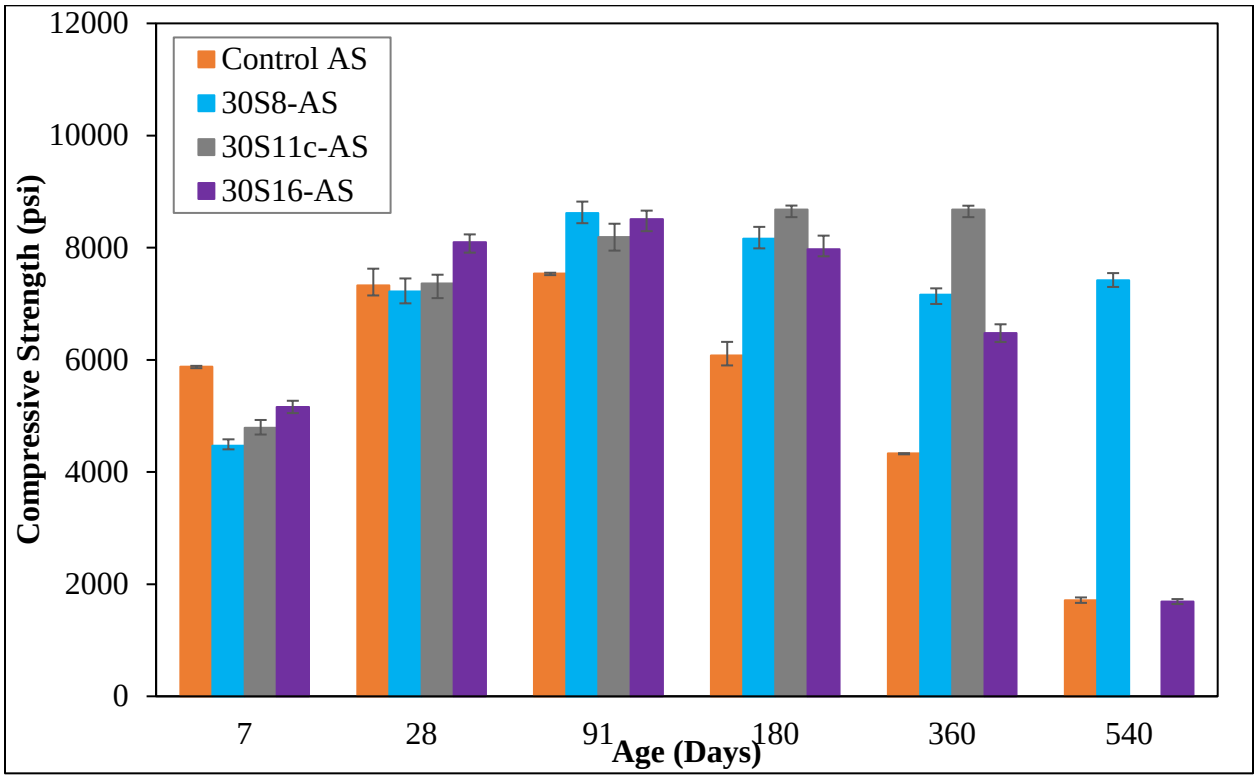

Figure 3-10: Compressive strength development of Cement A-30% slag mortars stored in 5% sodium sulfate solution

In order to quantify any potential decrease in strength due to sulfate attack, compressive strength ratios expressed in terms of their respective 28-day strength of all the mortars at 91, 180,

360 and 540 days were determined. Table 3-1 shows that out of all the slag mortars only the 30S16-A mixture experienced a drop in relative strength at 180 days. Slag S16 had the highest Al_2O_3 content of 16%, which is likely responsible for the observed decrease in strength.

Table 3-1: Compressive strengths at later ages relative to the 28-day strength (%) for Cement A-30% slag mixtures exposed to 5% sodium sulfate solution

Age (days)	**Control A**	**30S8-A**	**30S11c-A**	**30S16-A**
91	103	119	111	105
180	83	113	118	98
360	59	99	118	80
540	23	103	N/A	21

For Cement B with 30% slag (Figure 3-11) the trends in sulfate solution were also similar to those observed in lime solution (Figure 3-4), except for 30S16-BS mortar. As with Cement A, a decrease in strength was observed for 30S16-BS compared to its 28-day value (Table 3-2), except the drop in strength was higher than that of 30S16-AS and started earlier, at 91 days rather than at 180 days. Although ASTM C989 [27] does not address the effect of slags with Al_2O_3 contents in the range of 11-18%, the standard states that addition of slag with Al_2O_3 content of 18% or higher can have a negative effect on sulfate resistance when cement replacement levels are 50% or lower. Although a decrease in sulfate resistance compared to the control was not observed in this study, it appears that low additions of 16% Al_2O_3 slag only delay the drop in strength associated with sulfate attack, and that improvement in sulfate resistance decreases with an increase in C_3A content of cement and increase in the slag alumina content.

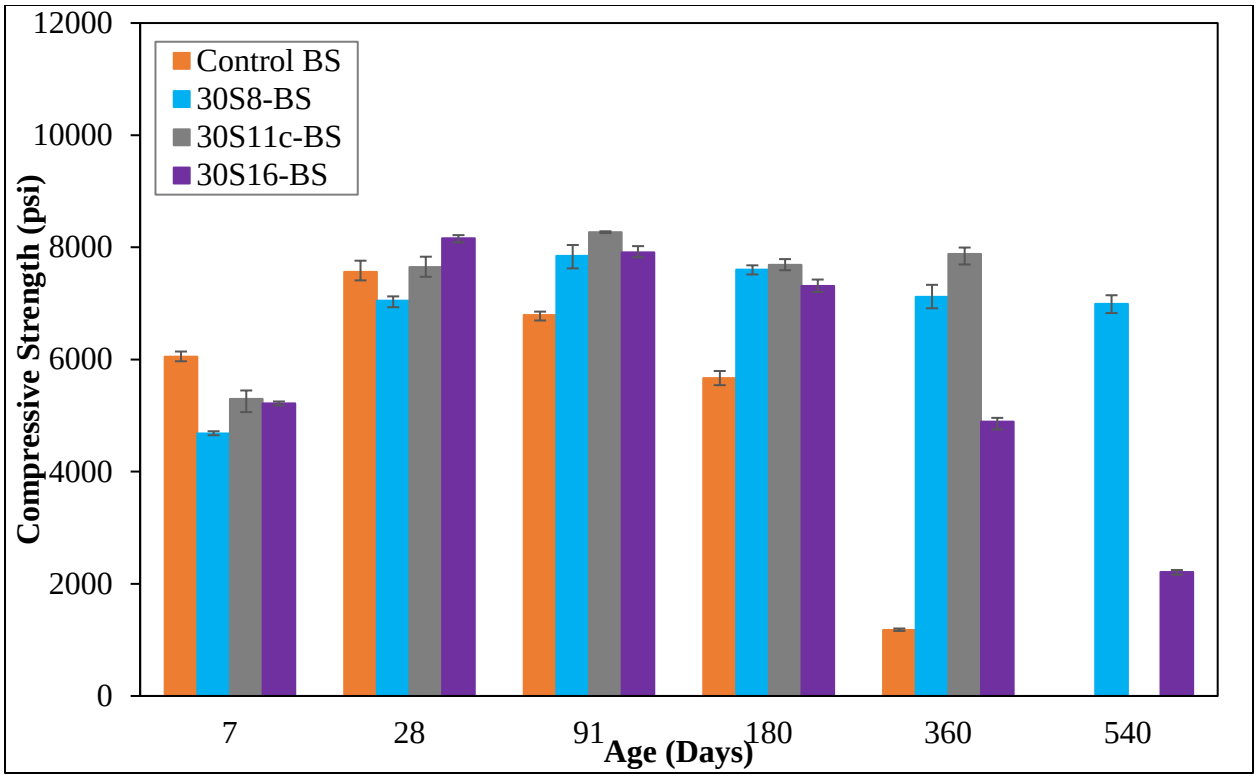

Figure 3-11: Compressive strength development of Cement B-30% slag mortars stored in 5% sodium sulfate solution

Table 3-2: Compressive strengths at later ages relative to the 28-day strength (%) for Cement B-30% slag mixtures exposed to 5% sodium sulfate solution

Age (days)	Control B	30S8-B	30S11c-B	30S16-B
91	90	111	108	97
180	75	108	101	90
360	16	101	103	60
540	disintegrated	99	N/A	27

At 50% cement replacement, and for 180 days of exposure, no strength drop was observed for any of the Cement A-slag mixtures compared to their respective 28-day strength values (Figure 3-12 and Table 3-3). The same trend was observed for Cement B-slag mortars (Figure 3-13 and Table 3-4). It appears that increasing cement replacement from 30 to 50% improves sulfate resistance of cement-slag mixtures.

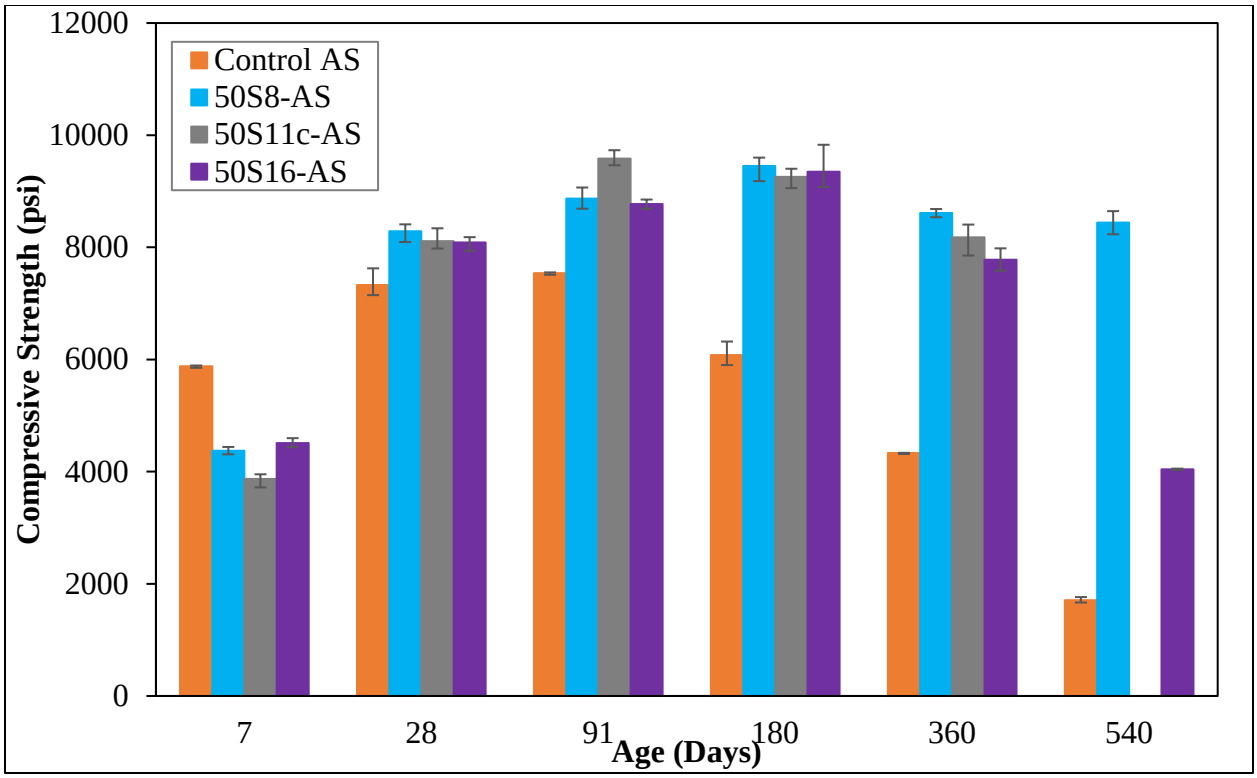

Figure 3-12: Compressive strength development of Cement A-50% slag mortars stored in 5% sodium sulfate solution

Table 3-3: Compressive strengths at later ages relative to the 28-day strength (%) for Cement A-50% slag mixtures exposed to 5% sodium sulfate solution

Age (days)	Control A	50S8-A	50S11c-A	50S16-A
91	103	107	118	108
180	83	114	114	116
360	59	104	101	96
540	23	102	N/A	50

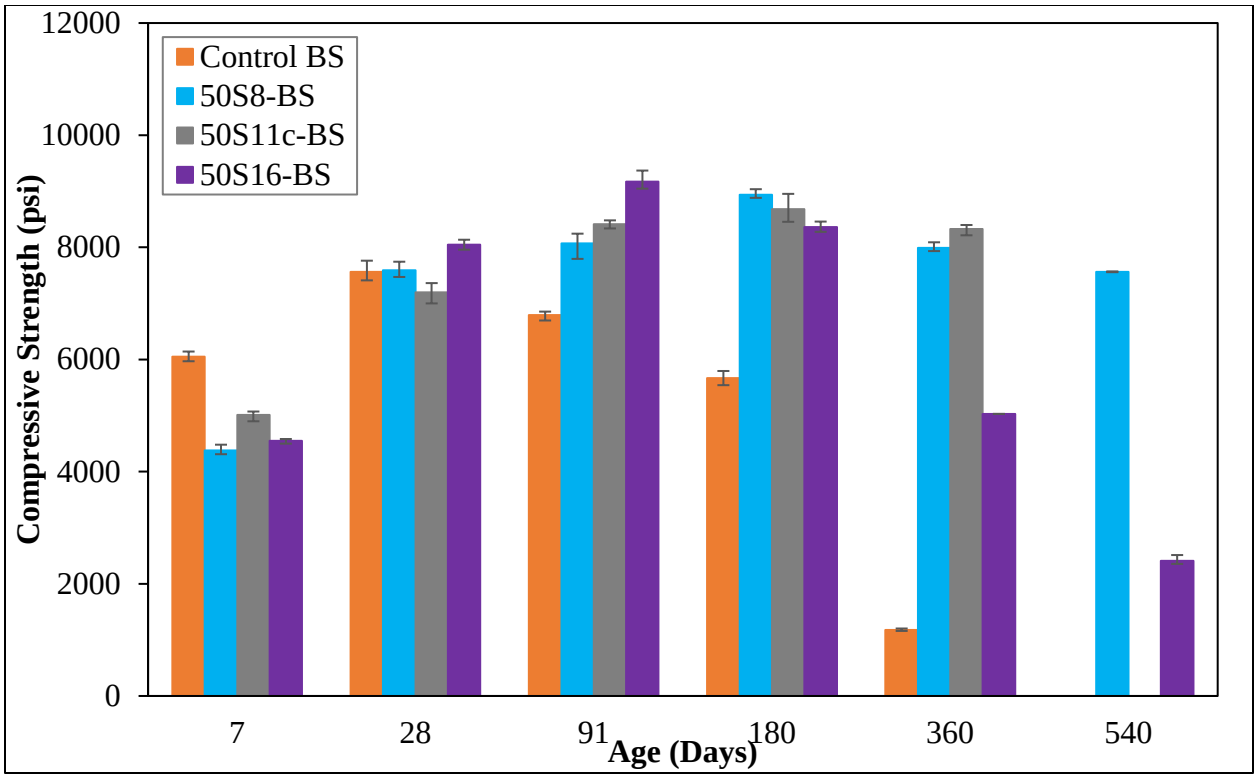

Figure 3-13: Compressive strength development of Cement B-50% slag mortars stored in 5% sodium sulfate solution

Table 3-4: Compressive strengths at later ages relative to the 28-day strength (%) for Cement B-50% slag mixtures exposed to 5% sodium sulfate solution

Age (days)	Control B	50S8-B	50S11c-B	50S16-B
91	90	106	117	114
180	75	118	121	104
360	16	105	116	62
540	disintegrated	100	N/A	30

Improvement in sulfate resistance with 70% slag addition compared to 30% slag addition was observed as well (Figure 3-14, Figure 3-15. Table 3-5, Table 3-6). At 180 days, all the Cement A-slag and Cement B-slag mixtures maintained compressive strengths above their respective 28-day strength values.

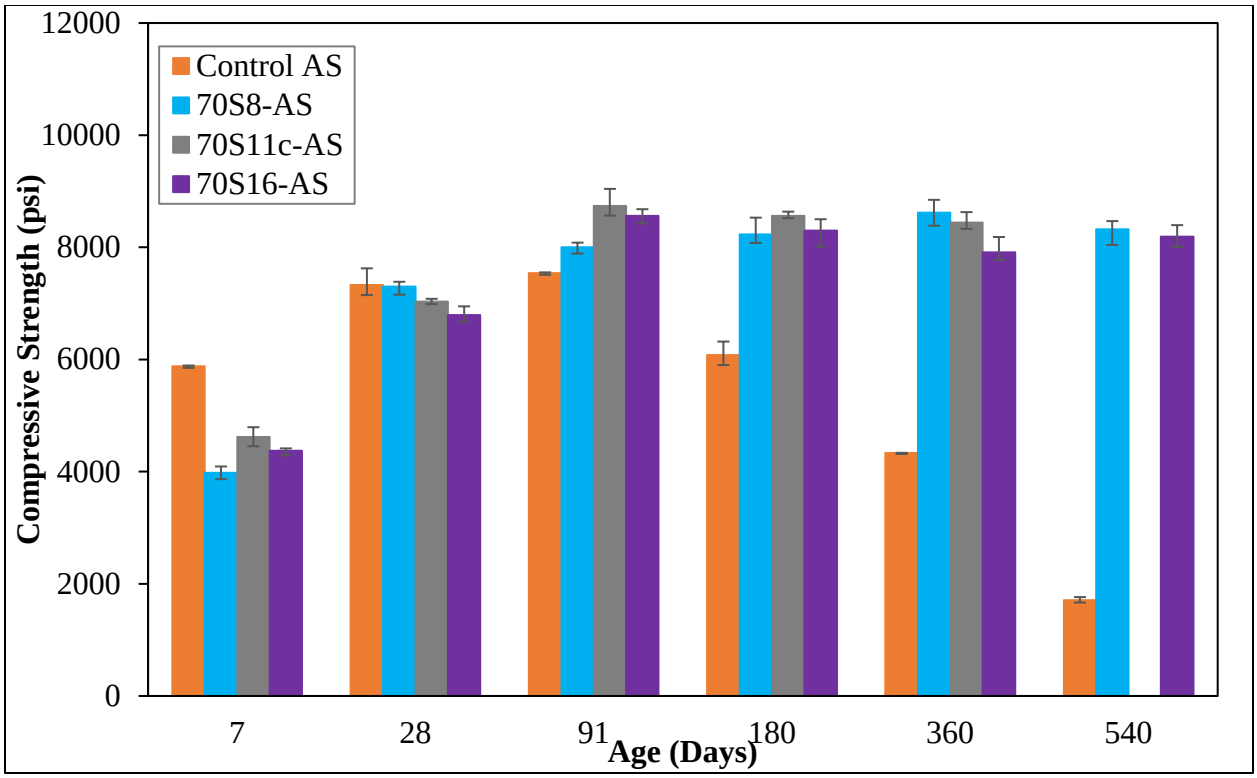

Figure 3-14: Compressive strength development of Cement A-70% slag mortars stored in 5% sodium sulfate solution

Table 3-5: Compressive strengths at later ages relative to the 28-day strength (%) for Cement A-70% slag mixtures exposed to 5% sodium sulfate solution

Age (days)	Control A	70S8-A	70S11c-A	70S16-A
91	103	110	124	126
180	83	113	122	122
360	59	118	120	116
540	23	114	N/A	121

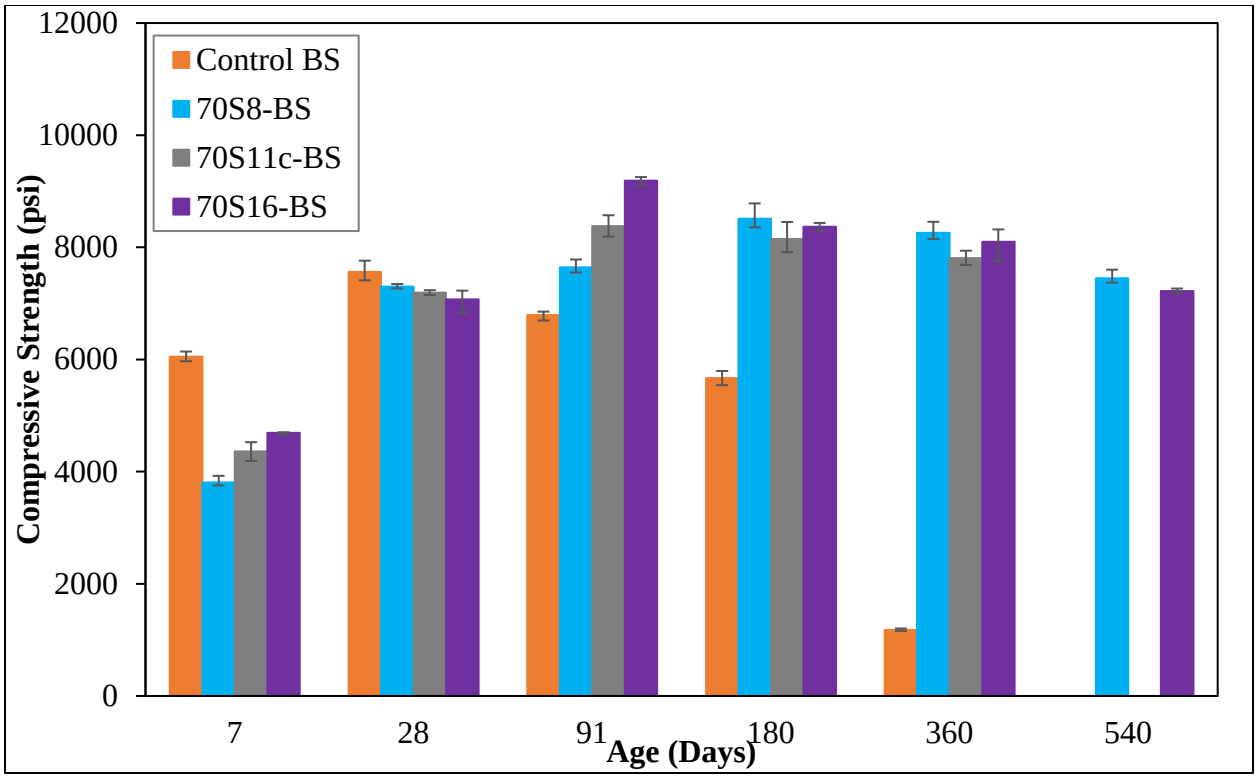

Figure 3-15: Compressive strength development of Cement B-70% slag mortars stored in 5% sodium sulfate solution

Table 3-6: Compressive strengths at later ages relative to the 28-day strength (%) for Cement B-70% slag mixtures exposed to 5% sodium sulfate solution

Age (days)	Control B	70S8-B	70S11c-B	70S16-B
91	90	105	117	130
180	75	117	113	118
360	16	113	109	115
540	disintegrated	102	N/A	102

3.4 Conclusions

Compressive strength data were collected for mortar cubes exposed to lime and sulfate solution for mixtures prepared using Type II and Type I cements. The findings indicate:

1. Compressive strengths of cements A and B in lime solution were very similar.
2. Cement replacement with slag decreased compressive strengths at 7 and, in some cases, 28 days in lime solution. However, by 91 days compressive strengths of all the slag mixes were comparable to those of their respective control and exceeded the strength of the control at 181 days.
3. In lime solution, 50% slag addition resulted in maximum compressive strength for most slag mixtures compared to 30 and 70% cement replacement.
4. Both control mixtures, exposed to sulfate solution, experienced a significant strength drop by 180 days. Control B disintegrated at an age of 540 days due to the higher tricalcium aluminate and silicate content of the cement.
5. Cement replacement with slag content of 70% improved sulfate resistance compared to the plain cement mixtures regardless of slag composition. However, mixtures with cement A sustained better performance compared to their respective 28-day strength up to an age of 540 days.
6. At lower replacement levels of 30 and 50%, the slag with lower alumina (S8) content showed better performance than slag with higher alumina (S16). A substantial drop in strength was observed for S16 at 540 days of exposure to a sulfate solution, corresponding to 30% of its respective 28-day compressive strength. This was attributed to the high Al_2O_3 content of this slag.

3.5 References

[1] P. K. Mehta and P. J. M. Monteiro, *Concrete: Microstructure, Properties and Materials*, 3rd ed. New York, NY: McGraw-Hill, 2006.

[2] S. Mindess, J. F. Young, and D. Darwin, *Concrete*, 2nd ed. Upper Saddle River, NJ: Prentice Hall, 2003.

[3] P. K. Mehta, "Mechanism of expansion associated with ettringite formation," *Cem. Concr. Res.*, vol. 3, pp. 1–6, 1973.

[4] I. Odler and J. Colán-Subauste, "Investigations on cement expansion associated with ettringite formation," *Cem. Concr. Res.*, vol. 29, no. 5, pp. 731–735, 1999.

[5] N. Shanahan and A. Zayed, "Cement composition and sulfate attack," *Cem. Concr. Res.*, vol. 37, no. 4, pp. 618–623, Apr. 2007.

[6] B. Tian and M. D. Cohen, "Expansion of Alite Paste Caused by Gypsum Formation during Sulfate Attack," *J. Mater. Civ. Eng.*, vol. 12, no. 1, pp. 24–25, 2000.

[7] B. Tian and M. D. Cohen, "Does gypsum formation during sulfate attack on concrete lead to expansion?," *Cem. Concr. Res.*, vol. 30, no. 1, pp. 117–123, Jan. 2000.

[8] N. Shanahan and A. Zayed, "Role of tricalcium silicate in sulfate resistance," *Adv. Cem. Res.*, vol. 27, no. 7, pp. 409–416, 2015.

[9] M. Whittaker, M. Zajac, M. Ben Haha, and L. Black, "The impact of alumina availability on sulfate resistance of slag composite cements," *Constr. Build. Mater.*, vol. 119, pp. 356–369, 2016.

[10] ASTM C989/ C989M-17, "Standard Specification for Slag Cement for Use in Concrete and Mortars," West Conshohocken, PA: ASTM International, 2017.

[11] ASTM C109/ C109M-16a, "Standard Test Method for Compressive Strength of Hydraulic Cement Mortars (Using 2-in. or [50-mm] Cube Specimens)," West Conshohocken, PA: ASTM International, 2016.

[12] ASTM C305-14, "Standard Practice for Mechanical Mixing of Hydraulic Cement Pastes and Mortars of Plastic Consistency," West Conshohocken, PA: ASTM International, 2014.

[13] ASTM C1012/C1012M-15, "Standard test method for length change of hydraulic-cement mortars exposed to sulfate solution," West Conshohocken, PA: ASTM International, 2015.

[14] ASTM C1702-15b, "Standard Test Method for Measurement of Heat of Hydration of

Hydraulic Cementitious Materials Using Isothermal Conduction Calorimetry," West Conshohocken, PA: ASTM International, 2015.

[15] ASTM C150/C150M-16, "Standard Specification for Portland Cement," West Conshohocken, PA: ASTM International, 2016.

[16] M. Gonzalez and E. Irassar, "Ettringite Formation in Low C3A Portland Cement Exposed to Sodium Sulfate Solution," *Cem. Concr. Res.*, vol. 27, no. 7, pp. 1061–1072, 1997.

[17] P. K. Mehta, D. Pirtz, and M. Polivka, "Properties of alite cements," *Cem. Concr. Res.*, vol. 9, no. 4, pp. 439–450, Jul. 1979.

[18] H. T. Cao, L. Bucea, A. Ray, and S. Yozghatlian, "The effect of cement composition and pH of environment on sulfate resistance of Portland cements and blended cements," *Cem. Concr. Compos.*, vol. 19, no. 2, pp. 161–171, 1997.

[19] M. Ben Haha, B. Lothenbach, G. Le Saout, and F. Winnefeld, "Influence of slag chemistry on the hydration of alkali-activated blast-furnace slag — Part II: Effect of Al_2O_3," *Cem. Concr. Res.*, vol. 42, no. 1, pp. 74–83, 2012.

[20] M. Ben Haha, B. Lothenbach, G. Le Saout, and F. Winnefeld, "Influence of slag chemistry on the hydration of alkali-activated blast-furnace slag — Part I: Effect of MgO," *Cem. Concr. Res.*, vol. 41, no. 9, pp. 955–963, 2011.

[21] D. P. Bentz, T. Barrett, I. De la Varga, and W. J. Weiss, "Relating Compressive Strength to Heat Release in Mortars," *Adv. Civ. Eng. Mater.*, vol. 1, no. 1, p. 20120002, 2012.

[22] T. Oey, J. Stoian, J. Li, C. Vong, M. Balonis, A. Kumar, W. Franke, and G. Sant, "Comparison of Ca(NO3)2 and CaCl2 Admixtures on Reaction, Setting, and Strength Evolutions in Plain and Blended Cementing Formulations," *J. Mater. Civ. Eng.*, vol. 27, no. 10, pp. 04014267-1–12, Oct. 2015.

[23] A. Oner and S. Akyuz, "An experimental study on optimum usage of GGBS for the compressive strength of concrete," *Cem. Concr. Compos.*, vol. 29, no. 6, pp. 505–514, Jul. 2007.

[24] C. Poon, S. Azhar, M. Anson, and Y. Wong, "Comparison of the strength and durability performance of normal- and high-strength pozzolanic concretes at elevated temperatures," *Cem. Concr. Res.*, vol. 31, pp. 1291–1300, 2001.

[25] H. Lee, X. Wang, L. Zhang, and K. Koh, "Analysis of the Optimum Usage of Slag for the Compressive Strength of Concrete," *Materials (Basel).*, vol. 8, pp. 1213–1229, 2015.

[26] F. Sajedi and P. Shafigh, “Optimum Level of Replacement Slag in OPC – Slag Mortars,” *J. Civ. Eng. Archit.*, vol. 4, no. 1, pp. 11–19, 2010.

[27] ASTM C989/C989M-14, “Standard Specification for Slag Cement for Use in Concrete and Mortars,” West Conshohocken, PA: ASTM International, 2014.

Chapter 4 Effects of Slag Properties on Sulfate Durability of Cementitious Mixtures

4.1 Introduction

As discussed previously, sulfate attack is a durability issue of major concern in Florida. ASTM C1012 [1] is a laboratory test that is most commonly used to assess sulfate resistance of ordinary portland cement (OPC) and cementitious materials [2] exposed to an external sulfate source. This test measures expansion of mortar bars exposed to sulfate solution. Both secondary ettringite formation (conversion of monosulfate (C_4ASH_{12}) to ettringite ($C_6AS_3H_{32}$)) and secondary gypsum formation (reaction of CH with external sulfate ions to form gypsum) are accompanied by overall expansion caused by an increase in solid volume [3]–[9]. Sulfate attack by either of these mechanisms can be identified using ASTM C1012 [1]. Although more common in the presence of magnesium sulfate rather than sodium sulfate [10], sulfate attack can also be manifested through decalcification of C-S-H [11]. This form of sulfate deterioration is not accompanied by an increase in volume, but results in microcracking and loss of strength and cohesion [2], [10].

Cement replacement with supplementary cementitious materials (SCMs) is one of the common approaches to improve concrete sulfate durability. ASTM C989 [12] states that cement replacement with low-alumina slag, defined as slag of alumina content of 11%, can improve sulfate resistance of the mixture, while cement replacement with high-alumina slag (18%) can decrease sulfate resistance at replacement levels of 50% and lower. However, the standard does not address the effect of slags with alumina contents between 11 and 18% on sulfate resistance of the blended mixtures. Since commercials slags with alumina contents of 12% and higher are commonly available in Florida, it is imperative to assess the effect of slag Al_2O_3 content in this range on sulfate durability.

4.2 Materials and Experimental Methods

Four cements (Cement A, Cement B, Cement C and Cement D) and five slags (S8, S11c, S11f, S14 and S16) were used in this part of the study. Cements A and B were ordinary portland cements (OPCs) with similar fineness and an equivalent alkali (Na_2O_{eq}) content of less than 0.6%,

and differed mainly in their C_3A and C_3S contents. Cements C and D had oxide compositions similar to Cement B except they had higher SO_3 and higher equivalent alkali contents (approximately 4% and 1%, respectively). Cement D had a higher fineness compared to Cement C. Slags were selected based on Al_2O_3 contents (8-16%), finenesses, and MgO contents. The characterization of these cements and slags is presented in Table 4-1, Table 4-2,

Table 4-3 and Table 4-4.

Table 4-1: Chemical oxide composition and physical properties of cements

Analyte	**Cement A (wt %)**	**Cement B (wt %)**	**Cement C (wt %)**	**Cement D (wt %)**
SiO_2	21.2	20.1	19	18.8
Al_2O_3	5.15	5.6	5.9	5.7
Fe_2O_3	3.61	2	2.8	2.5
CaO	63.91	64.4	60.8	61
MgO	0.7	0.9	2.5	2.7
SO_3	2.59	3.6	4	4.2
Na_2O	0.14	0.08	0.32	0.3
K_2O	0.31	0.47	1.1	1.02
L.O.I. (950°C)	1.66	1.8	2.4	2.9
Total	99.89	99.56	99.82	100
Na_2O_{eq}	0.35	0.39	1.05	0.97
Mean size (MPS) (µm)	12.26	13.81	16.50	10.32
Blaine Fineness (m^2/kg)	413	474	436	522

Table 4-2: Mineralogical composition of cements determined by Rietveld analysis

Phase	**Cement A Type II(MH) wt %)**	**Cement B Type I (wt %)**	**Cement C Type I (wt %)**	**Cement D Type III (wt %)**
C_3S	48.1	54	48.1	49.5
C_2S	23.1	17.3	15.6	13.4
C_3A	5.5	8.4	8.3	8.1
Ferrite	9.9	5.6	7.6	6.8
Gypsum	2.6	4.3	3.8	2.2
Hemihydrate	1.5	1.4	1.7	3
Anhydrite	0	0.1	0	0
Calcite	1.2	0.3	1.6	1.8
Portlandite	-	0.2	0.2	0.2
Syngenite	0.7	0.4	0.9	0.7
Quartz	0.1	0.1	0.2	0.3
Aphthitalite	-	0.2	0.5	0.4
Amorphous/ unidentified	7.2	7.8	9.1	10.5

Table 4-3: Chemical oxide composition and physical properties of slags

Analyte	**Slags**					
	S8	**S11c**	**S11f**	**S14**	**S14(S)**	**S16**
SiO_2	38.59	36.15	35.67	35.44	33.7	32.86
Al_2O_3	8.09	10.71	10.82	14.25	13.67	16.29
Fe_2O_3	0.51	0.7	0.54	0.45	0.69	0.36
CaO	38.11	37.41	41.93	41.06	41.48	37.98
MgO	10.83	11.27	7.9	5.25	5.33	8.88
Total SO_3	2.21	2.33	1.91	1.99	3.02	2.61
S as sulfide (slag)	0.89	-	0.68	0.67	0.635	0.952
SO_3 as sulfate (slag)	-0.02	-	0.22	0.31	1.43	0.23
Na_2O	0.3	0.26	0.2	0.2	0.25	0.37
K_2O	0.38	0.37	0.37	0.3	0.26	0.44
L.O.I(950˚C)	1.15	-	0.53	1.06	1.37	0.4
Total	99.89	100.09	99.85	99.84	99.77	100.41
Na_2O_{eq}	0.55	0.51	0.44	0.4	0.42	0.66
Mean particle size (MPS) (µm)	9.16	10.855	8.36	11.15	12.344	11.80
Blaine fineness (m^2/kg)	642	589	680	574	595	466

Table 4-4: Mineralogical composition of slags determined by Rietveld analysis

Phase	Slags					
	S8	**S11c**	**S11f**	**S14**	**S14(S)**	**S16**
Calcite	0.7	0.5	0.3	0.6	0.6	0.3
Melilite	0.5	0.4	0.2	0.5	0.5	0.7
Merwinite	-	0.7	0.7	-	-	-
Quartz	-	0.1	-	1.5	0.1	-
Gypsum	-	-	-	0.4	1.1	-
Amorphous/ unidentified	98.9	98.3	98.8	97	97	99.0

The effect of slag characteristics on sulfate durability were evaluated by measuring length change of mortar bars stored in 5% sodium sulfate solution in addition to mortar cube strength discussed previously in Chapter 3. Mortar bars were prepared and tested following ASTM C1012 [1], except the water-to-cementitious materials (w/cm) ratio was maintained constant at 0.485 for all the mixtures. Initial curing was conducted in an oven maintained at 35°C (+/-3ºC). Per specifications mortar cubes, of matching mixture design to the mortar bars, must reach a strength of 3000 (+/-150) psi prior to mortar bar exposure to the sulfate environment. Slag mixtures were prepared with Cements A, B, C and D. According to the Mill Certificates, Cement A is a Type II(MH) OPC while Cement B and C are Type I OPC and Cement D is a Type III OPC cement, ASTM C150 [13]. Four cement replacement levels of 0, 30, 50, and 70% were used in this study to assess the effect of slag alumina content. Additional mixtures were prepared to study the effect of slag fineness at a replacement level of 70%. For this part, two slags of different grinds S11c (Blaine fineness = 589 m^2/kg) and S11f (Blaine fineness = 680 m^2/kg) were obtained from the same commercial source. Mixtures were prepared with the 4 cements (Cement A, B, C and D). A limited expansion set prepared with a slag of alumina content of 14% was initiated to study the effect of calcium sulfate addition on the expansion trends of high-alumina slag using Cements B, C and D. Both unsulfated slag (S14) and its sulfated form (S14(S)) were obtained from the same commercial source.

For all expansion bars, length change measurements were carried out at 1, 2, 3, 4, 8, 13, and 15 weeks, and also at 4, 6, 9, and 12 months after immersion in the sulfate solution as

prescribed by ASTM C1012 [1]. The sulfate solution was changed at these intervals as well. For some mixtures, data was collected for 18 months and for those mixtures the solution was changed also at 15M. Additional length change measurements were taken when rapid expansion of the bars was observed, although the solution was not changed after these additional readings. Each time the solution was changed, the pH of the freshly prepared solution was measured using a pH meter, to ensure its value is within the specified range (pH= 6-8).

The effect of slag characteristics on microstructure was studied using x-ray diffraction (XRD) for selected mixtures prepared with slags of low, medium and high alumina content and Type II(MH) cement (Cement A). In order to characterize phase content before sulfate exposure, pastes were prepared by hand mixing for 5 minutes and cured at the same conditions as the mortar bars, at 35˚C during the first 24 hours and then at 23˚C until the age of immersion into sulfate solution. Additionally, XRD measurements were performed on the high (16%) and low (8%) alumina slag-blended mortar bars after 1 year of sulfate exposure. The phase composition was determined at the surface of the bars, which would have the highest concentration of external sulfate ions, and the core, which should only contain background levels of sulfates [14], [15]. Approximately 1 mm of the bar was removed from the surface for the XRD measurements, and the remainder was used to prepare the core sample for samples that did not show deterioration. For deteriorated samples that exhibited spalling and softening of the surface, the softened material was removed until the intact solid core remained. After crushing, mortar samples were gently ground by hand with mortar and pestle in order to minimize formation of additional x-ray amorphous content due to the grinding effects [16]–[18]. The material was then sieved through a 45-µm sieve to separate the sand. The fraction passing 45 µm was then mixed with an internal standard in order to determine the amorphous/unidentified content of each sample [19], [20]. Standard reference material (SRM) 676a obtained from the National Institute of Standards and Technology was used as an internal standard in this study. SRM 676a is a corundum (α-Al_2O_3) powder of high purity and high crystallinity (99.02% crystalline) [21], which is considered to be the best material for this application [22]. SRM 676a was mixed with the sample by hand in order to avoid increasing the amorphous content. No specific technique was used to stop the hydration, as samples were loaded into the diffractometer immediately after preparation.

XRD measurements were performed using a Phillips X'Pert PW3040 Pro diffractometer equipped with the X'Celerator Scientific detector and a CuKα x-ray source. Tension and current were set to 45 kV and 40 mA, respectively. Scans were performed in the range of 7 - 70° 2θ, with a step size of 0.0167° 2θ. Samples were then loaded into the sample holder using a back-loading technique in order to minimize preferred orientation, and placed onto a spinner stage that was rotating at 30 rpm in order to improve counting statistics [23]. Phase quantification was performed using the Rietveld refinement functionality of the PANalytical HighScore Plus 4.5 software.

In addition, thermodynamic modeling was performed on the same mixtures analyzed by X-ray diffraction using the Gibbs free energy minimization software GEMS 3 [24]–[26]. Thermodynamic data was taken from the default Nagra-PSI database [27] and CEMDATA14 [28] for cement-specific compounds. GEMS models phase assemblage at equilibrium. Therefore, 100% and 70% degrees of hydration were assumed for ordinary portland cement (OPC) and slag, respectively. This degree of slag hydration is widely used in the literature for GEMS modeling of OPC-slag blends [29], [30] and can be expected in samples at the age of 1 year [31]. Sulfate attack was modeled by varying the cementitious-materials-to-Na_2SO_4 solution ratio. This assumes that the cores of the bars are exposed to very small amounts of sulfate solution, while the surfaces are exposed to large volumes of solution. This approach has been described in several publications [32]–[35], and, as Lothenbach et al. [32] pointed out, is fast and convenient, although "the calculated data relate neither to time nor to distance and merely the sequence of changes is reproduced."

4.3 Results and Discussion

4.3.1 Length change measurements

4.3.1.1 Effect of slag alumina content

Figure 4-1 shows the expansion of the control mortar mixtures prepared with as-received cements A and B. Control B had a well-defined induction period of approximately 50 days, during which only minor changes in length were recorded. After 50 days, the rate of expansion of Control B increased dramatically, and expansion of almost 1% was recorded at 105 days. Although the

induction period for Control A was not as well-defined, it was approximately 180 days. The subsequent rate of expansion was significantly lower compared to Control B. This was expected based on the lower C_3A and C_3S content of Cement A as both are known to influence cement sulfate durability [3], [6], [36]–[38]. Control B bars broke following the 105-day measurement as indicated in Figure 4-1, where "X" indicates the last measurement, after which the set could not be measured.

Compressive strength results for the control mixes were in line with the expansion results. The drop in compressive strength for Control B cubes stored in sulfate solution was observed after 28 days, while for Control A the strength started to decrease after 91 days, Figure 3-2. Additionally, the drop in strength for Control B at 360 days compared to its 28-day strength was significantly higher than for Control A.

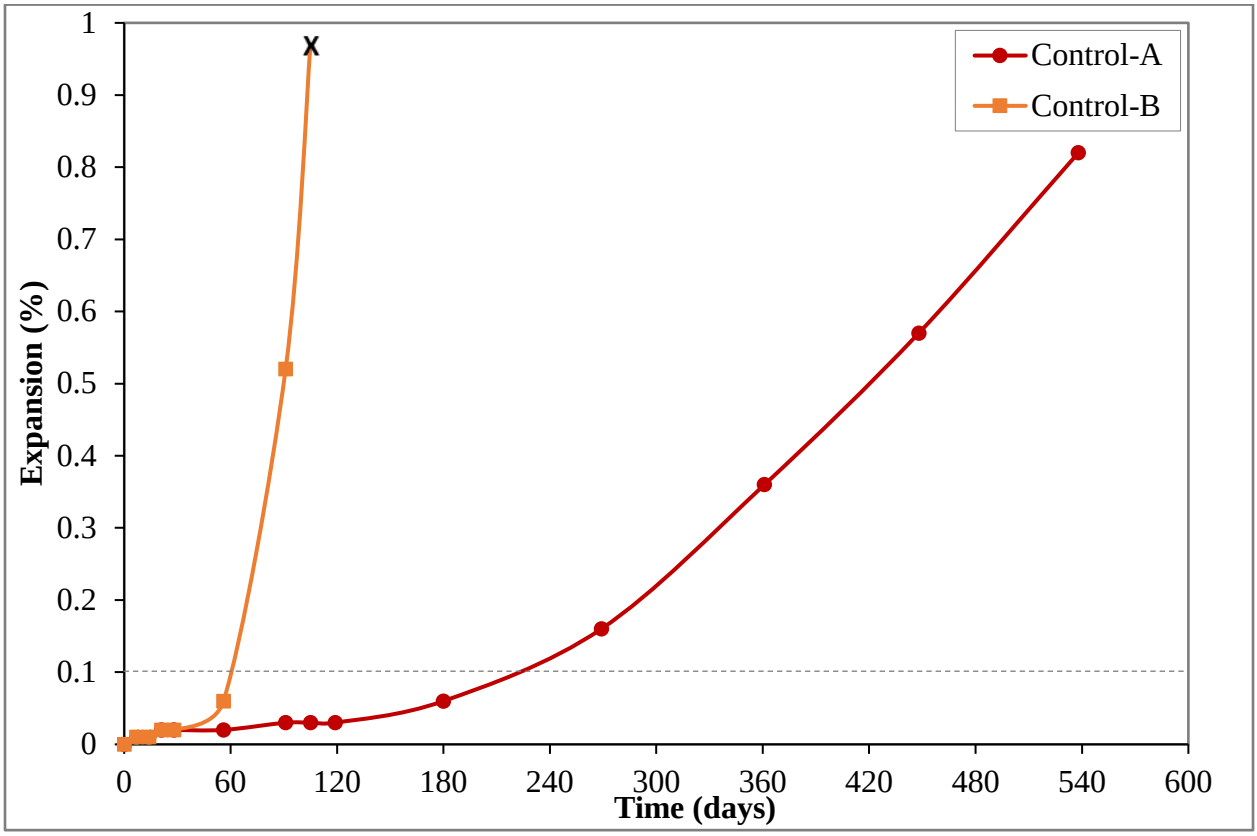

Figure 4-1: Length change of as-received cements mortar bars in 5% sodium sulfate solution

Addition of S8 slag significantly reduced expansion compared to Control A (Figure 4-2a). In fact, no significant expansion was recorded for S8-A mixtures regardless of the cement

replacement level. At 1 year, the expansion of S8-A bars was well below 0.1%, and all the mixtures appeared to still be in the induction period. Expansion of 0.10% at 1 year is specified by ACI 201.2R [39] as the limit for the S2 (severe) category of sulfate exposure. At an age of 18 months, all S8 replacement levels were below 0.1% expansion, thus passing the expansion limit specified for the S3 (very severe) exposure condition, [39].

The same trend was observed with S8 addition to Cement B (Figure 4-2b) for the first 360 days. This is consistent with the findings reported in the literature [40], [41] and ASTM C989 [12], which states that low-alumina (11%) slags improve sulfate resistance regardless of cement characteristics or cement replacement level. However, when data collection was extended to 18 months, the low replacement level mixture (30S8-B) showed an expansion of 0.34%, well above the S3 exposure limit. This is not surprising as Cement B has tricalcium aluminate content of 11% and S8 has a Blaine fineness of 640 m^2/kg; both factors can increase the sulfate demand for optimum performance in a sulfate environment. It is to be noted that compressive strength data for all replacement levels for S8 mixtures with cement A or Cement B did not show significant strength drop at 540 days of exposure to sulfate solution, though performance in blended mixtures with Cement A was better than those with Cement B.

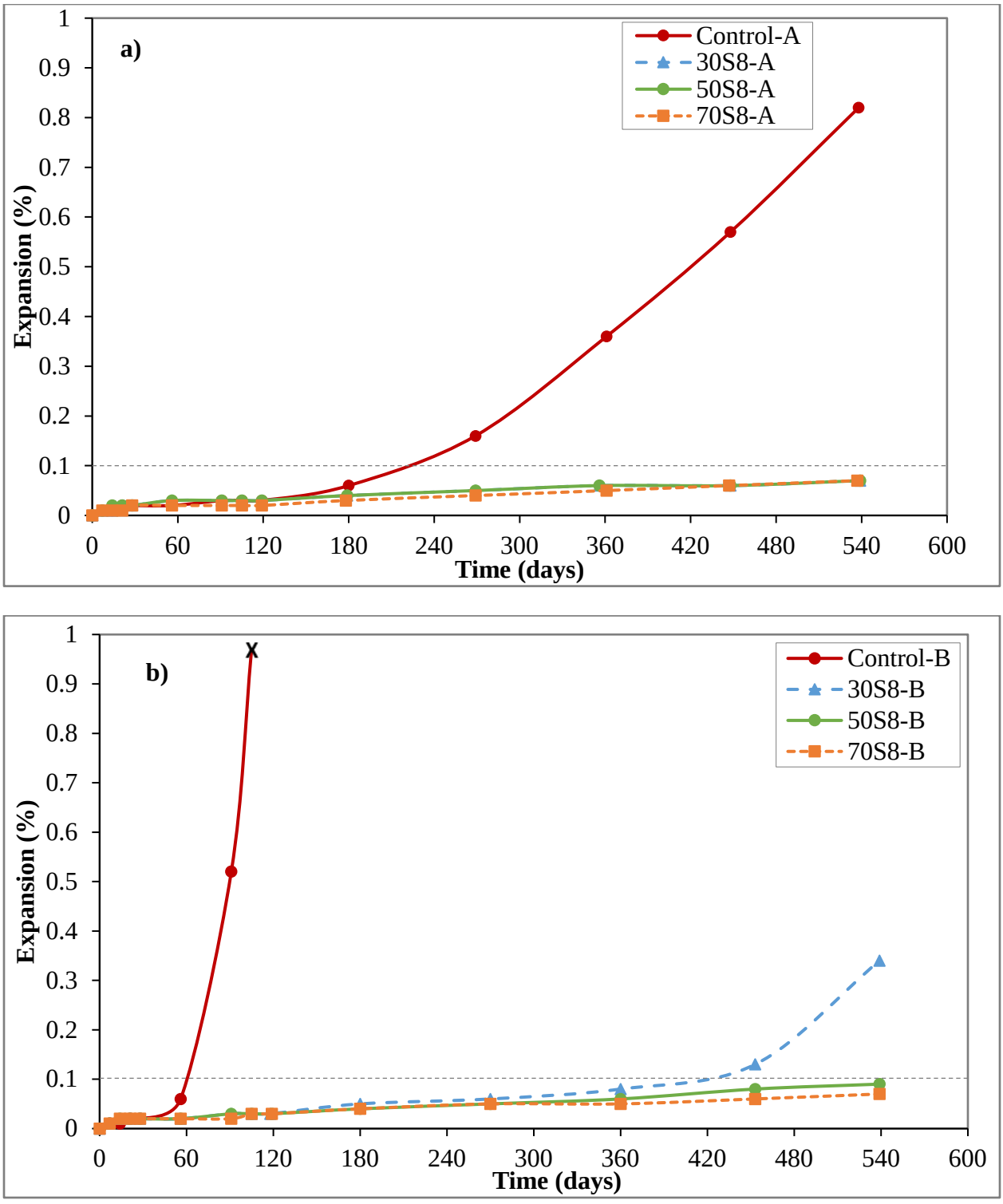

Figure 4-2: Length change of S8 mortar bars blended with a) Cement A and b) Cement B

Slag S11c behavior was very similar to that of S8 with Cement A up to 300 days, except expansions recorded for the S11c-A mixtures (approximately 0.08%) were slightly higher than those recorded for the S8-A mixtures (0.06%) (Figure 4-3a). All Figures have been noted with "**o**" to indicate the first broken bar and "X" to indicate the last measurement, after which the set could not be measured. With Cement B, addition of S11c slag also significantly reduced expansion compared to Control B, and had similar expansion compared with Cement A during the induction period (Figure 4-3b). However, the onset of rapid expansion was observed at an earlier time than with Cement A, and 30S11c-B bars had the highest expansion (0.36%) out of the S11c-B mixes at 360 days. The end of the induction period for this mixture was observed at 240 days. As with Cement A, none of the S11c-B bars exceeded the 0.10% expansion at 1 year except for the 30S11c-B mixture. The higher expansion of S11c compared to S8 is not unexpected. Hooton and Emery [41] reported an increase in expansion with increasing Al_2O_3 content from 8.4% (Blaine fineness of 396 m^2/kg) to 11.4% (Blaine fineness of 398 m^2/kg) at a constant cement replacement level of 50%. Only slight differences in expansion, similar to those observed in the current study, were reported during the induction period, after which time the expansion rate of the 11.4% Al_2O_3 slag increased dramatically. Slag replacement levels above 50% are expected to increase sulfate durability [12], [42], [43] and has been noted here for S11c with Cement A and Cement B. Both mixtures showed expansion less than 0.1% at 18 months.

As discussed earlier in Chapter 1, the literature indicates that the Blaine fineness of slag affect its rate of reaction. It is therefore expected to affect phase assemblage and subsequently sulfate durability. The 11.4% Al_2O_3 slag used in [41] had a Blaine fineness of 398 m^2/kg compared to S11c with a Blaine fineness of 589 m^2/kg. Higher slag fineness increases slag reactivity and subsequently the blended system sulfate demand. While assessing phase assemblage prior to and post sulfate exposure can be helpful in explaining expansion trends noted here, it would be interesting to assess expansion trends with different grinds of slag. This data will be presented later in this chapter.

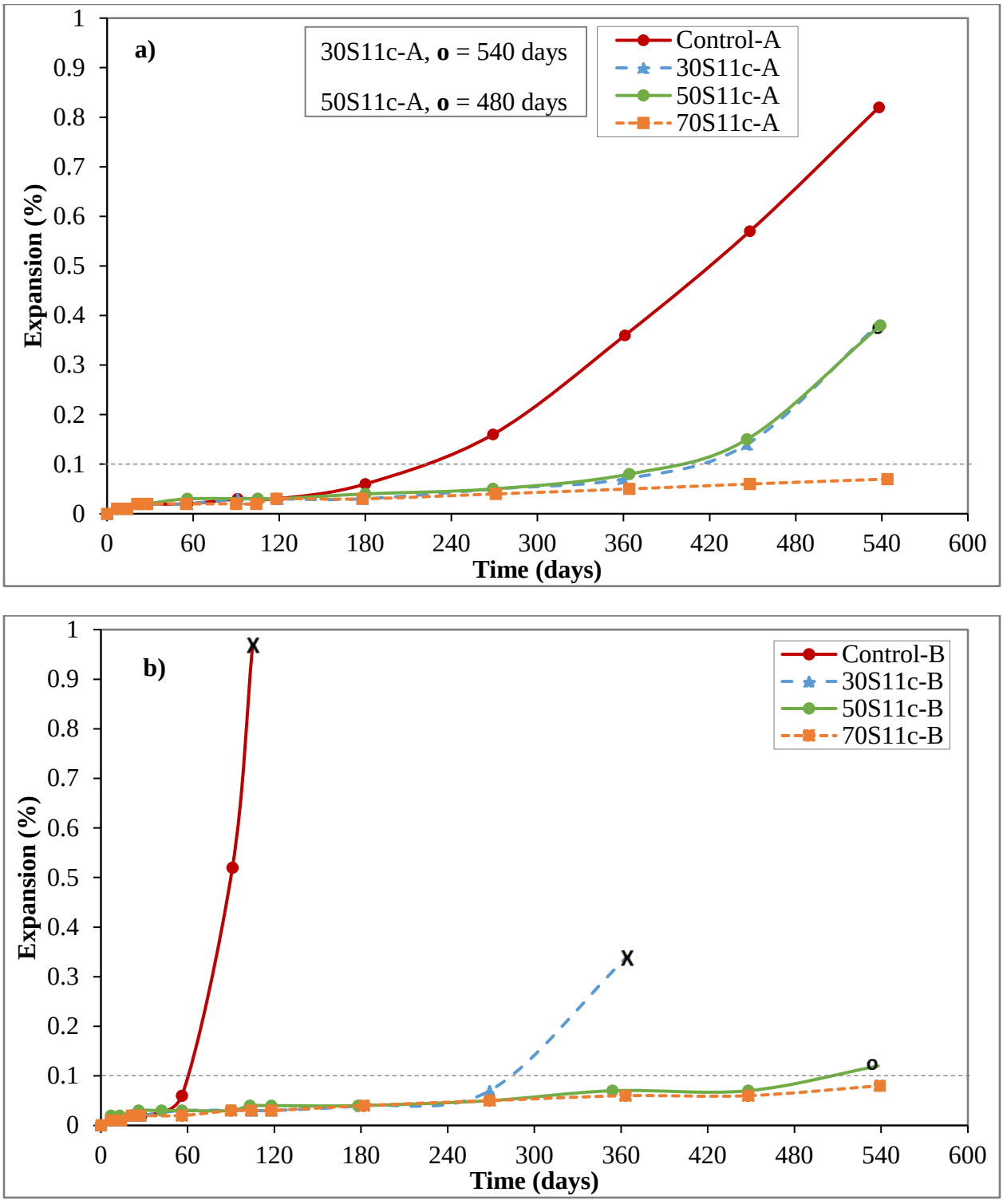

Figure 4-3: Length change of S11c mortar bars blended with a) Cement A and b) Cement B

Increasing slag Al_2O_3 content from 8-11% to 16% dramatically changed the behavior of slag mortar bars in sulfate environment (Figure 4-4). Addition of S16 slag to Cement A at 30 and 50% cement replacement decreased sulfate resistance compared to Control A mixture, as it reduced the length of the induction period by almost half, (Figure 4-4a). While no large expansions were recorded, length change measurements for these mixtures had to be terminated as all the bars broke when they reached an expansion of approximately 0.15-0.2%. As mentioned previously, based on the Bogue-calculated C_3A content (8%), Cement A is classified as moderate-sulfate resistant according to ASTM C150 [13]. Rietveld refinement showed that the actual C_3A content of this cement was even lower (5%). Based on Figure 4-4a, it appears that replacement of a moderate-C_3A cement with high-Al_2O_3 slag at 50% or lower had a negative effect on sulfate durability. 70% cement replacement, however, was sufficient to improve sulfate resistance as 70S16-A bars were still in the induction period at the age of 1 year, and their expansion was below 0.1%. However, extending measurements to an age of 540 days, all bars failed prior to an age of 540 days whether prepared with Cement A or B. This indicates that data monitoring for a period of 12 months might not be adequate to assess performance of slag-blended mixtures exposed to a sulfate environment or where high sulfate resistance is required.

Addition of S16 slag to Cement B improved the sulfate resistance compared to Control B (Figure 4-4b). The induction period was extended to 90 and 150 days with 30 and 50% cement replacement, respectively, and at 70% cement replacements no onset of expansion was observed up to the age of 300 days though all bars broke by an age of 480 days. However, the 30S16-B and 50S16-B bars broke when their expansion reached approximately 0.1%, which indicates that even though the onset of expansion was delayed compared to Control B with addition of S16 slag, 30-50% cement replacement was not adequate to provide improvement in sulfate resistance. This is in agreement with compressive strength data (Chapter 3) where S16 blended mixtures at 30% and 50% replacement showed substantial strength loss at 360 and 540 days.

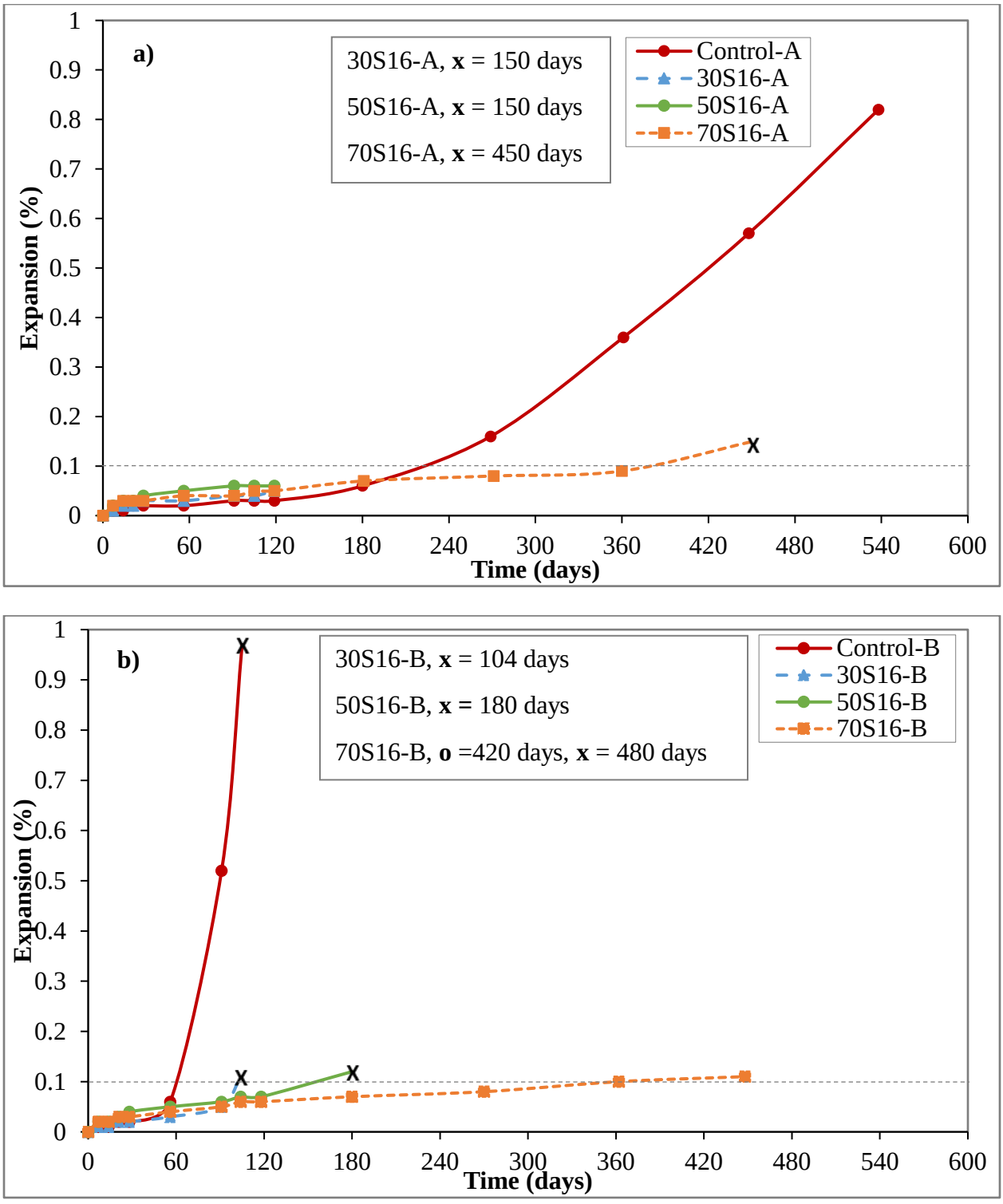

Figure 4-4: Length change of S16 mortar bars blended with a) Cement A and b) Cement B

4.3.1.2 Effect of slag fineness

In order to study the effect of slag fineness on performance and durability of slag-blended cementitious systems, a finer grind or a Grade 120 was requested from the commercial S11c source. The fine grind of S11c, S11f, had a Blaine fineness of 680 m^2/kg compared to S11c, which had a Blaine fineness of 589 m^2/kg. The results are presented in Figure 4-5 for S11 blends with Cement A (Type II(MH), Na_2O_{eq} = 0.35), Cement B (Type I, Na_2O_{eq} = 0.39), Cement C (Type I, Na_2O_{eq} = 1.05) and Cement D (Type III, Na_2O_{eq} = 0.97) at 70% replacement. The highest replacement level was selected here as it showed the lowest expansion among all replacement levels of 30, 50 and 70% studied with S11c. Though 70S11c samples showed performance similar to S8 in that it passed the criteria for the most aggressive exposure to sulfates (Class S3, ACI 201.2R-16 Table 6.1.4.1b), 70S11f samples (Slag S11f was Grade 120 and had a significantly higher Blaine fineness than S11c) did not perform well in three out of the four cements blends used here. The mixtures for Cement D, with the coarse and the fine grind of S11, are not yet available for data collection at an exposure time of 18 months. The rate of reaction of cementitious materials is known to affect phase assemblage [44]. Higher slag fineness indicates more surface area available to participate in the hydration reactions and can affect the sulfate balance in the pore solution, alumina availability, and therefore affect the calcium aluminate hydration products. This can result in a higher sulfate demand for durable performance. Locher [45] indicates that increasing slag fineness from 300 m^2/kg to 500 m^2/kg decreased sulfate resistance, and a slag replacement higher than 65% is needed to improve sulfate resistance of the higher fineness slag. Though the low- and high-fineness slags used in Locher's study had lower fineness than the coarsest slag used here, slag 70S11c of Blaine fineness of 589 m^2/kg did improve sulfate resistance with Type I, Type II(MH) and Type III cements and met "S3" exposure classification. However, slag 70S11f (680 m^2/kg), though improving performance compared to its respective controls with Type I and Type II(MH) cements, cannot be used for "S3" exposure classification, even at such a high replacement level.

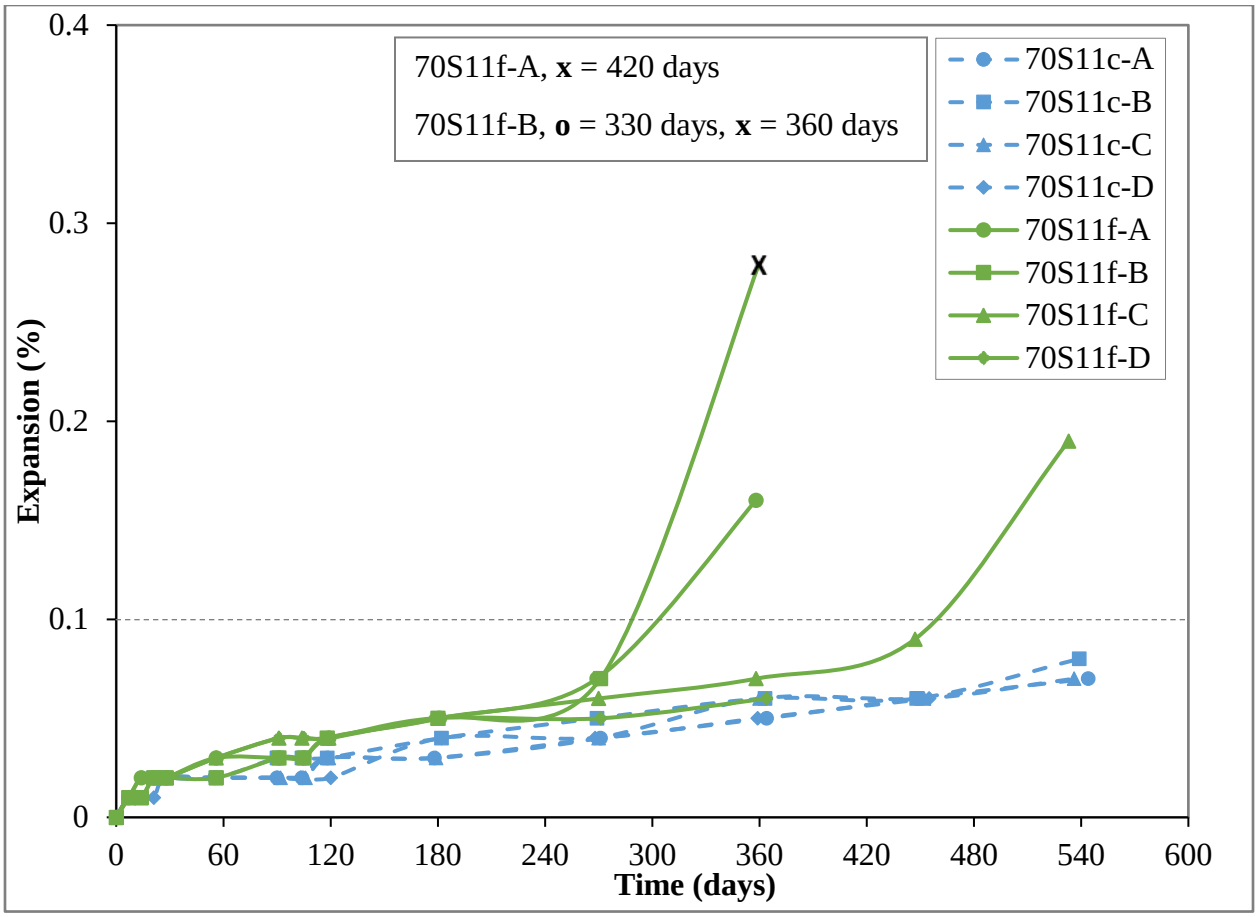

Figure 4-5: Effect of slag fineness on expansion behavior (Blaine fineness of S11c is 589 m^2/kg and Blaine fineness of S11f is 680 m^2/kg)

4.3.1.3 Effect of sulfate optimization

Calcium sulfate and limestone are added in order to improve performance of high-alumina slags in regions where there is shortage of low-alumina slag [46]. Addition of sulfates stabilizes ettringite in the high-alumina slag while addition of limestone results in the formation of hemi- or monocarboaluminates. Though hemi-and monocarboaluminates will eventually convert to ettringite, the phenomena of external sulfate attack will be substantially delayed. A commercial slag with alumina content of 14% was collected without calcium sulfate addition, S14, and with about 1.4% calcium sulfate addition, S14(S). The elemental oxide composition and Blaine fineness are reported in

Table 4-3. Expansion data were collected for three cements at 3 replacement levels and are depicted in Figure 4-6 through Figure 4-8. At 30% replacement, Cement B blended with slag S14(S) passed the 180 days criteria (ASTM C989-18), for moderate sulfate resistance (expansion $\leq$ 0.1% at 6 months), but all specimens broke beyond the 6 month reading, while S14 broke prior to the 6 month reading. This is similar to the behavior noted at the 50% replacement level where all specimens broke in the time interval between 4 months and 6 months for the unsulfated slag, while the sulfated slag broke between 6 months and 9 months. Expansion of S14(S) at 6 months was 0.07%. At 12 months and a replacement level of 70 % , mortar bars showed expansion of 0.08% and 0.06% for S14 and S14(S), respectively. The S14 expansion at 18 months exceeded the ACI criteria of 0.1% for very severe sulfate exposure (S3) [2] by 0.01%. Data is not yet available for S14(S) at 18 months to verify meeting the 0.1% criteria for Class S3 expsoure. It appears that at lower replacement levels of slags, the chemical characteristics of the parent cement are of significance to the performance of high-alumina slag-blended systems. Cements B had a sulfate content of 3.6% and SO_3/Al_2O_3 ratio of 0.64 while for Cement C the sulfate content was 4.0% and a SO_3/Al_2O_3 ratio of 0.68 and Cement D has an SO_3 content of 4.2% and SO_3/Al_2O_3 ratio of 0.74. Using cements of the same tricalcium aluminate content of 11% but higher sulfate content lowered the expansion at all replacement levels for the sulfated S14(S) as well as the unsulfated S14 slag-blended systems. This can be seen when comparing Cement B blends versus Cement C or Cement D blends. For S14 at 30% replacement of Cement B, the specimens had expansion of 0.35% at 4 months and broke at 5 months while for Cement C blends, expansion for the same replacement level was at 0.19% at 6 months and the specimens broke at a later age of 7 months. Cement D had an expansion of 0.56% at 12 months when it broke. At 50% replacement, it appears that for high-alumina slags, sulfate durability is affected by the cement chemistry as well as the slag sulfate content. The SO_3/Al_2O_3 ratio of the slag as well as the portland cement affects sulfate durability of the slag-blended system. Though the blended systems performed better than their respective control at higher replacement level, the performance of high-alumina slag-blended systems was not as good as the low-alumina slag even when sulfated, Figure 4-9 through Figure 4-11.

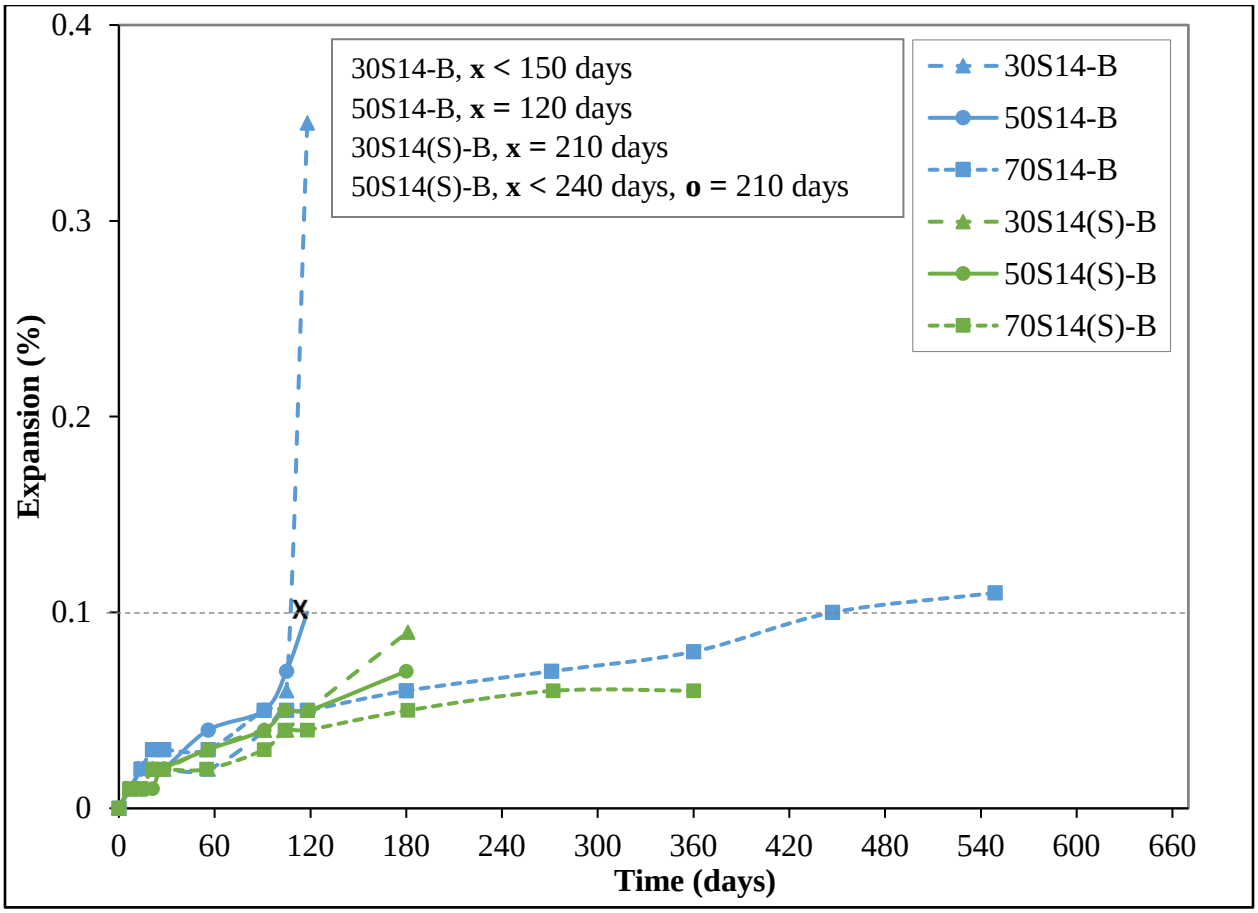

Figure 4-6: Length change of mortar bars for unsulfated slag (S14) and sulfated slag S14(S) blended with Cement B

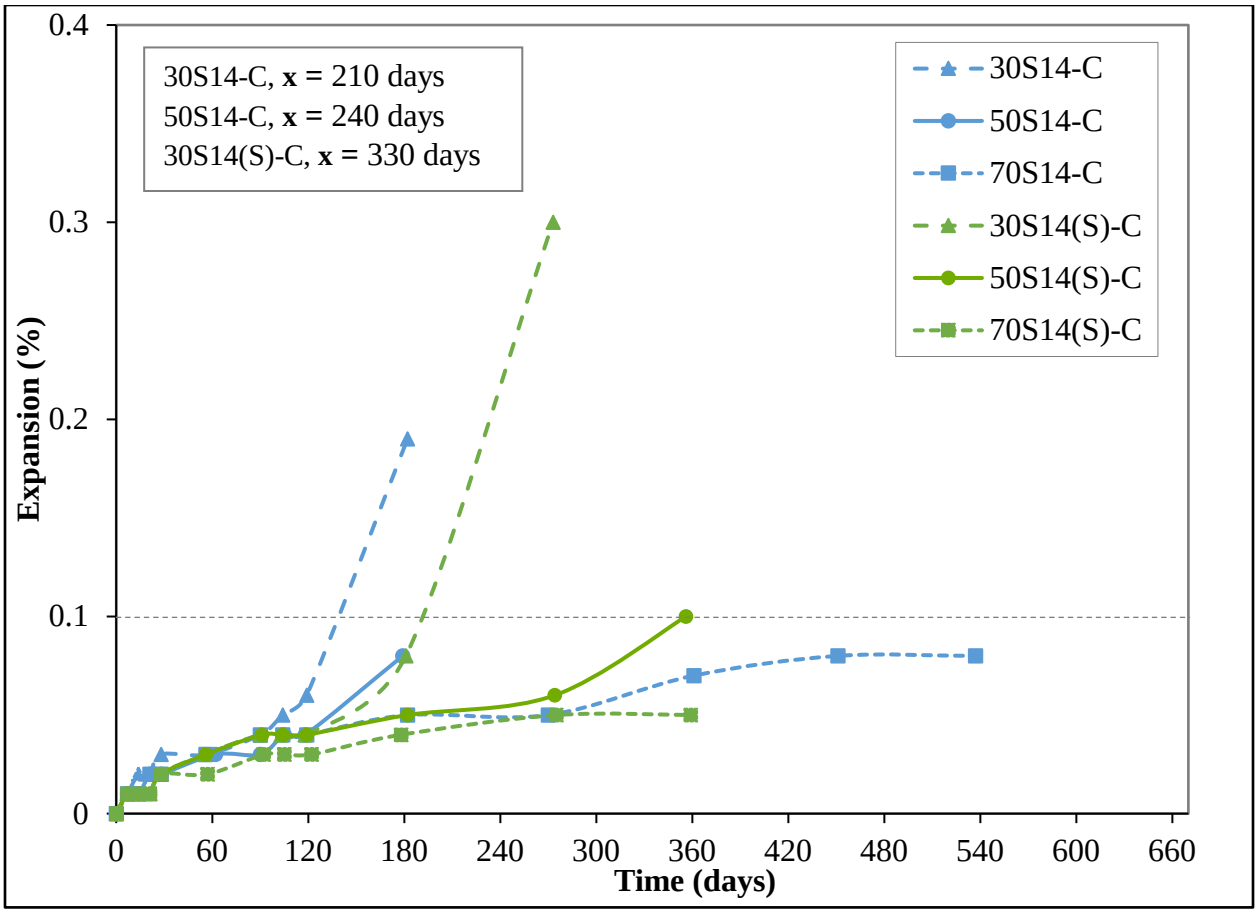

Figure 4-7: Length change of mortar bars for unsulfated slag (S14) and sulfated slag S14(S) blended with Cement C

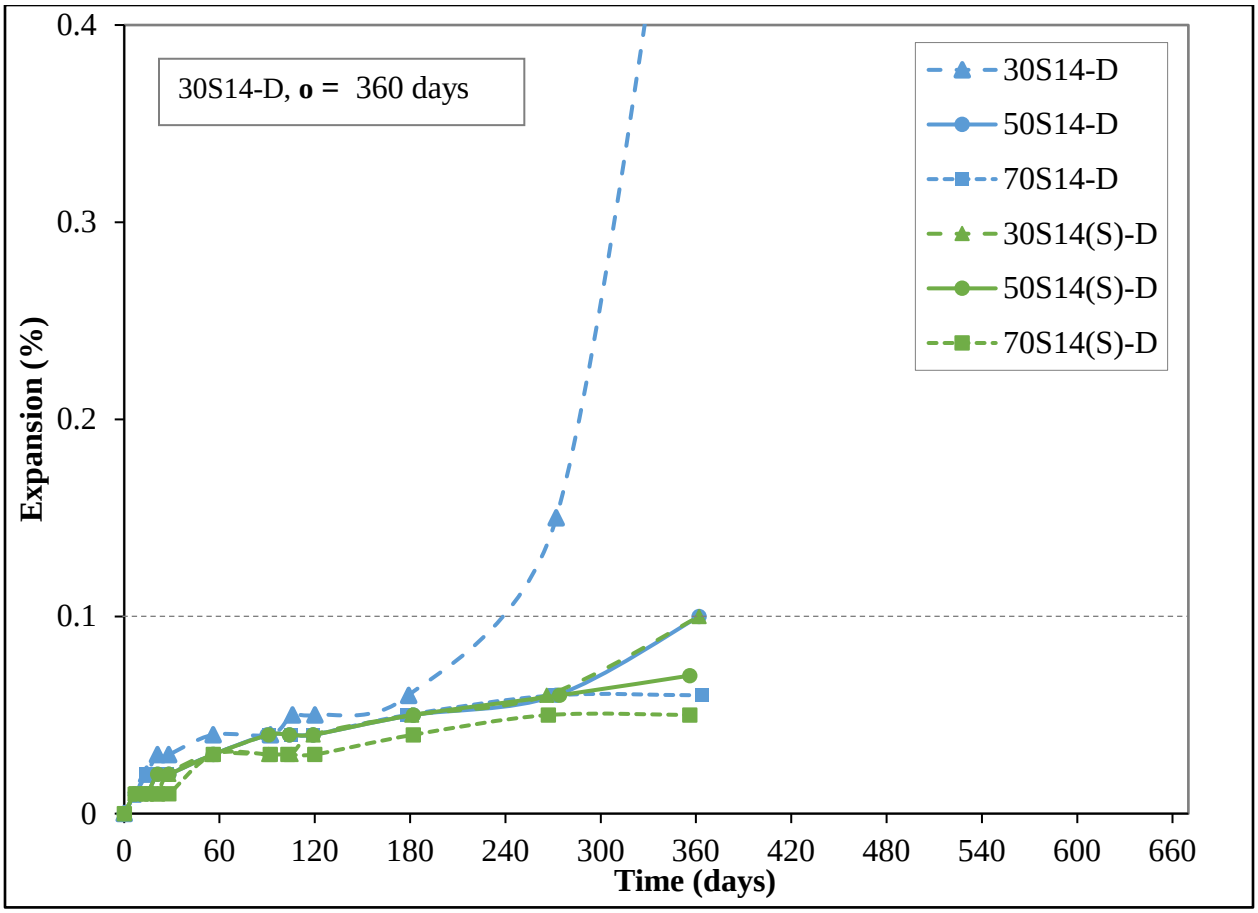

Figure 4-8: Length change of mortar bars for unsulfated slag (S14) and sulfated slag S14(S) blended with Cement D

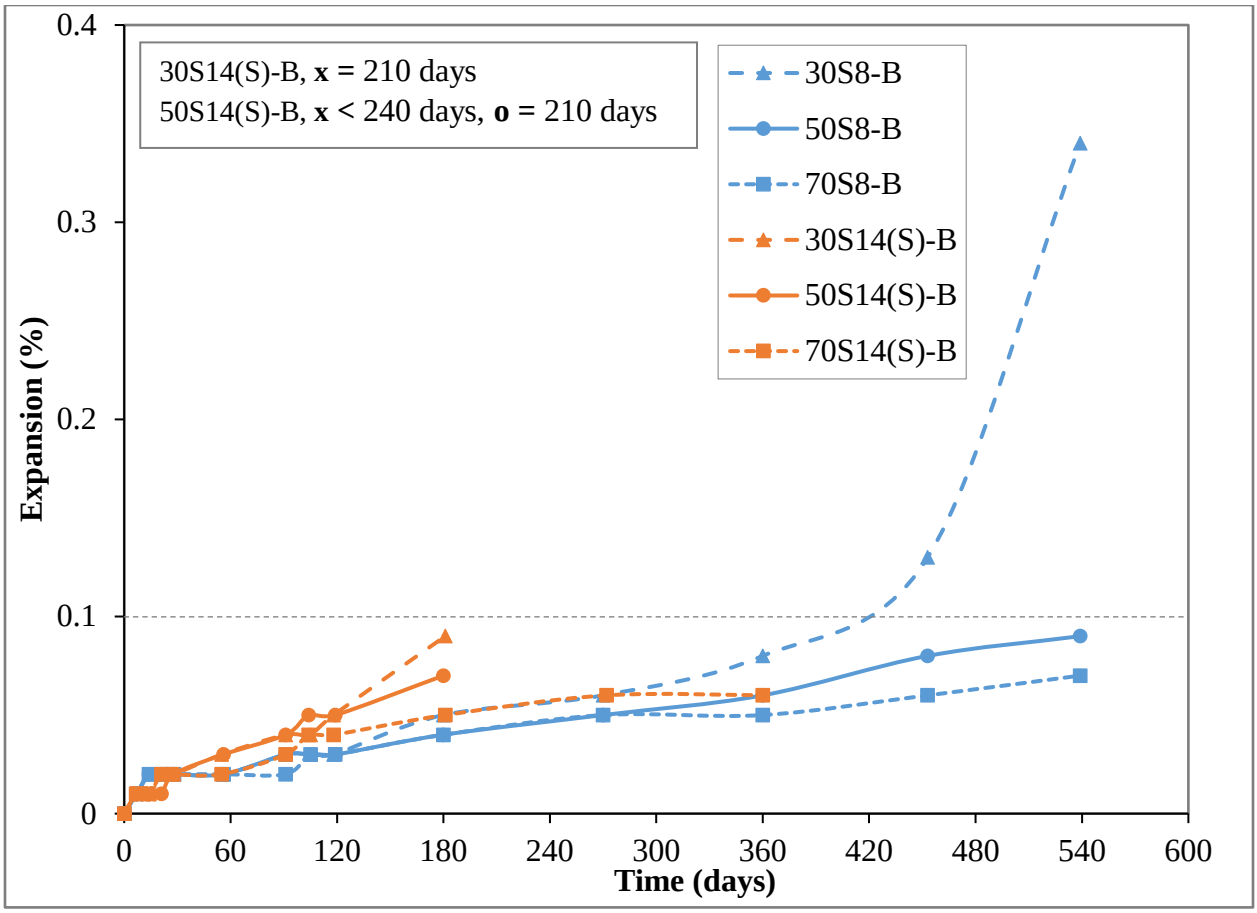

Figure 4-9: Comparison of expansion behavior of low-alumina slag S8 and sulfated high-alumina slag S14(S) blended with Cement B

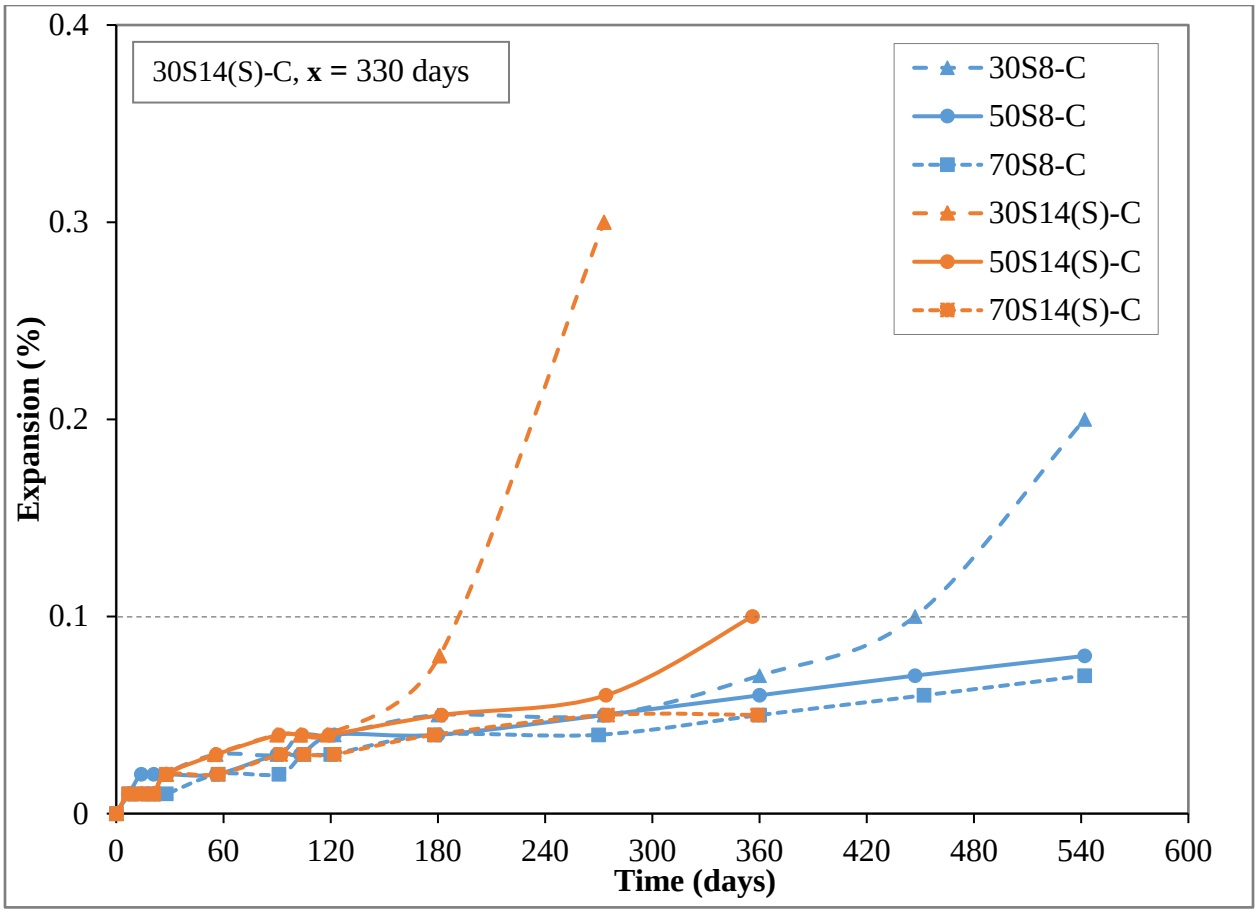

Figure 4-10: Comparison of expansion behavior of low-alumina slag S8 and sulfated high-alumina slag S14(S) blended with Cement C

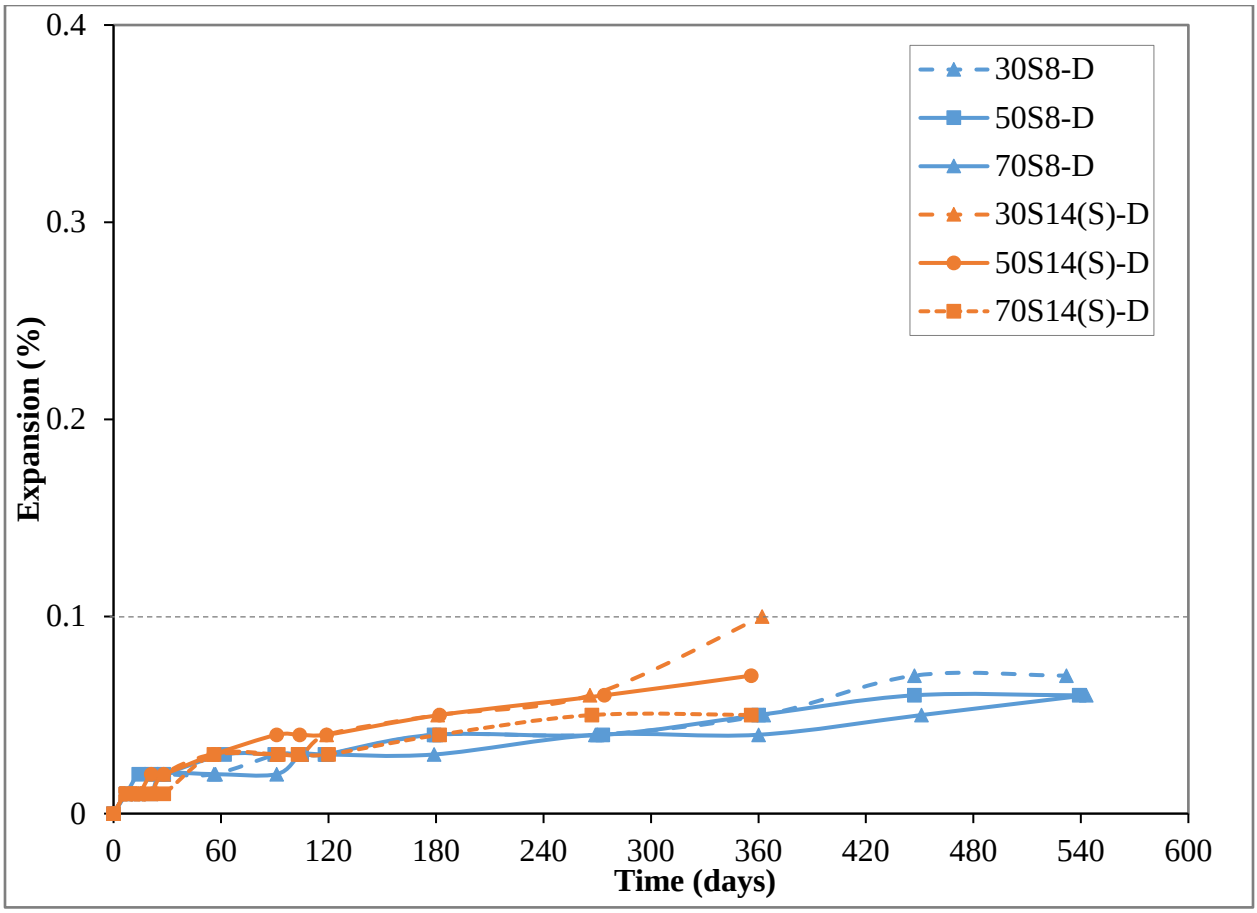

Figure 4-11: Comparison of expansion behavior of low-alumina slag S8 and sulfated high-alumina slag S14(S) blended with Cement D

4.3.2 Visual observation at 1 year

The visual progress of deterioration for slag mortars differed from OPC mortars. Figure 4-12a shows the appearance of Control B bars at 91 days, at the first signs of warping, which corresponded to an expansion of approximately 0.52%. Some deterioration and spalling were observed at the corners, as well as overall warping of the bars. Increased warping and warping-induced cracking that initiated at the bottom of the bars were observed at 105 days (Figure 4-12b), which corresponded to an expansion of 0.97%. By 120 days, most of the bars were broken and could not be measured (Figure 4-12c). For Control A, only minor spalling at the edges and corners was observed at 1 year (Figure 4-13).

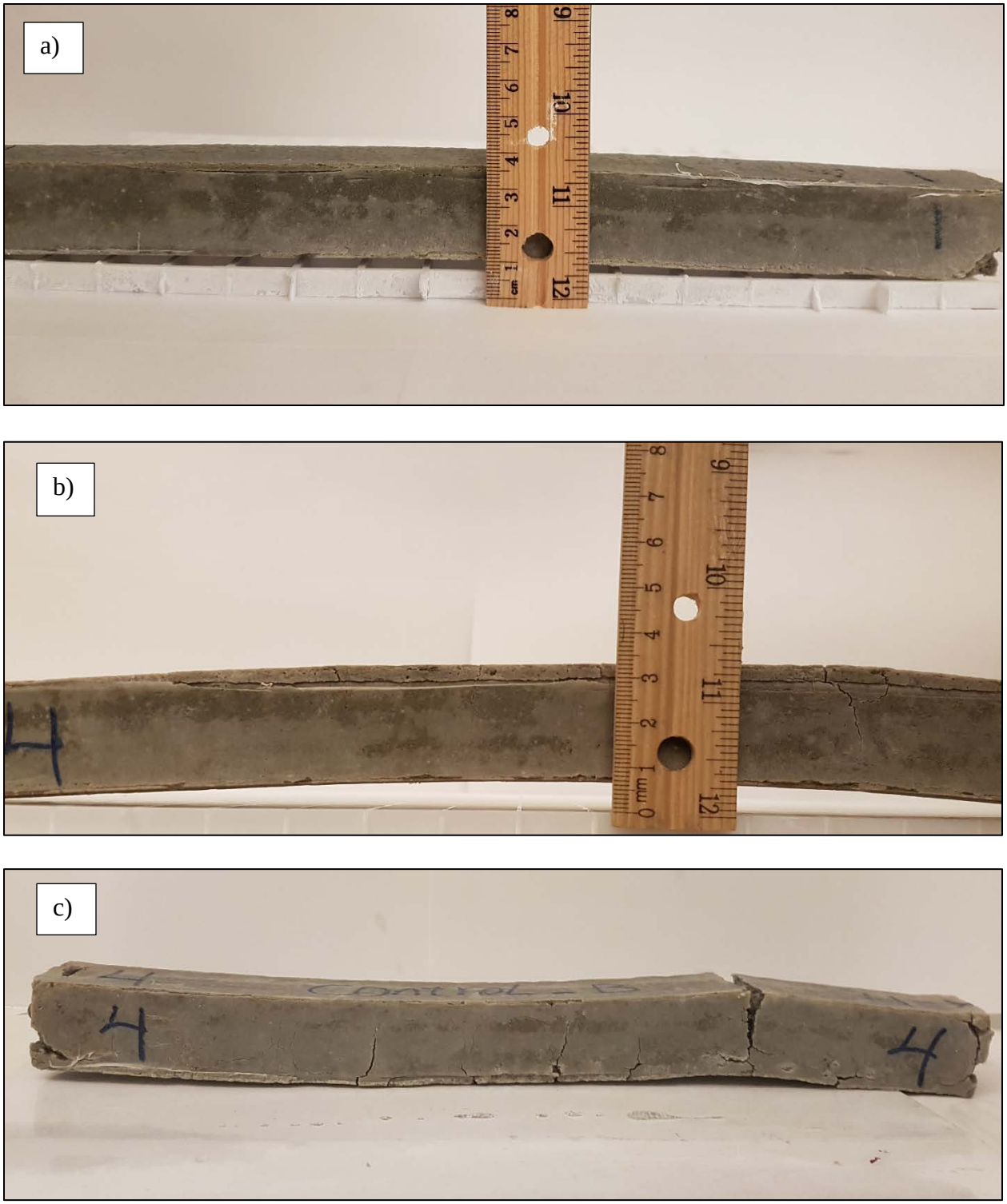

Figure 4-12: Control B sample after a) 91 days, b) 105 days and c) 120 days of exposure to 5% sodium sulfate solution

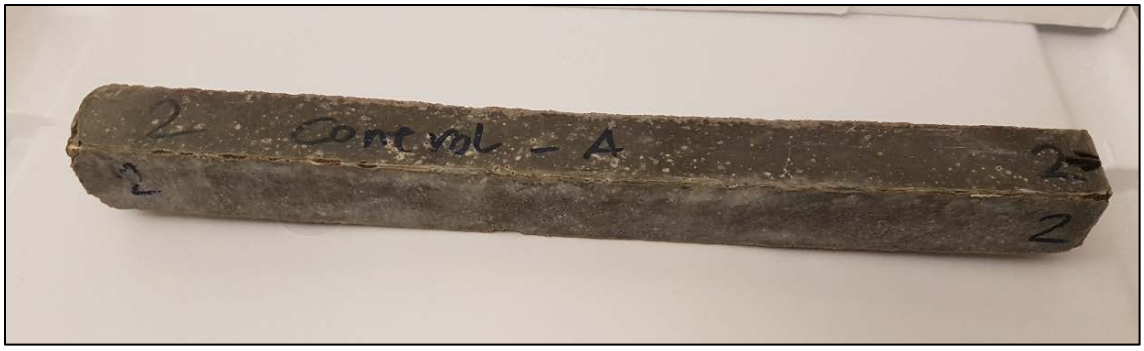

Figure 4-13: Control A sample after 1 year of exposure to 5% sodium sulfate solution

As for the slag mixtures, no visual deterioration has been observed for mortars with S8 at any cement replacement level, whether with Cement A (Figure 4-14) or B. This is consistent with the length change measurements that showed no expansion for the S8 mortars with either cement up to the age of 1 year.

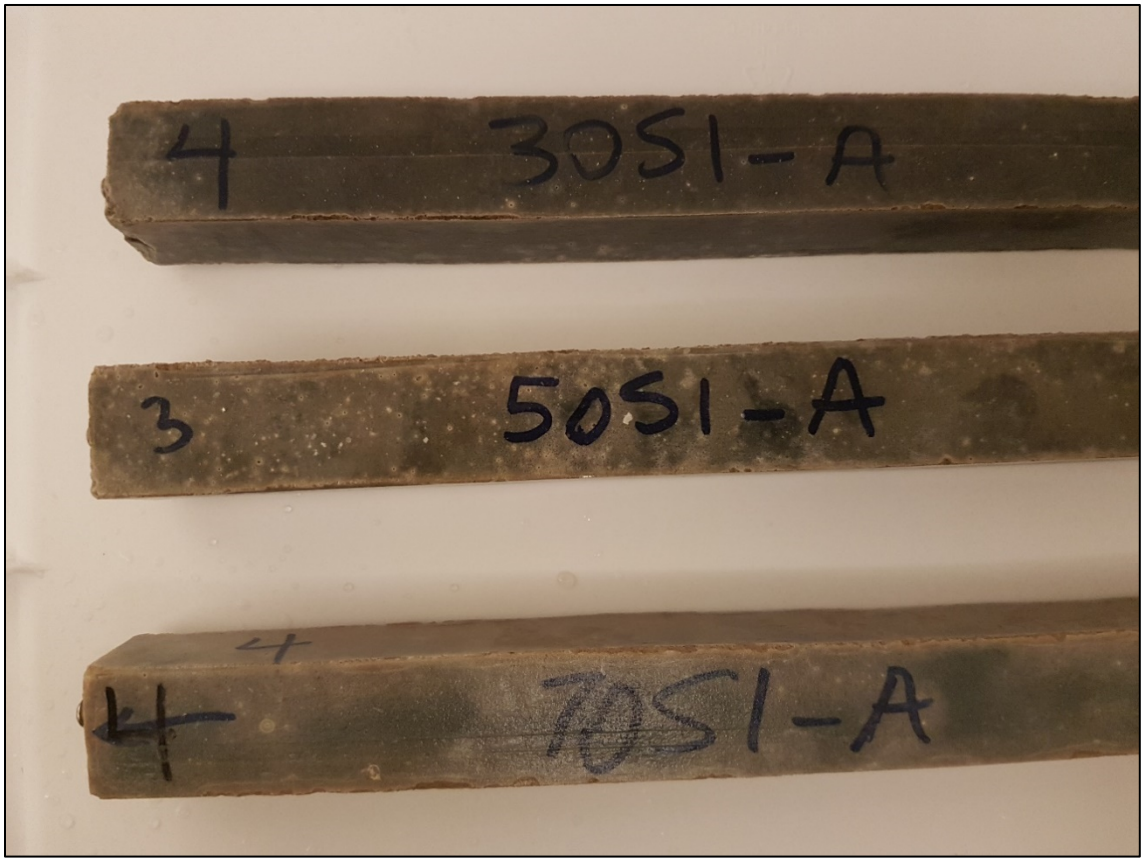

Figure 4-14: S8-A bars after 1 year of exposure to 5% sodium sulfate solution

Similar to S8 samples, the S11c-A samples did not show any deterioration for the first year at all replacement levels. However, for mixtures prepared with S11c and Cement B, deterioration was observed at the 30% replacement level at one year. The higher slag fineness (Blaine fineness of 680 m^2/kg) of the S11f-A samples resulted in deterioration, even at the highest replacement level (70%), as can be seen in Figure 4-15. This is consistent with the expansion measurements, where higher expansion was recorded for the 70S11f-A mortar bars (Figure 4-5). Deterioration of the S11f-A mortar bars was observed in the form of spalling, and was mostly confined to the ends of the bars.

Figure 4-15: S11f-A bars at 1 year of exposure to 5% sodium sulfate solution

The most rapid deterioration was observed for the 30S16-B bars; however, the deterioration progress was different from the control mixture. Only one measurement could be taken after the onset of rapid expansion as shown in Figure 4-4. At 105 days, more extensive spalling was observed (Figure 4-16a) than in the Control B samples, despite significantly lower expansion (0.11%). At 120 days, a majority of the bars had a single crack as shown in Figure 4-16b, and extensive spalling at the edges was observed (Figure 4-16c), more severe than in Control B samples. No evidence of warping was observed. Similar deterioration was observed for 30S16-A bars.

This difference in failure between the OPC and OPC-slag mortars is in line with the observations by Yu et al. [14], who also reported that test failure in OPC-slag mortar bars that were exposed to sodium sulfate solution occurred by cracking rather than by excessive expansion. They proposed that deterioration of slag mixtures in sodium sulfate environments was due to progressive spalling of the surface layer, rather than internal expansion and cracking, as found with OPC mortars. The authors attributed this to pore refinement in sulfate-exposed OPC-slag samples since sulfate ions in the slag samples were concentrated within 1 mm of the surface. Whittaker et al. [15] also reported that the depth of sulfate ion penetration was lower for slag-containing mortars, with the highest concentration observed at 0.5-1 mm below the surface. A sharp drop in sulfate concentration was observed after 1 mm, while a concentration gradient existed in the plain OPC mortar.

Figure 4-16: 30S16-B bars after a) 105 days and b) 120 days of exposure to 5% sodium sulfate solution; c) close-up view of the deterioration at 120 days.

More extensive spalling was observed for 50S16-B bars as can be seen in Figure 4-17. Deterioration was noted at 91 days, before the onset of rapid expansion, and became severe by 180 days, even though expansion at this age was only 0.12%. Similar deterioration was observed with Cement A for 50S16-A bars after 150 days (0.09% expansion), which was the last measurement age before all the bars broke (Figure 4-18). It appears that the length change measurements alone are not able to capture the progress of deterioration due to sulfate attack in the slag-containing mortars, as expansion of slag mortars prior to failure was significantly lower than that of their respective control mixtures. Visual signs of damage should also be used as a performance indicator. It has also to be noted that the strength measurements presented in Chapter 3 for S16 showed a substantial drop in strength on exposure to the sulfate environment at the 30 and 50% replacement levels for both Cement A and Cement B blends.

Figure 4-17: 50S16-B bars after a) 91 days and b) 180 days of exposure to 5% sodium sulfate solution.

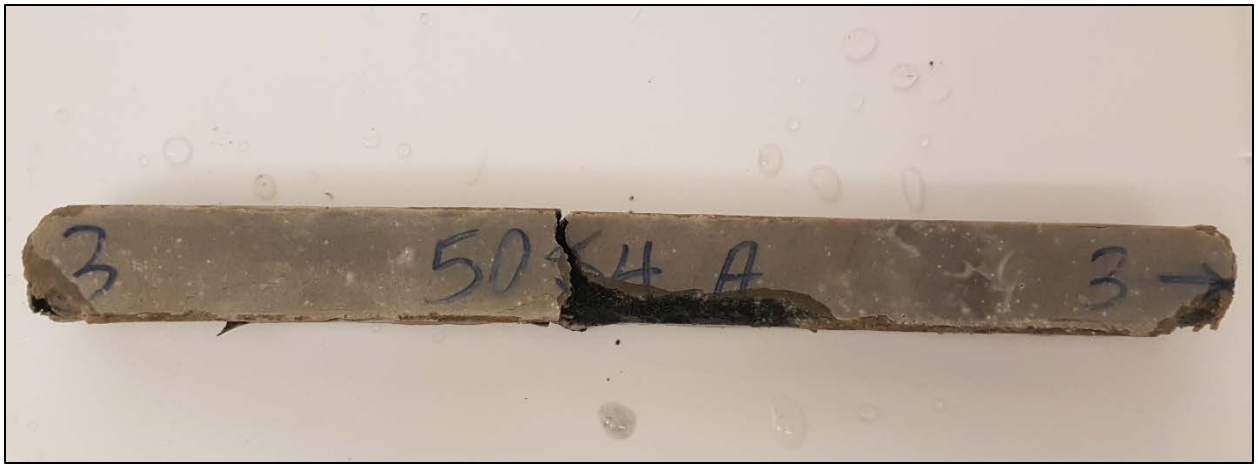

Figure 4-18: 50S16-A bars after 150 days of exposure to 5% sodium sulfate solution

Greater visual deterioration of sulfate-exposed OPC-slag mortar samples with increase in slag Al_2O_3 content was previously reported by Gollop and Taylor [42]. The authors also reported increased decalcification of C-S-H with increasing Al_2O_3 content of slag. They speculated that due to the low amount of CH observed, the calcium ions from C-S-H were used in the formation of ettringite [42], [47].

4.3.3 Microstructural Characterization

4.3.3.1 Characterization of Microstructure Prior to Sulfate Exposure

ASTM C1012 [1] specifies that the compressive strengths for companion cubes, prepared and match-cured together with the mortar bars, must reach 20.0 ± 1.0 MPa [3000 ± 150 psi] or higher prior to exposure of the bars to sulfate solution. Both bars and cubes are stored in saturated lime solution until this strength is reached. The control bars had reached minimum strengths at 24 hours and did not need curing in lime solution; however, the OPC-slag samples required curing in lime solution for lengths of time that were proportional to the cement replacement level. The lengths of curing time in lime solution needed to reach minimum strengths for cement replacements of 30%, 50%, and 70% were 1 day, 2 days, and 3 days, respectively. In order to assess the phase assemblage and characteristics of the pore network at the time of sulfate exposure, which play an important role in determining sulfate resistance, pastes were cured under the same conditions as the mortar bars and selected mixtures were analyzed to better understand the effect

of slag alumina content on the performance of slag-blended cementitious mixtures in sulfate environment.

4.3.3.1.1 X-Ray Diffraction Analysis of Pastes

Table 4-5 presents the phase composition of selected samples made with Cement A prior to sulfate immersion, at an age of 2 days for 30% replacement and 3 days for 50% replacement and 4 days for 70% replacement. Those ages correspond to the ages at which the specimens reached the specified strength requirement per ASTM C1012 for sulfate immersion. Generally, cement replacement with slag lowered the amounts of CH, ettringite, and unreacted clinker phases due to reduction of cement content. Formation of hemicarboaluminate (hemicarbonate) and hydrotalcite was noted in the presence of slag, and their amounts increased with increasing slag content. Monosulfoaluminate (monosulfate) was also observed in 70S11f-A, 50S16-A, and 70S16-A samples. Formation of monosulfoaluminate and hydrotalcite in OPC-slag samples has been previously reported in the literature and is attributed to the release of alumina during slag hydration [15], [47], [48], [49]. Presence of monosulfoaluminate indicates potentially lower durability of these mixes in sulfate environments as monosulfate will convert to ettringite on exposure to sulfates. It can also indicate that the system might not be sulfate-optimized for external sulfate exposure. However, the pore structure of the paste component will be an important factor in determining how much sulfate will reach these phases to cause secondary ettringite formation. Also noted is the belite content at 70% replacement with S16 and S11f, which is lower compared to 70S8 and 70S11c mixtures. This can possibly indicate that the blended system belite reactivity is higher in the presence of high-alumina slag, high-fineness slag, or both.

Table 4-5: Phase quantification before sulfate exposure of paste samples using Cement A

Sample ID / Phase (%)	Control A	30S8-A	50S8-A	70S8-A	30S11c-A	50S11c-A	70S11c-A	70S11f-A	30S16-A	50S16-A	70S16-A
Alite	8.5	1.8	1.1	0.3	1.6	1.1	0.2	0.7	1.2	0.6	0.5
Belite	10.1	6.4	5.0	2.9	5.9	4.0	2.8	2.0	5.7	4.2	1.6
Aluminate	1.2	0.2	0	0	0.2	0.0	0.0	0	0.2	0	0
Ferrite	2.1	0.9	0.4	0	0.8	0.0	0.0	0	0.4	0	0
Calcite	0.2	0	0	0	0.0	0.0	0.0	0	0	0	0
Quartz	0	0	0	0	0.1	0.1	0.1	0.1	0	0.1	0.1
CH	8.2	6.8	3.9	1.4	6.6	3.6	1.1	1.1	5.7	3.4	1.2
Ettringite	4.2	3.3	2.1	1.7	3.8	1.8	1.0	0	3.8	0.4	0
Monosulfate	0	0	0	0	0.0	0.0	0.0	0.5	0	1.1	1.3
Hemicarbonate	0	0.6	1.2	1.6	0.8	1.4	1.4	0.5	0	0.8	1.0
Hydrotalcite	0	0	0	0.19	0.0	0.0	0.6	0.5	0	0.1	0.6
Amorphous	65.5	80.0	86.2	92.0	80.1	87.9	92.9	94.6	82.9	89.4	93.51

4.3.3.1.2 Mercury Intrusion Porosimetry

Mercury intrusion porosimetry was used to evaluate the effect of slag composition and replacement level on pore structure of the paste samples prior to sulfate exposure at the same ages as the XRD samples. Figure 4-19 through Figure 4-21 present the cumulative and differential intruded pore volumes for all the samples. Examination of these plots shows that cement replacement with slag generally resulted in an increase in the intruded pore volume compared to the control, except for the 70S11f-A and the 70S16-A samples. Slag additions also produced a broadening of the intruded pore size distribution, indicated by reduced slopes of the cumulative curves, in which there was both coarsening (more larger pores) and refining of the pore structure (more smaller pores). The 70S11f-A and 70S16-A samples also showed a broadening of the intruded pore size distribution; however, only refining of the pore structure occurred, resulting in a reduction in cumulative intruded pore volume, which may have been related to the higher fineness of the S11f slag and the higher reactivity of S16 high-alumina slag.

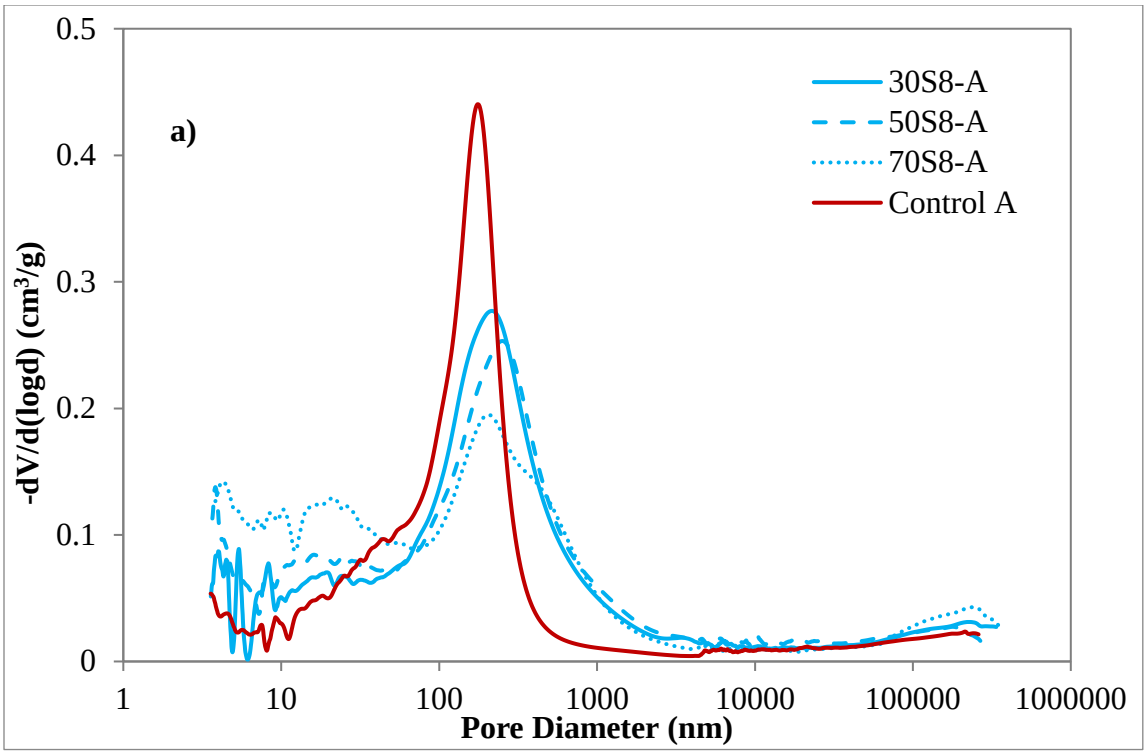

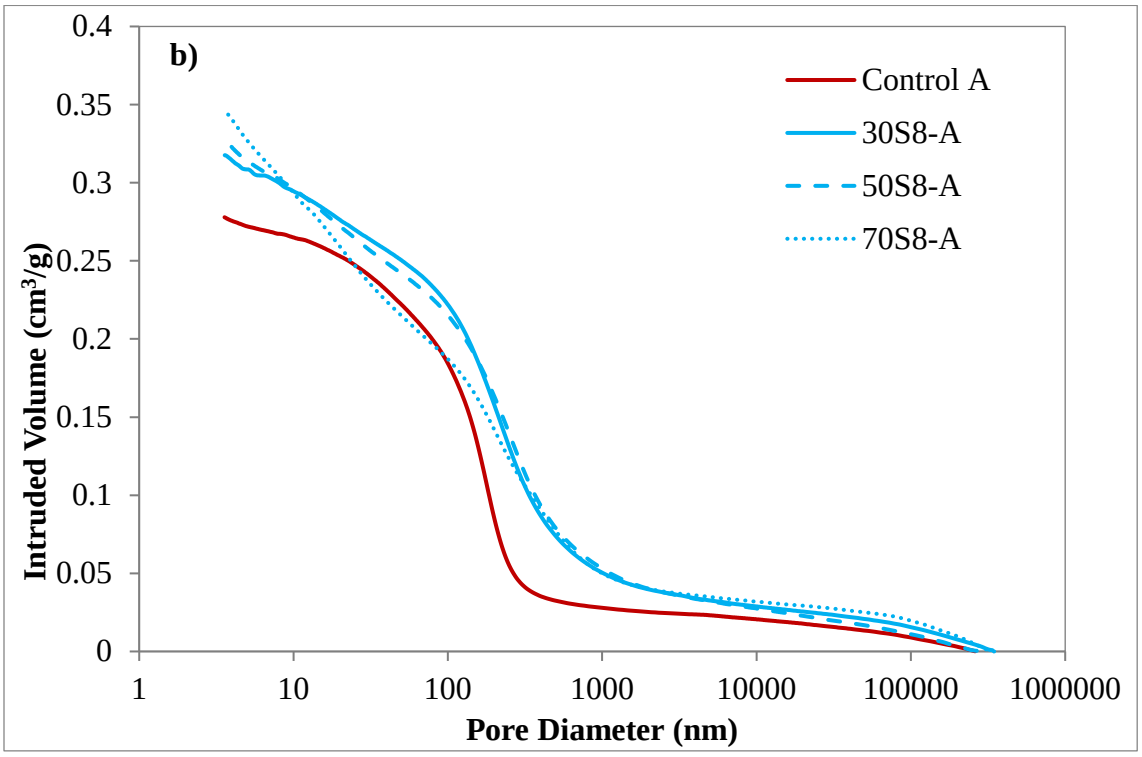

Figure 4-19: a) Differential pore size distribution and b) cumulative intruded volume for Control A and S8-A pastes prior to sulfate immersion.

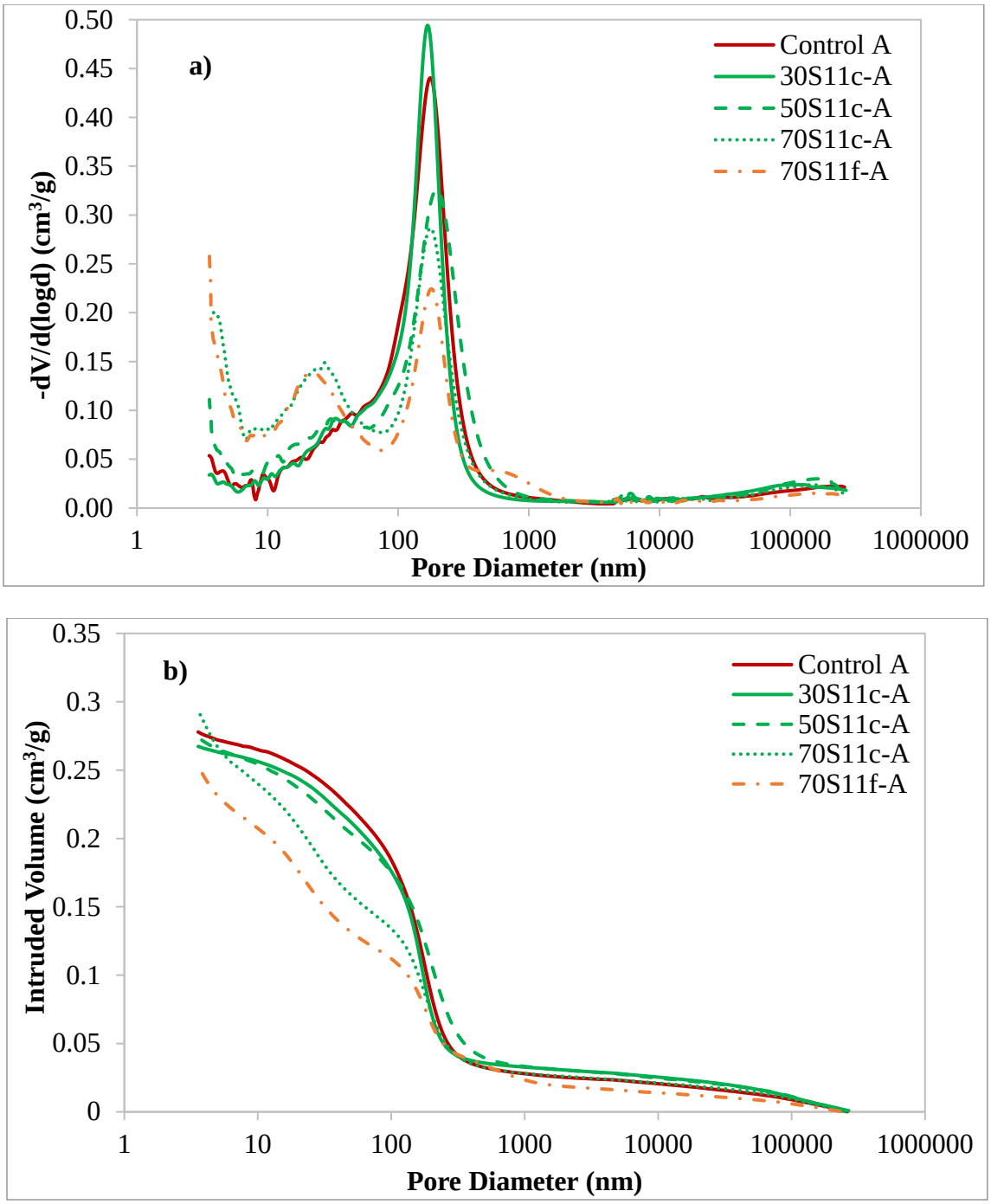

Figure 4-20: a) Differential pore size distribution and b) cumulative intruded volume for Control A and S11-A pastes prior to sulfate immersion

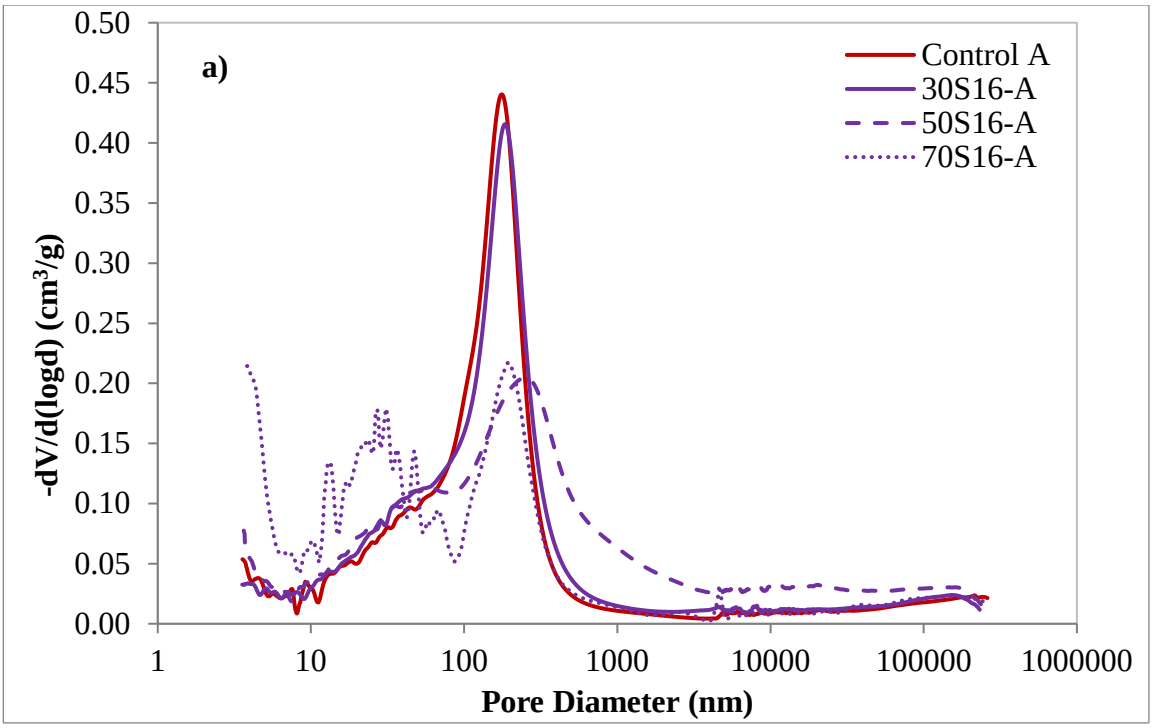

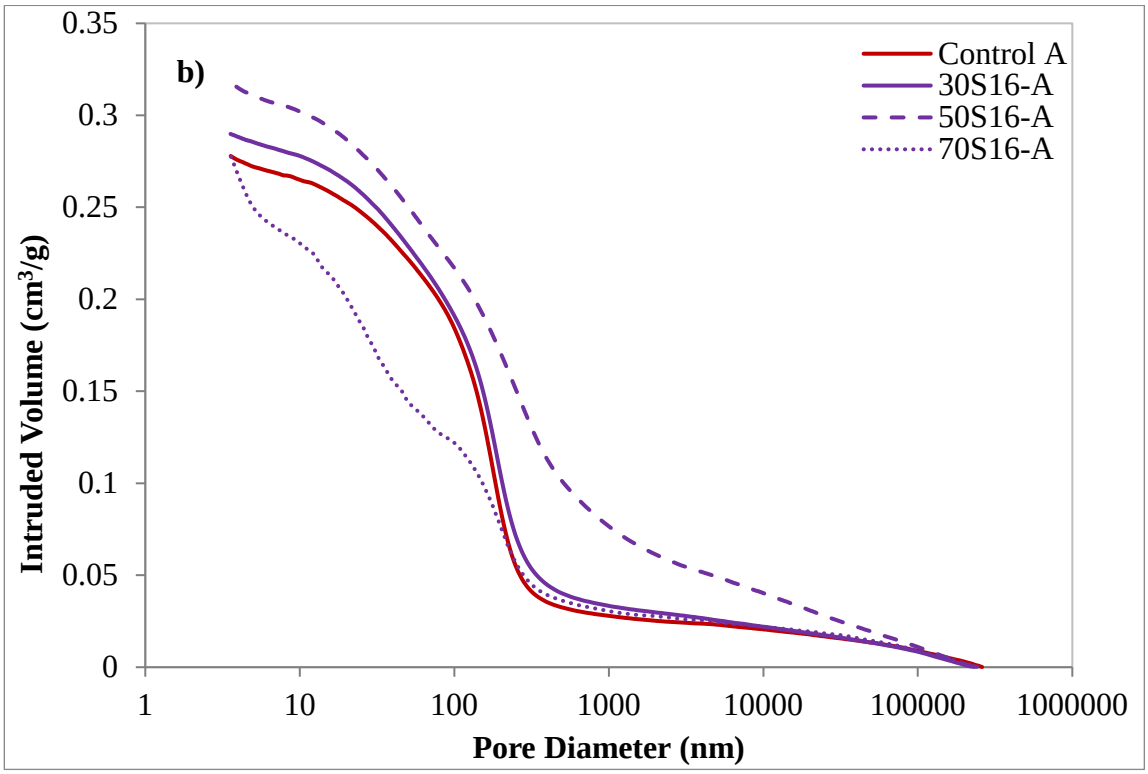

Figure 4-21: a) Differential pore size distribution and b) cumulative intruded volume for Control A and S16-A pastes prior to sulfate immersion

Three parameters are typically obtained from the MIP curves: total intrudable porosity (ϕ_{in}), critical pore diameter (d_c), and threshold pore diameter (d_{th}) [50], [51]. Total porosity corresponds to the maximum volume of mercury intruded on the cumulative porosity curve and describes the volume of mercury-entering the accessible interconnected pores in the sample. Critical pore diameter can also be obtained from the cumulative porosity curve and is defined as the pore size corresponding to the steepest slope, but it is more easily determined from the differential porosity curve and corresponds to the pore diameter at the highest peak. In terms of the pore network, d_c describes the most common size of interconnected pores or "the maximum continuous pore radius" [50]. Critical pore diameter has been related to transmissivity and permeability of the material [50], [52]–[54]. Halamickova et al. [54] also reported a linear relationship between d_c and the coefficient of chloride ion diffusion.

Threshold pore diameter is defined as "the largest pore diameter at which significant intruded pore volume is detected" [50]. While ϕ_{in} and d_c can be unequivocally determined, determination of d_{th} is still rather ambiguous [50], [51]. The following methods have been proposed to establish the d_{th} value: using the first inflection point in the cumulative intruded volume curve [50], the diameter corresponding to 5% of the total intruded volume [55], the lowest point on the difference curve between first and second cumulative intruded volumes [56], and the tangent method, where d_{th} is found at the intersection of tangents before and after the inflection point [51], [57]. The tangential method is illustrated in Figure 4-22. Due to the ambiguity of d_{th} determination and subjectivity in its determination, only the values of ϕ_{in}, and d_c are listed in Table 4-6.

Another parameter included in Table 4-6 is the volume of pores in the 10-50 nm diameter range labeled as $\phi_{10\text{-}50}$. Müllauer et al. [58] attributed deterioration due to sulfate attack to ettringite crystallization in pores of this size. He reported that ettringite crystallization in these pores can generate crystallization pressure well above the tensile strength of the hydrated cementitious system, resulting in expansion and cracking, while ettringite formation in larger pores is not expansive.

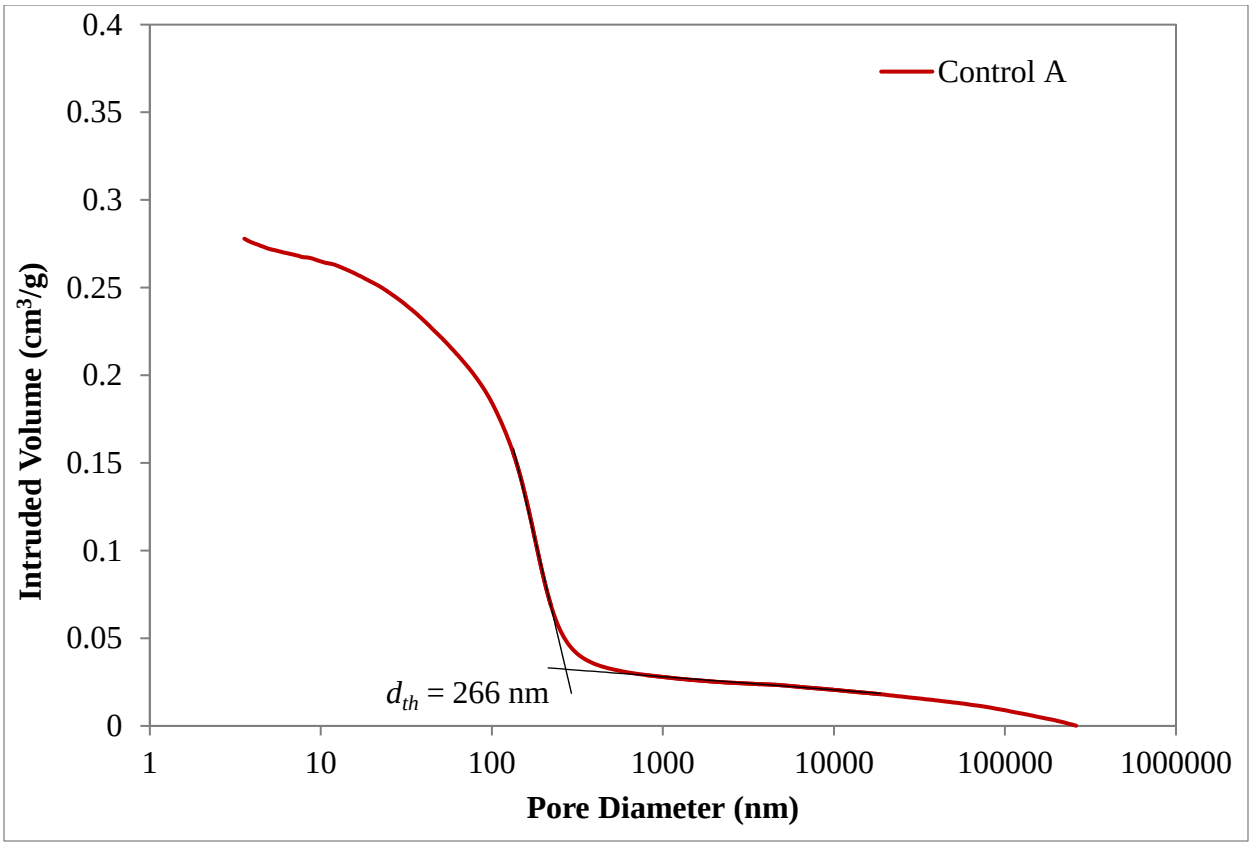

Figure 4-22: Tangential method illustration

Table 4-6: Porosity Indices Obtained from MIP

	ϕ_{in} (cm^3/g)	d_c (nm)	$\phi_{10\text{-}50}$ (cm^3/g)
Control A	0.278	175	0.043
30S8-A	0.318	217	0.044
50S8-A	0.329	250	0.054
70S8-A	0.347	206	0.078
30S11c-A	0.267	167	0.045
50S11c-A	0.274	195	0.051
70S11c-A	0.294	176	0.081
70S11f-A	0.254	178	0.076
30S16-A	0.290	185	0.049
50S16-A	0.318	251	0.052
70S16-A	0.278	193	0.085

As can be seen from Table 4-6, addition of slag resulted in a higher value of ϕ_{in} for S8, at all replacement levels compared the control. This is in line with the results of Choi et al. [59], who also reported an increase in intruded pore volume with increasing cement replacement by slag at the age of 3 days. However, 70S11f showed the lowest intruded pore volume, among all slags and at all replacement levels, consistent with its highest fineness and lower belite content at testing age and thus confirming its higher reactivity.

While d_c increased with addition of slag compared to Control A, at hydration time of 1 to 3 days, its value decreased with increasing slag content to 70% but was still above Control A. This is not surprising as slag reactivity is lower than portland cement, at early ages. This also indicates that increasing slag content to 70% would decrease permeability and, consequently, reduce penetration of the sulfate ions to the core of the mortar bars as indicated by decreasing d_c, which explains the better performance of mixes containing 70% slag. Additionally, the cummulative intruded volume curves for the 70% slag samples showed the presence of multiple inflection points or "choke points" [60], the presence of which has been associated in increased tortuosity [57]. It is also noted that 70S11f had a d_c value consistent with Control A, even at such high replacement level, indicating again the effect of fineness and reactivity on the pore structure at early age.

As for the volume of pores in the 10-50 nm range, it appeared to be dependent on cement replacement level. The values of $\phi_{10\text{-}50}$ were similar for Control A and 30% slag mixes and increased with increasing slag content. No significant differences were observed between slags at the same replacement level. This indicates that if the same trend in $\phi_{10\text{-}50}$ is maintained at later ages, higher-Al_2O_3 slags would be more prone to cracking as they have a higher potential for secondary ettringite formation, but the same volume of pores as the lower-Al_2O_3 slags that can accommodate this ettringite.

4.3.3.2 Thermodynamic Modeling

Figure 4-23 and Figure 4-24 show the predicted phase assemblages for Control A and Cement A with 50% Slag S8 replacement. The left side of the plots represents the phases at the core of the bars, while the right side of the plots represents the surface of the bars in contact with sulfate solution. For Control A, the phases predicted at the core are C-S-H, CH, ettringite,

monocarboaluminate, hydrogarnet and hydrotalcite (Figure 4-23). At large volumes of Na_2SO_4 solution, decomposition of CH and formation of gypsum is predicted as well as decomposition of monocarboaluminate. These phases are generally consistent with the XRD results at 1 year. In addition, this modeling approach is able to predict the effects of leaching [32], which can be observed as a decrease in the volumes of C-S-H, ettringite and gypsum.

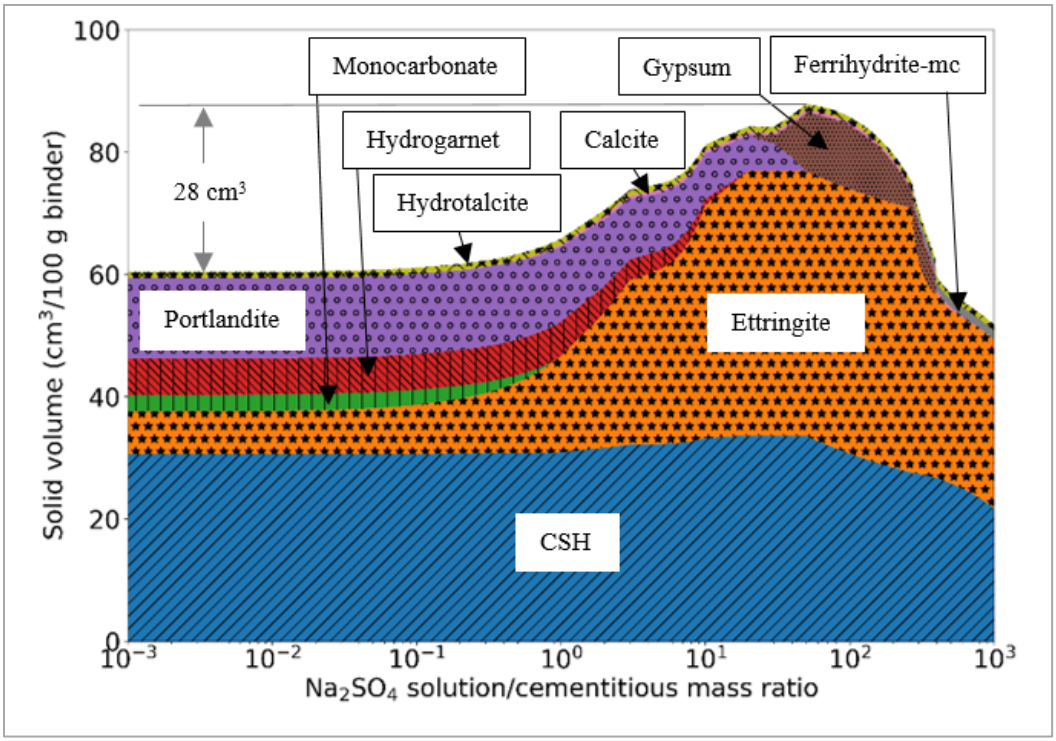

Figure 4-23: Control A phase assemblage prediction

When 50% of cement was replaced with slag S8, thermodynamic modeling predicted an increase in C-S-H solid volume and a decrease in ettringite compared to the Control A mixture (Figure 4-24). Addition of slag S8 also significantly reduced the overall predicted solid volume increase, which is consistent with the observed length changes (Figure 4-2). While no monosulfate was predicted with S8 addition, this phase was predicted for 50S16-A mixture at low sulfate solution amounts (Figure 4-24 and Figure 4-25). Additionally, the predicted solid volume increase for this mixture was higher than for 50S8-A, and appeared to increase with the Al_2O_3 content of slag. This is consistent with expansion measurements and the increase in deterioration with increasing Al_2O_3 content of slag. It is interesting to note that for 50S16-A mortar, GEMS modeling

predicted a slight decrease in the solid volume of C-S-H due to leaching at a solution to binder mass ratio of 1, while a later decrease in C-S-H solid volume was predicted for other mixtures. This decrease in C-S-H solid volume for 50S16-A coincides with a notable increase in predicted volume of ettringite. Gollop and Taylor [47] stated that in slag-OPC mixes some calcium ions necessary for formation of ettringite are obtained through decalcification of C-S-H. The higher overall alumina content of 50S16-A may, therefore, be responsible for this decrease in C-S-H solid volume. Additionally, Whittaker et al. [15] reported that decalcification of C-S-H in OPC-slag samples occurred at earlier ages compared to the plain cement paste, which is consistent with the results of thermodynamic modeling.

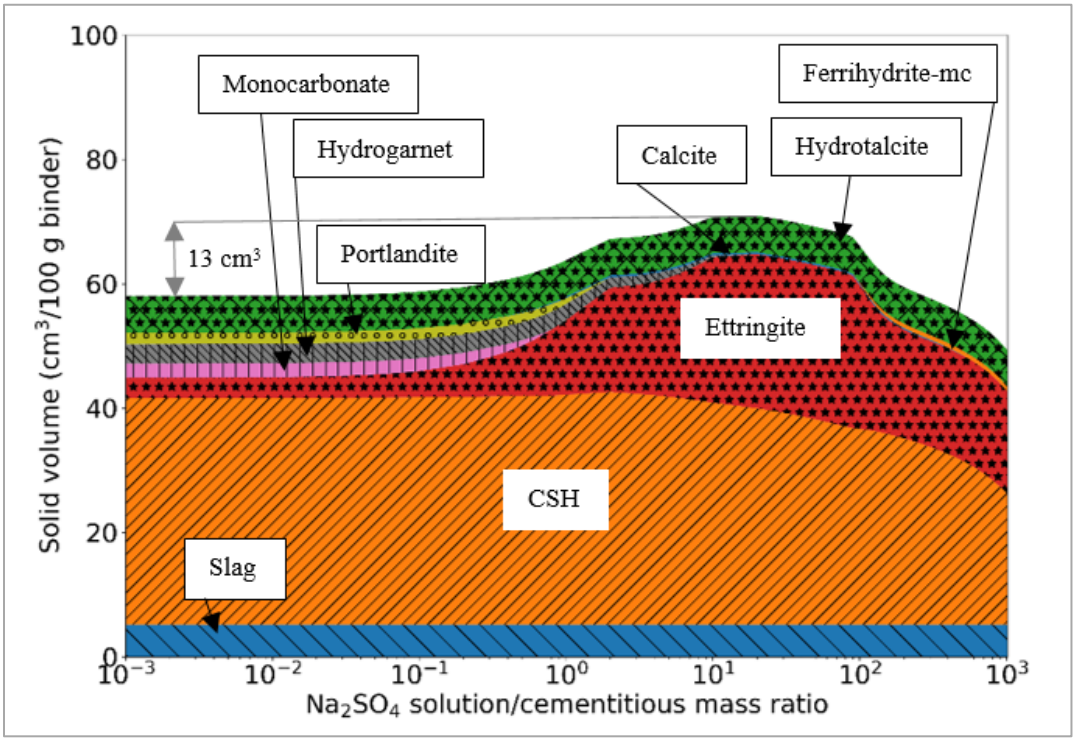

Figure 4-24: 50S8-A phase assemblage prediction

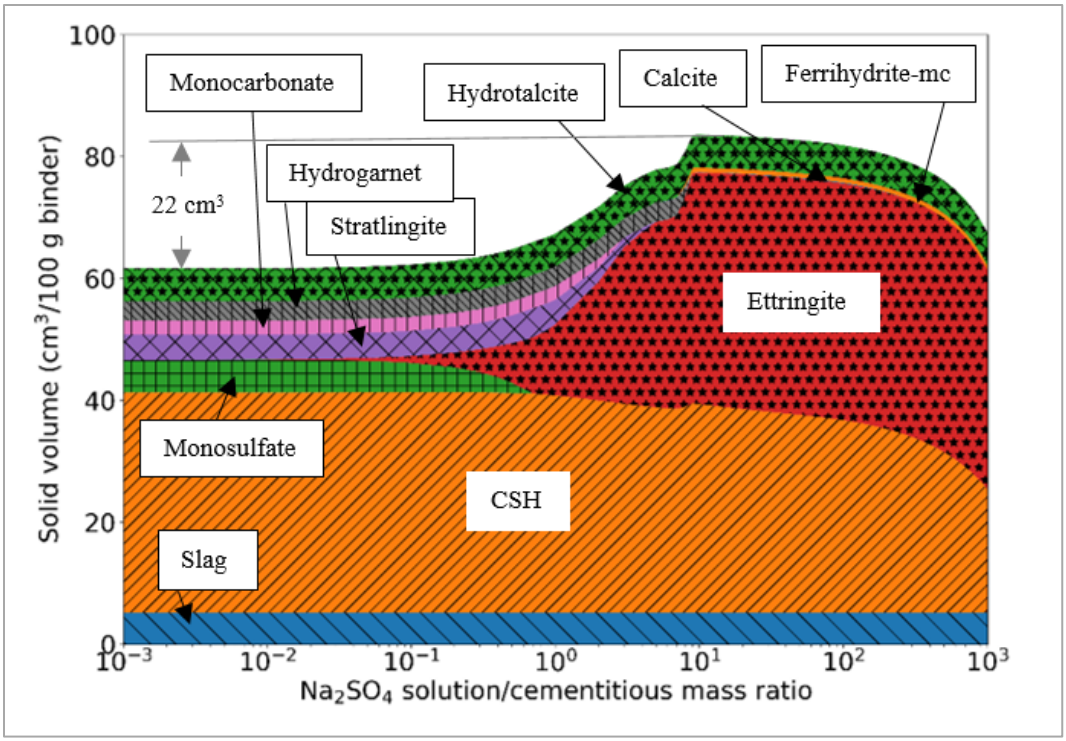

Figure 4-25: 50S16-A phase assemblage prediction

4.3.3.3 X-ray Diffraction Analysis

Phase quantification results of selected core and surface samples of the bars prepared with Cement A and 50% slag at 1 year are presented in Table 4-7. Amorphous content refers to the sum of C-S-H and unhydrated slag. For the clinker phases, only a small amount of belite was observed in all the samples, indicating that cement hydration was nearly 100%, as assumed in the GEMS modeling. Comparison of the core and surface samples for Control A showed a higher amount of CH in the core, while gypsum and ettringite were higher in the surface sample, which is expected during sulfate attack [6], [11], [61], and is consistent with the results of thermodynamic modeling (Figure 4-23). Calcite formation on exposure to high amounts of Na_2SO_4 solution was also predicted by GEMS, and is observed in the surface of Control A mortar. Cement replacement with slag significantly decreased the amount of CH and ettringite in the core samples both due to the reduction of cement content and the pozzolanic reaction of slag with CH. However, the amount of monosulfate increased. Although thermodynamic modeling predicted formation of monosulfate at the core only for 50S16-A samples, it was observed in the Control A and S8 slag sample by

QXRD. Some authors state that monosulfate formation due to slag hydration is not likely to cause damage in sulfate environments [15]. Whittaker et al. [15] reported that "less ettringite had formed in the slag systems despite the higher AFm content prior to sulfate attack." Additionally, the authors stated that "the C-A-S-H phase and hydrotalcite would have consumed all of the aluminium released by the slag" [15]. This is contrary to the increase in ettringite observed in the current study both in the core and surface samples with increasing Al_2O_3 content of slag (Figure 4-26). The amount of ettringite in the 50S16-A surface sample was very similar to that observed in the Control A surface. Based on the length change measurements (Figure 4-2, and Figure 4-4), it appears that the increase in ettringite content caused some expansion, particularly in the mortars prepared with S16 slag, and its formation resulted in cracking, which lead to spalling on the surface and cracking of the bars.

Table 4-7: Phase quantification of the core and surface samples of mortar bars stored in 5% Na_2SO_4 solution for 1 year

Sample ID / **Phase (wt.%)**	**Control A**		**50S8-A**		**50S16-A**	
	Core	**Surface**	**Core**	**Surface**	**Core**	**Surface**
Belite	1.5	1.0	1.3	0.5	1.1	0.0
Calcite	1.3	9.3	1.1	15.9	0.6	11.9
CH	17.6	4.9	5.9	0.2	3.1	0.0
Gypsum	1.8	8.8	1.3	4.1	1.2	0.6
Ettringite	14.6	21.4	4.0	9.5	8.0	20.0
Monosulfate	0.2	0.0	1.3	0.0	1.8	0.0
Hydrotalcite	0.0	0.0	1.7	0.0	1.7	0.8
Amorphous	63.0	54.5	83.5	70.0	82.5	66.7

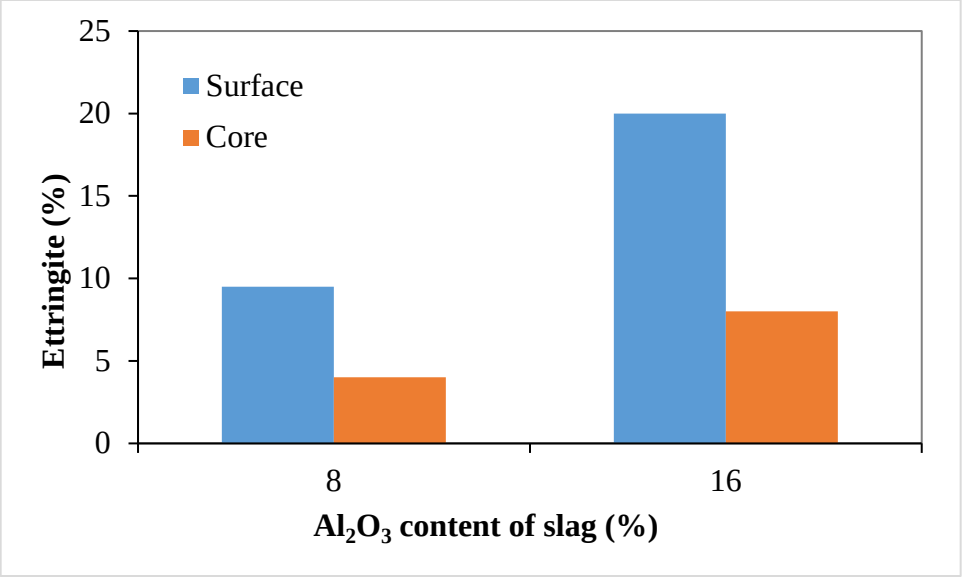

Figure 4-26: Variation in ettringite amount with Al_2O_3 content of slag in the core and surface of the mortar bars prepared with 50% slag (S8, S16) and Cement A at 1 year

4.4 Conclusions

Cement replacement with slag had a varied effect on durability of mortar in 5% sodium sulfate solution tested according to ASTM C1012-18, and appeared to be related to the slag alumina content, A/M ratio, Blaine fineness, slag replacement level, and the parent cement chemistry and mineralogy. Generally, addition of slag at a replacement level of 70%, regardless of its characteristics, improved sulfate resistance of the high-C_3A Cement B by extending the induction period. However, the extent of the improvement in durability was related to the chemical and physical characteristics of slag. For Cement A with the lower C_3A content, improvement in sulfate resistance was only observed with low-Al_2O_3 slags S8 and S11c. Bars prepared with S8 slag (8% Al_2O_3) showed excellent performance, with no expansion observed during the first year. XRD analysis showed that no monosulfate was formed in mixes prepared with S8 prior to sulfate exposure. The smallest amount of ettringite formed in OPC-slag samples after 1 year of sulfate exposure was observed for bars prepared with slag S8 and Cement A. Additionally, for slag-OPC samples, thermodynamic modeling predicted the lowest solid volume increase for S8-OPC samples. The higher alumina content of S11c-OPC samples resulted in higher expansions compared to S8-OPC mixes. Increasing slag fineness, alumina content and A/M ratio (S11f)

resulted in higher expansion. The highest solid volume increase was predicted for S16, which corresponded to the earliest deterioration of the mortars bars. Monosulfate was detected prior to sulfate exposure in S16 mixes, and S16 bars had the highest amount of ettringite at the age of 1 year.

Extending the measurements to 18 months or 540 days, showed clear trends on the effect of the slag chemical and physical characteristics as well as replacement levels on durability, especially for the Type II (MH) OPC cement (Cement A). At replacement levels between 30% and 70%, slag S8-blended samples showed excellent performance and can be used for the most aggressive sulfate exposure conditions. For slag alumina content of 11% (S11c), 70% replacement level was required to attain similar performance to the S8 slag. The data also showed that grinding slag of the same alumina content to higher fineness (from 589 to 680 m^2/kg) increased the susceptibility of S11 to sulfate attack and renders the slag unsuitable for Class "S3" exposure [39], up to 70% replacement. Increasing slag alumina content to 16% (S16) did not result in improving sulfate resistance when compared to the control at replacement levels of 30 and 50%. Increasing replacement level of S16 to 70% improved performance compared to Control A; however, the slag-blended mixtures broke at an age of 480 days. Though strength measurements for 70S16 showed good performance at 540 days of exposure to the same sodium sulfate solution used for mortar bar exposure, it appears that mortar bar expansion and failure was due to a substantially higher ettringite formation as confirmed by quantitative X-ray diffraction and thermodynamic modelling.

The mode of failure for the mortar bars containing slag differed from those prepared with plain cement. While the control bars showed significant expansion that was accompanied by warping until cracking eventually occurred, bars containing slag showed lower expansion; however, significant surface deterioration was observed, in the form of spalling, that was followed by cracking.

4.5 References

[1] ASTM C1012/C1012M-18, "Standard test method for length change of hydraulic-cement mortars exposed to sulfate solution," West Conshohocken, PA: ASTM International, 2018.

[2] ACI Committee 201, *ACI 201.2R-16 Guide to Durable Concrete*. 2016.

[3] S. Mindess, J. F. Young, and D. Darwin, *Concrete*, 2nd ed. Upper Saddle River, NJ: Prentice Hall, 2003.

[4] P. K. Mehta, "Mechanism of expansion associated with ettringite formation," *Cem. Concr. Res.*, vol. 3, pp. 1–6, 1973.

[5] I. Odler and J. Colán-Subauste, "Investigations on cement expansion associated with ettringite formation," *Cem. Concr. Res.*, vol. 29, no. 5, pp. 731–735, 1999.

[6] N. Shanahan and A. Zayed, "Cement composition and sulfate attack," *Cem. Concr. Res.*, vol. 37, no. 4, pp. 618–623, Apr. 2007.

[7] B. Tian and M. D. Cohen, "Expansion of Alite Paste Caused by Gypsum Formation during Sulfate Attack," *J. Mater. Civ. Eng.*, vol. 12, no. 1, pp. 24–25, 2000.

[8] B. Tian and M. D. Cohen, "Does gypsum formation during sulfate attack on concrete lead to expansion?," *Cem. Concr. Res.*, vol. 30, no. 1, pp. 117–123, Jan. 2000.

[9] N. Shanahan and A. Zayed, "Role of tricalcium silicate in sulfate resistance," *Adv. Cem. Res.*, vol. 27, no. 7, pp. 409–416, 2015.

[10] P. K. Mehta and P. J. M. Monteiro, *Concrete: Microstructure, Properties and Materials*, 3rd ed. New York, NY: McGraw-Hill, 2006.

[11] R. S. Gollop and H. F. W. Taylor, "Microstructural and microanalytical studies of sulfate attack. I. Ordinary portland cement paste," *Cem. Concr. Res.*, vol. 22, no. 6, pp. 1027–1038, 1992.

[12] ASTM C989/C989M-17, "Standard Specification for Slag Cement for Use in Concrete and Mortars," West Conshohocken, PA: ASTM International, 2017.

[13] ASTM C150/C150M-16, "Standard Specification for Portland Cement," West Conshohocken, PA: ASTM International, 2016.

[14] C. Yu, W. Sun, and K. Scrivener, "Mechanism of expansion of mortars immersed in sodium sulfate solutions," *Cem. Concr. Res.*, vol. 43, pp. 105–111, 2013.

[15] M. Whittaker, M. Zajac, M. Ben Haha, and L. Black, “The impact of alumina availability on sulfate resistance of slag composite cements,” *Constr. Build. Mater.*, vol. 119, pp. 356–369, 2016.

[16] D. Jansen, F. Goetz-Neunhoeffer, C. Stabler, and J. Neubauer, “A remastered external standard method applied to the quantification of early OPC hydration,” *Cem. Concr. Res.*, vol. 41, no. 6, pp. 602–608, Jun. 2011.

[17] D. Jansen, S. T. Bergold, F. Goetz-Neunhoeffer, and J. Neubauer, “The hydration of alite: A time-resolved quantitative XRD approach using the G-factor method compared with heat release,” *J. Appl. Crystallogr.*, vol. 44, no. 5, pp. 895–901, 2011.

[18] D. Jansen, C. Stabler, F. Goetz-Neunhoeffer, S. Dittrich, and J. Neubauer, “Does Ordinary Portland Cement Contain Amorphous Phase? A Quantitative Study Using an External Standard Method,” *Powder Diffr.*, vol. 26, no. 1, pp. 31–38, Mar. 2011.

[19] R. Snellings, A. Bazzoni, and K. Scrivener, “The existence of amorphous phase in Portland cements: Physical factors affecting Rietveld quantitative phase analysis,” *Cem. Concr. Res.*, vol. 59, pp. 139–146, May 2014.

[20] I. C. Madsen, N. V. Y. Scarlett, and A. Kern, “Description and survey of methodologies for the determination of amorphous content via X-ray powder diffraction,” *Zeitschrift für Krist.*, vol. 226, no. 12, pp. 944–955, Dec. 2011.

[21] J. P. Cline, R. B. Von Dreele, R. Winburn, P. W. Stephens, and J. J. Filliben, “Addressing the amorphous content issue in quantitative phase analysis: the certification of NIST standard reference material 676a,” *Acta Crystallogr. A.*, vol. 67, no. Pt 4, pp. 357–67, Jul. 2011.

[22] A. G. De La Torre, S. Bruque, and M. A. G. Aranda, “Rietveld quantitative amorphous content analysis,” *J. Appl. Crystallogr.*, vol. 34, pp. 196–202, 2001.

[23] D. Bish and R. J. Reynolds, “Sample Preparation for X-Ray Diffraction,” in *Modern Powder Diffraction*, D. Bish and J. Post, Eds. Washington, DC: The Mineralogical Society of America, 1989, pp. 73–99.

[24] Paul Scherrer Institut (PSI), “GEMS 3 [Software].” .

[25] D. A. Kulik, T. Wagner, S. V. Dmytrieva, G. Kosakowski, F. F. Hingerl, K. V. Chudnenko and U. Berner, “GEM-Selektor geochemical modeling package: revised algorithm and

GEMS3K numerical kernel for coupled simulation codes," *Comput. Geosci.*, vol. 17, pp. 1–24, 2013.

[26] T. Wagner, D. A. Kulik, F. F. Hingerl, and S. V. Dmytrieva, "GEM-Selektor geochemical modeling package: TSolMod library and data interface for multicomponent phase models," *Can. Mineral.*, vol. 50, pp. 1173–1195, 2012.

[27] W. Hummel, U. Berner, E. Curti, F. J. Pearson, and T. Thoenen, "Nagra/PSI chemical thermodynamic data base 01/01," *Radiochim. Acta*, vol. 90, no. 9–11, pp. 805–813, 2002.

[28] EMPA, "CEMDATA14." [Online]. Available: https://www.empa.ch/web/s308/cemdata.

[29] A. Schöler, B. Lothenbach, F. Winnefeld, and M. Zajac, "Hydration of quaternary Portland cement blends containing blast-furnace slag, siliceous fly ash and limestone powder," *Cem. Concr. Compos.*, vol. 55, pp. 374–382, 2015.

[30] W. Kunther, B. Lothenbach, and K. L. Scrivener, "On the relevance of volume increase for the length changes of mortar bars in sulfate solutions," *Cem. Concr. Res.*, vol. 46, pp. 23–29, 2013.

[31] V. Kocaba, E. Gallucci, and K. L. Scrivener, "Methods for determination of degree of reaction of slag in blended cement pastes," *Cem. Concr. Res.*, vol. 42, no. 3, pp. 511–525, 2012.

[32] B. Lothenbach, B. Bary, P. Le Bescop, T. Schmidt, and N. Leterrier, "Sulfate ingress in Portland cement," *Cem. Concr. Res.*, vol. 40, no. 8, pp. 1211–1225, 2010.

[33] E. Menendez, T. Matschei, and F. P. Glasser, "Sulfate Attack of Concrete," in *Performance of Cement-Based Materials in Aggressive Aqueous Environments*, M. Alexander, A. Bertron, and N. De Belie, Eds. New York, NY: Springer, 2013, pp. 7–74.

[34] B. Lothenbach, W. Kunther, and A. E. Idiart, "Thermodynamic modeling of sulfate interaction," *Concr. Repair, Rehabil. Retrofit. III - Proc. 3rd Int. Conf. Concr. Repair, Rehabil. Retrofit. ICCRRR 2012*, no. Kulik, pp. 1444–1449, 2012.

[35] T. Schmidt, B. Lothenbach, M. Romer, J. Neuenschwander, and K. Scrivener, "Physical and microstructural aspects of sulfate attack on ordinary and limestone blended Portland cements," *Cem. Concr. Res.*, vol. 39, no. 12, pp. 1111–1121, 2009.

[36] C. F. Ferraris, J. R. Clifton, P. E. Stutzman, and E. J. Garboczi, "Mechanisms of degradation of Portland cement-based systems by sulfate attack," in *Mechanisms of Chemical*

Degradation of Cement-Based Systems, K. L. Scrivener and J. F. Young, Eds. London, UK: E & FN Spon, 1997, pp. 185-.

[37] H. T. Cao, L. Bucea, A. Ray, and S. Yozghatlian, "The effect of cement composition and pH of environment on sulfate resistance of Portland cements and blended cements," *Cem. Concr. Compos.*, vol. 19, no. 2, pp. 161–171, 1997.

[38] P. J. M. Monteiro and K. E. Kurtis, "Time to failure for concrete exposed to severe sulfate attack," *Cem. Concr. Res.*, vol. 33, no. 7, pp. 987–993, 2003.

[39] ACI Committee 201, "ACI 201.2R - 16 Guide to Durable Concrete," American Concrete Institute, Farmington Hills, MI, 2016.

[40] R. D. Hooton, "Canadian use of ground granulated blast-furnace slag as a supplementary cementing material for enhanced performance of concrete," *Can. J. Civ. Eng.*, vol. 27, no. 4, pp. 754–760, 2000.

[41] R. D. Hooton and J. Emery, "Sulfate Resistance of a Candian slag cement," *ACI Mater. J.*, no. 87, pp. 547–555, 1990.

[42] R. S. Gollop and H. F. W. Taylor, "Microstructural and Microanalytical Studies of sulfate Attack. V. Comparison of Different Slag Blends," *Cem. Concr. Res.*, vol. 26, no. 7, pp. 1029–1044, 1996.

[43] R. D. Hooton and J. Emery, "Sulfate Resistance of a Candian slag cement," *ACI Mater. J.*, vol. 87, no. 6, pp. 547–555, 1990.

[44] A. Sedaghat, N. Shanahan, and A. Zayed, "Predicting One-Day, Three-Day, and Seven-Day Heat of Hydration of Portland Cement," *J. Mater. Civ. Eng.*, vol. 27, no. 9, p. 04014257, 2015.

[45] F. W. Locher, "The Problems of the Sulfate Resistance of Slag Cements," *Zement-Kalk-Gips*, vol.19, no. 9, pp.395-401, 1966.

[46] S. Ogawa, T. Nozaki, K. Yamada, H. Hirao, and R. D. Hooton, "Improvement on sulfate resistance of blended cement with high alumina slag," *Cem. Concr. Res.*, vol. 42, no. 2, pp. 244–251, Feb. 2012.

[47] R. S. Gollop and H. F. W. Taylor, "Microstructural and microanalytical studies of sulfate attack. IV. Reactions of a slag cement paste with sodium and magnesium sulfate solutions," *Cem. Concr. Res.*, vol. 26, no. 7, pp. 1013–1028, 1996.

[48] C. Yu, W. Sun, and K. Scrivener, “Degradation mechanism of slag blended mortars immersed in sodium sulfate solution,” *Cem. Concr. Res.*, vol. 72, pp. 37–47, 2013.

[49] E. F. Irassar, “Sulfate attack on cementitious materials containing limestone filler - A review,” *Cem. Concr. Res.*, vol. 39, no. 3, pp. 241–254, 2009.

[50] K. K. Aligizaki, *Pore Structure of Cement-Based Materials: Testing, Interpretation and Requirements*. New York, NY: Taylor & Francis, 2006.

[51] H. Ma, “Mercury intrusion porosimetry in concrete technology: Tips in measurement, pore structure parameter acquisition and application,” *J. Porous Mater.*, vol. 21, no. 2, pp. 207–215, 2014.

[52] A. Kumar, S. Ketel, K. Vance, T. Oey, N. Neithalath, and G. Sant, “Water Vapor Sorption in Cementitious Materials-Measurement, Modeling and Interpretation,” *Transp. Porous Media*, vol. 103, pp. 69–98, 2014.

[53] A. J. Katz and A. H. Thompson, “Quantitative prediction of permeability in porous rock,” *Phys. Rev. B*, vol. 34, no. 11, pp. 8179–8181, 1986.

[54] P. Halamickova, R. J. Detwiler, D. P. Bentz, and E. J. Garboczi, “Water permeability and chloride ion diffusion in portland cement mortars: Relationship to sand content and critical pore diameter,” *Cem. Concr. Res.*, vol. 25, no. 4, pp. 790–802, 1995.

[55] P. Pipilikaki and M. Beazi-Katsioti, “The assessment of porosity and pore size distribution of limestone Portland cement pastes,” *Constr. Build. Mater.*, vol. 23, no. 5, pp. 1966–1970, 2009.

[56] J. Kaufmann, R. Loser, and A. Leemann, “Analysis of cement-bonded materials by multi-cycle mercury intrusion and nitrogen sorption,” *J. Colloid Interface Sci.*, vol. 336, no. 2, pp. 730–737, 2009.

[57] N. Alderete, Y. Villagrán, A. Mignon, D. Snoeck, and N. De Belie, “Pore structure description of mortars containing ground granulated blast-furnace slag by mercury intrusion porosimetry and dynamic vapour sorption,” *Constr. Build. Mater.*, vol. 145, pp. 157–165, 2017.

[58] W. Müllauer, R. E. Beddoe, and D. Heinz, “Sulfate attack expansion mechanisms,” *Cem. Concr. Res.*, vol. 52, pp. 208–215, Oct. 2013.

[59] Y. C. Choi, J. Kim, and S. Choi, “Mercury intrusion porosimetry characterization of

micropore structures of high-strength cement pastes incorporating high volume ground granulated blast-furnace slag," *Constr. Build. Mater.*, vol. 137, pp. 96–103, 2017.

[60] S. Diamond, "Mercury porosimetry An inappropriate method for the measurement of pore size distributions in cement-based materials," *Cem. Concr. Res.*, vol. 30, pp. 1517–1525, 2000.

[61] E. F. Irassar, V. L. Bonavetti, and M. González, "Microstructural study of sulfate attack on ordinary and limestone Portland cements at ambient temperature," *Cem. Concr. Res.*, vol. 33, no. 1, pp. 31–41, 2003.

Chapter 5 Effect of Slag Composition and Fineness on Cracking Potential

5.1 Introduction

Granulated blast furnace slag is extensively used in mass concrete to reduce concrete temperature rise and improve resistance to early-age cracking [1]. Although cement replacement with slag is expected to reduce concrete temperature rise, several studies have shown that heat evolution during slag hydration varies significantly with slag chemistry [2]–[7]. An increase in heat evolution, especially at early ages, has been observed with increasing Al_2O_3 content of the slag [2], [3], [6]. Ben Haha et al. [7] also observed that at the same Al_2O_3 content, a decreasing MgO content increased the cumulative heat release during the first 2 days. Since heat evolution is indicative of reactivity, which affects the mechanical properties and stress development in restrained concrete elements, slags with higher reactivity may not be as effective in preventing early-age cracking as those with lower early-age reactivity. While the effect of slag composition has been studied with regard to heat evolution, there are currently no systematic studies that examine the effect of slag chemistry on cracking potential.

5.2 Methodology

Two cements, A and B, and seven slags (S8, S8F S11c, S11f, S14, S16 and S16G) were used to investigate the effect of slag characteristics on early-age cracking potential. Originally, four slags were obtained for this research. Slag S16 was ground using the Micronizer jet mill manufactured by Sturtevant to a mean particle size (MPS) of approximately 5 μm to examine the effect of fineness. This slag was named S16G. At a later date, a finer grind was obtained for S8, S8F, from the same source to examine the effect of fineness on cracking potential of concrete. Mean particle size (MPS) of the slags determined via laser scattering particle size analysis (wet method) is listed in Table 5-1.

Table 5-1: Slag alumina content, Blaine fineness and mean particle size

Slag	Blaine fineness (m^2/kg) b-value = 0.9	Mean particle size (µm)
S8	642	9.16
S8F	698	8.03
S11f	680	8.36
S11c	589	10.86
S14	574	11.15
S16	466	11.80
S16G	N/A	4.83

Control and slag concrete mixtures were prepared at a constant water-to-binder (w/b) ratio of 0.385 by mass and a total cementitious content of 395 kg/m^3 (666 lb/yd^3). In the blended mixtures, slag content was fixed at 60% replacement level on a mass basis (Table 5-2). Plain cement mixes were also prepared with each cement and were designated as Control A and Control B. The dosage of high-range water-reducing admixture (HRWR) was varied to maintain adequate workability. A dosage of 196 ml/100 kg (3.0 fl oz/100 lb) of cementitious material was used in mixes 60S8-A, 60S8f-A, 60S11c-A, 60S11c-B, 60S16-A, and 60S16-B. Mixes 60S11f-A, 60S14-A, 60S8-B and 60S14-B contained 280 ml/100 kg (4.3 fl oz/100 lb) of HRWR, while 365 ml/100 kg (5.6 fl oz/100 lb) of HRWR was used in mix 60S11f-B due to the higher slag fineness. In order to maintain a constant w/b ratio, mixing water was adjusted to account for the water contributed by the HRWR.

Table 5-2: Concrete mix proportions per 1 m^3

Material	Control A	Control B	Slag mixes
Cement (kg)	395	395	158
Slag (kg)	0	0	237
Coarse Aggregate #57 limestone (SSD) (kg)	1047	1047	1047
Fine Aggregate (SSD) (kg)	696	696	696
HRWR (ml/100 kg)	196	365	196 / 280 / 365
AEA (ml/100 kg)	6.5	6.5	6.5
w/b	0.385	0.385	0.385

Concrete mixtures were prepared in the laboratory following ASTM C192 [8]. Aggregates we first separated into different sieve sizes, washed, dried and recompiled to the specified grading curve prior to concrete mixing. The aggregates were brought to the SSD condition by re-soaking for a period of 24 hours prior to mixing. In order to simulate fresh concrete temperatures in the field, mixing water and aggregates were preheated prior to mixing. For semi-adiabatic calorimetry, which was performed following the guidelines provided by RILEM [9], a 150 mm x 300 mm fresh concrete cylinder was placed inside the calorimeter immediately after mixing. The concrete temperature at the beginning of the test was approximately 34.5˚C. Semi-adiabatic calorimetry was used to generate concrete temperature profiles for each mixture that were then imposed in the rigid cracking frame (RCF). The use of semi-adiabatic profiles is also favored as the effect of temperature on autogenous shrinkage is found to be unsystematic [10].

A rigid cracking frame, as shown in Figure 5-1, was used to evaluate the uniaxial stress development of the concrete specimens under restrained temperature profiles obtained for each concrete mixture from semi-adiabatic calorimetry during the first 96 hours. After 96 hours, cooling was induced at the rate of 1ºC/hr. until the age of 120 hours. The RCF restrains the concrete against thermal and autogenous volume changes and records resultant uniaxial stresses. It is noteworthy that development of the concrete modulus of elasticity, creep and stress relaxation

affects the stress in the concrete [11]. Further information about cracking frame testing can be found in [12], [13].

Figure 5-1: Rigid cracking frame

The following descriptors on the stress development curve were used as the indices for assessing the risk of early-age cracking:

1. 2nd Zero-Stress Temperature. This is the temperature at which the stress state shifts from compression to tension. 2nd Zero-Stress Temperature is expected to be higher than the final setting temperature as a large percentage of the early-age compressive stresses are relaxed due to the low modulus of elasticity of concrete at early ages. Higher autogenous shrinkage can increase the 2nd Zero-Stress Temperature [14]. Any decrease in temperature below the 2nd Zero-Stress Temperature would be expected to produce tensile stresses, therefore a 2nd Zero-Stress Temperature below ambient temperature could indicate a lower cracking tendency.

2. Cracking Temperature (T_{cr}). This is the temperature at which the concrete specimen cracks. A lower cracking temperature is global indicator lower cracking tendency [15]. The measured concrete temperature at the start of data collection in the RCF was approximately 31°C due to the longer placement time required. Prior to starting the test, the RCF was heated by circulating water at 45°C through the pipes for approximately 1 h before placing the concrete in the form. After the start of data collection, concrete temperature was in step with the imposed temperature profile typically within 30-45 minutes. The longer induction period observed for the slag mixtures was also helpful in ensuring that the concrete in the RCF was able to reach the imposed temperature profile within a short period. Temperature profiles imposed in the RCF were those recorded in the semi-adiabatic calorimeter for each mix during the first 96 h, after which time artificial cooling was imposed at the rate of 1˚C/h in order to induce cracking.

In order to assess mechanical properties development, 100 mm x 200 mm concrete cylinders were match-cured to their respective semi-adiabatic temperature profiles. Elastic modulus and tensile splitting strength were determined in accordance with ASTM C496 [16] and C469 [17], respectively, at the ages of 1, 3, 4 days and at the time of cracking. Two cylinders were tested at each age, and their average value is reported here. Mechanical properties of 60S8f and 60S16G-A were not tested due to limited available quantities of these slags.

5.3 Results and Discussion

5.3.1 Rigid Cracking Frame

Temperature profiles imposed in the cracking frame for Cement A-slag mixtures, based on the temperature of each mixture recorded in the semi-adiabatic calorimeter, are shown in Figure 5-2(a). Slags S8F, S11f and S16G had the highest fineness and were excluded from this initial comparison in order to separate the effect of fineness on stress development from the effect of alumina content. Their behavior is compared to that of their respective coarser counterparts (slags S8, S11c and S16) later in this report.

In general, incorporation of slag significantly reduced the maximum concrete temperature compared to the control as well as the rate of initial temperature rise (Figure 5-2(a)). However,

the maximum temperature for the slag mixes varied from approximately 46˚C to 49˚C for the Cement A concretes. Comparison between OPC-slag mixtures prepared with Cement A appears to suggest an increase in maximum temperature is attained as the alumina content increases from approximately 8 to 16%.

Although these differences between slag maximum temperatures may appear small, they are expected to be more exaggerated in mass concrete elements, where concrete in the center is better insulated than inside the semi-adiabatic calorimeter and approaches adiabatic conditions. Wei and Hansen [18] suggested that improvement of early-age cracking potential with the use of slag is due to reduction of cement content; however, the variability in the temperature profiles of the slag mixes indicates that slags are reacting at these early ages and contributing to the concrete temperature rise, and that their reactivity is likely different from one slag to another.

Stress development in the RCF is largely affected by the imposed temperature profile, although Wei and Hansen [18] reported a large contribution of autogenous shrinkage to stress development in mixes with high slag content. Stress development profiles displayed in Figure 5-2(b) show that while imposed temperature has a clear effect on stress development, thermal effects alone cannot explain the behavior of all the slag mixes.

The 60S8-A mix showed the largest reduction in tensile stress development in comparison to Control A, which is attributed to its lower maximum temperature and lower rate of subsequent cooling during the first 96 h. Although 60S14-A mix did not have the highest temperature profile, it showed the highest tensile stress development throughout the testing period. The main difference between S14 and the other slags used in this study, apart from its second highest Al_2O_3 content, was its low MgO content. Ben Haha et al. [7] reported that slag reactivity at early ages increases with decreasing MgO content (at the same Al_2O_3 content).

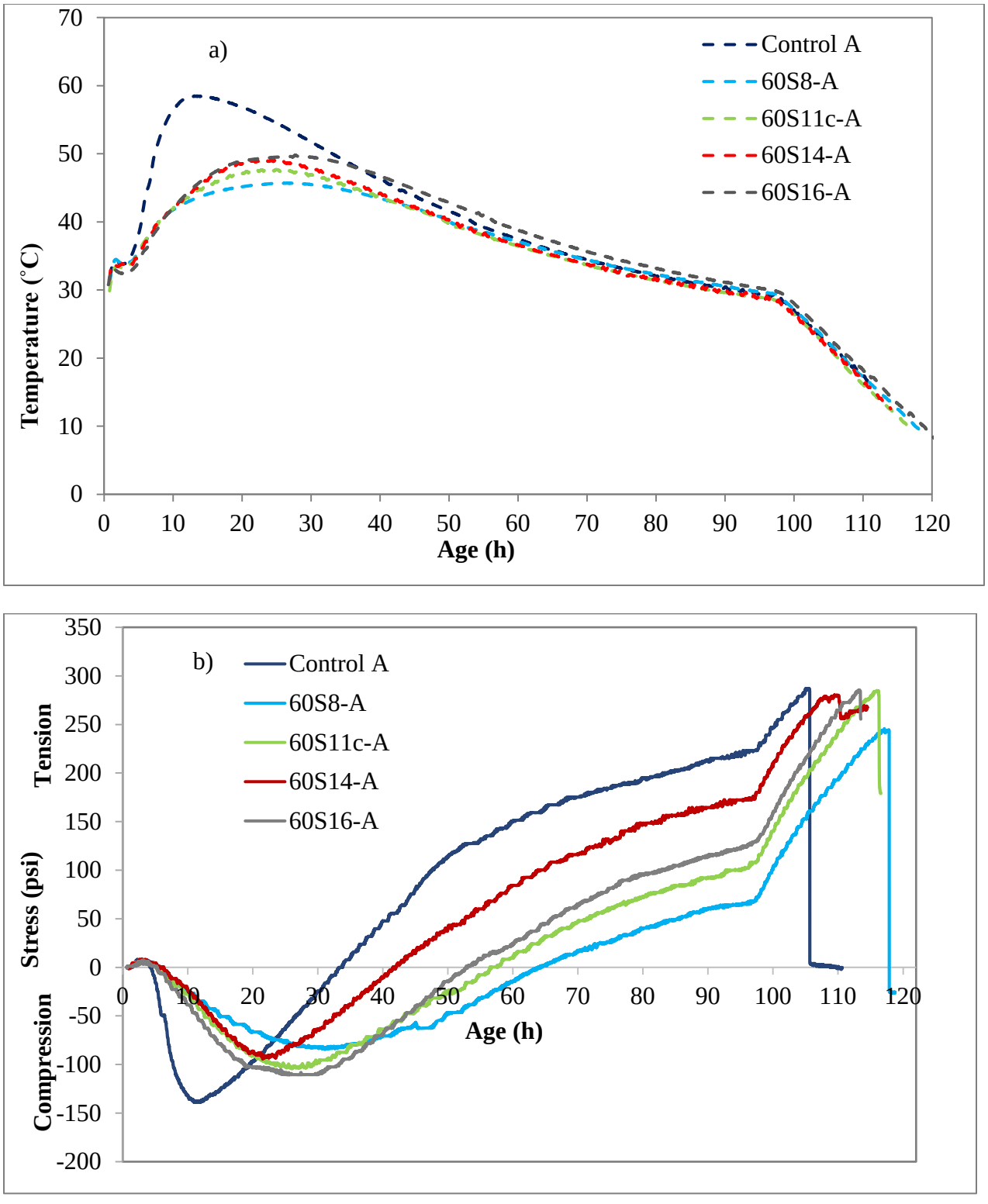

Figure 5-2: a) Temperature and b) stress development in the RCF for Cement A mixes

Figure 5-3(a) and Figure 5-3(b) show the temperature profiles and stress development for Cement B-slag mixes, respectively. A similar trend in temperature profiles was observed for the Cement B series to that of Cement A series. Addition of slag reduced the rate of heat evolution and maximum temperature rise compared to Control B regardless of slag characteristics. The maximum temperature for the slag mixes increased from approximately 46˚C to 53˚C with increasing Al_2O_3 content of the slag.

In terms of stress development of the Cement B series, 60S8-B mixture had the best performance, while the difference in the stress development of 60S14-B and 60S16-B was notably lower than between 60S14-A and 60S16-A mixes. This cannot be explained by the differences in their respective temperature profiles, as the difference in temperature development of these slags was more significant with Cement B. The major difference between Cements A and B was in their C_3A content. Therefore, it appears that cement chemistry has an important effect on stress development in OPC-slag blended mixtures.

Figure 5-4 through Figure 5-6 show a comparison of slags with similar alumina contents but different fineness. It appears that decreasing the slag MPS from 9.2 to 8 μm had no significant effect on temperature or stress development (Figure 5-4). However, an increase in fineness shifted the appearance of the first microcrack to an earlier time in the 60S8F-A mixture compared to 60S8-A (Table 5-3).

A larger difference in MPS (10.9 μm for S11c and 8.4 μm for S11f) resulted in an increase in temperature rise and a higher tensile stress development for the mixture with the finer slag (Figure 5-5). It is likely that the larger increase in fineness had influenced the hydration kinetics of the cementitious mixture by providing particles fine enough to act as nucleations sites that speed up the nucleation process [19]. Again, perhaps the most significant effect of increased fineness was observed in the earlier cracking time of the 60S11f-A mixture (Table 5-3).

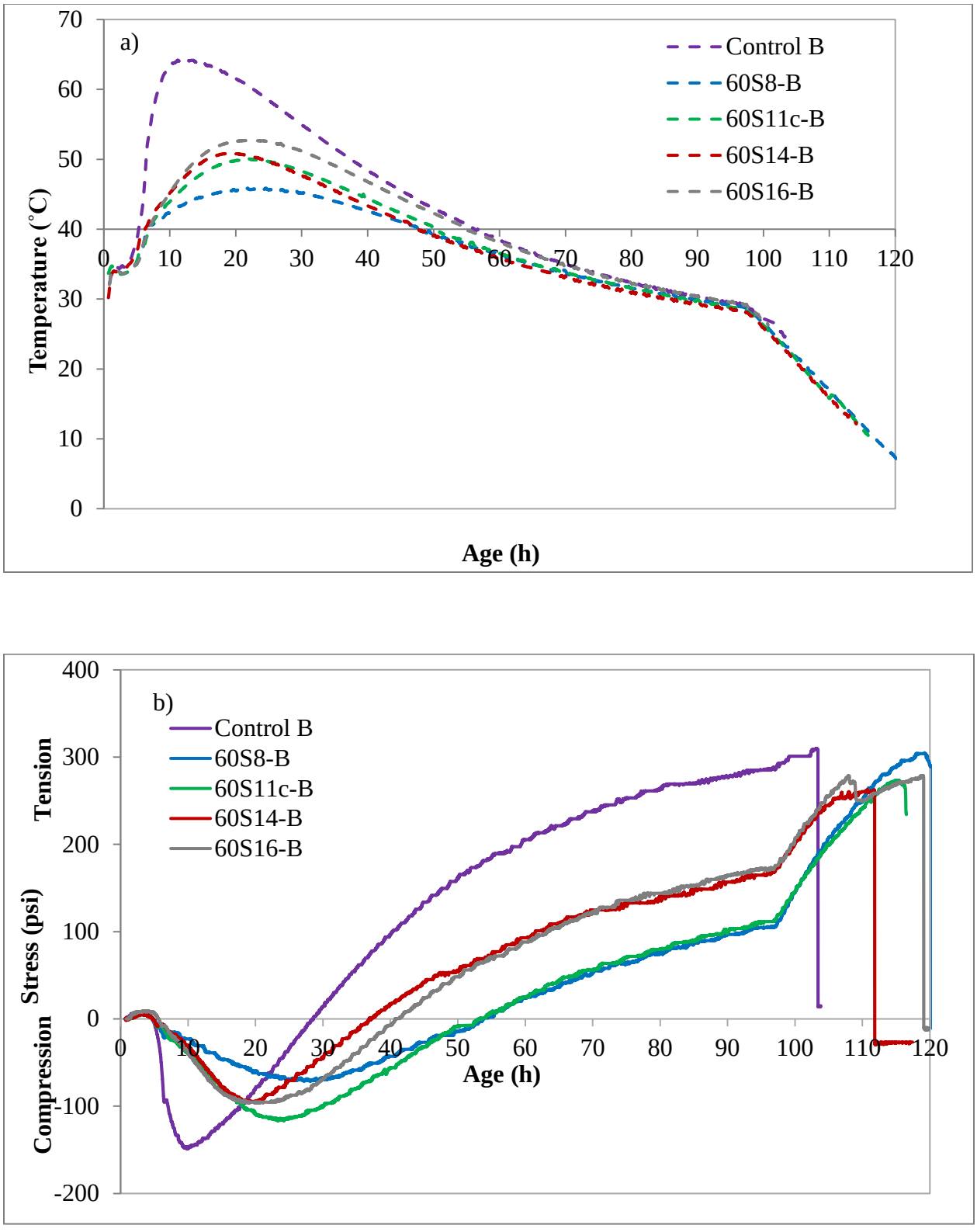

Figure 5-3: a) Temperature and b) stress development in the RCF for Cement B mixes

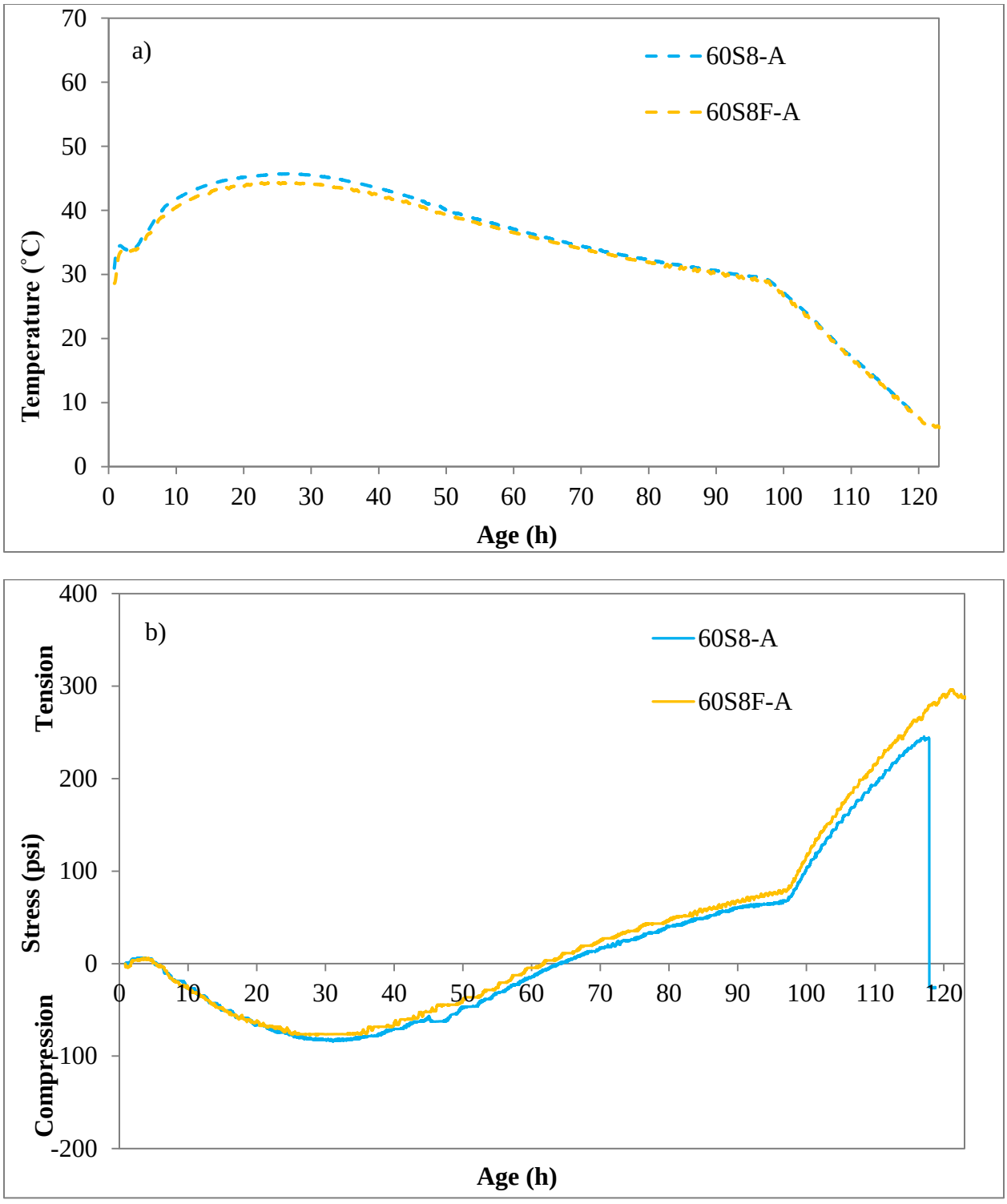

Figure 5-4: a) Temperature and b) stress development in the RCF for 60S8-A and 60S8F-A mixes

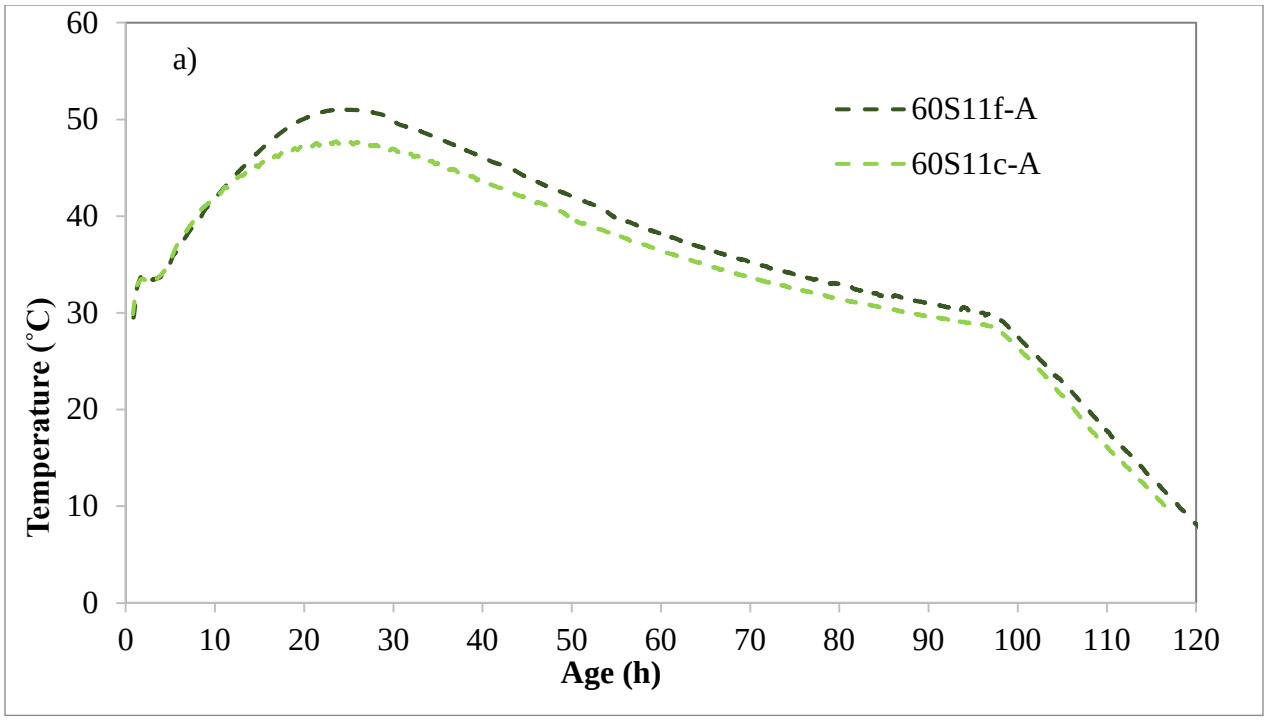

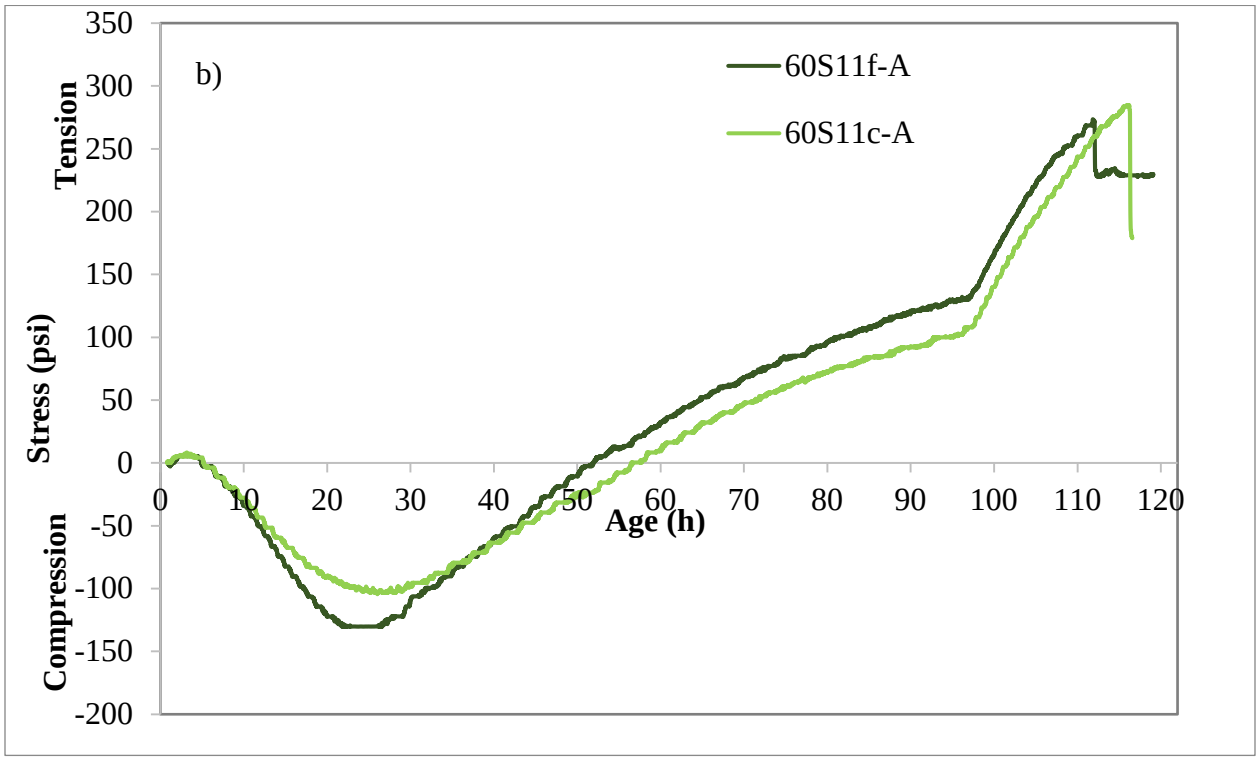

Figure 5-5: a) Temperature and b) stress development in the RCF for 60S11f-A and 60S11c-A mixes

Table 5-3: RCF cracking indices

	2nd Zero-Stress		Cracking		Slag MgO/Al_2O_3
Mix	**Time (h)**	**Temperature (°C)**	**Time (h)**	**Temperature (°C)**	
Control A	33.7	49.6	105.6	21.6	-
60S8-A	64.4	35.9	117.1	10.5	1.34
60S8F-A	61.7	36.0	113.7	13.5	1.33
60S11f-A	51.9	41.3	112.1	15.8	0.73
60S11c-A	57.6	37.2	116.1	10.2	0.90
60S14-A	42.0	43.4	110.1	16.5	0.37
60S16-A	53.0	41.6	113.4	15.0	0.55
60S16G-A	46.3	44.7	106.6	21.6	0.55
Control B	28.5	55.9	103.4	24.6	-
60S8-B	53.7	38.3	119.4	7.9	1.34
60S11f-B	45.8	43.7	107.8	18.9	0.73
60S14-B	37.1	44.6	111.8	17.7	0.37
60S16-B	40.9	46.4	108.4	19.1	0.55

Although an increase in temperature and stress development was also observed for the S16 slag ground in the laboratory (Figure 5-6), it was similar to that the increase observed for 60S11c-A and 60S11f-A mixtures despite a much larger difference in MPS (11.8 μm for S16 and 5.7 μm for S16G). This may be due to the difference in particle morphology between the laboratory air-jet mill and commercial ball-mill grinders. Nonetheless, T_{cr} was further reduced upon reduction in MPS (Table 5-3). An increase in fineness is expected to result in increased autogenous shrinkage, which Wei and Hansen [18] identified as the main reason for early-age cracking in slag mixtures. It is likely that increased autogenous shrinkage contributed to the increase in the T_{cr} with decreasing MPS.

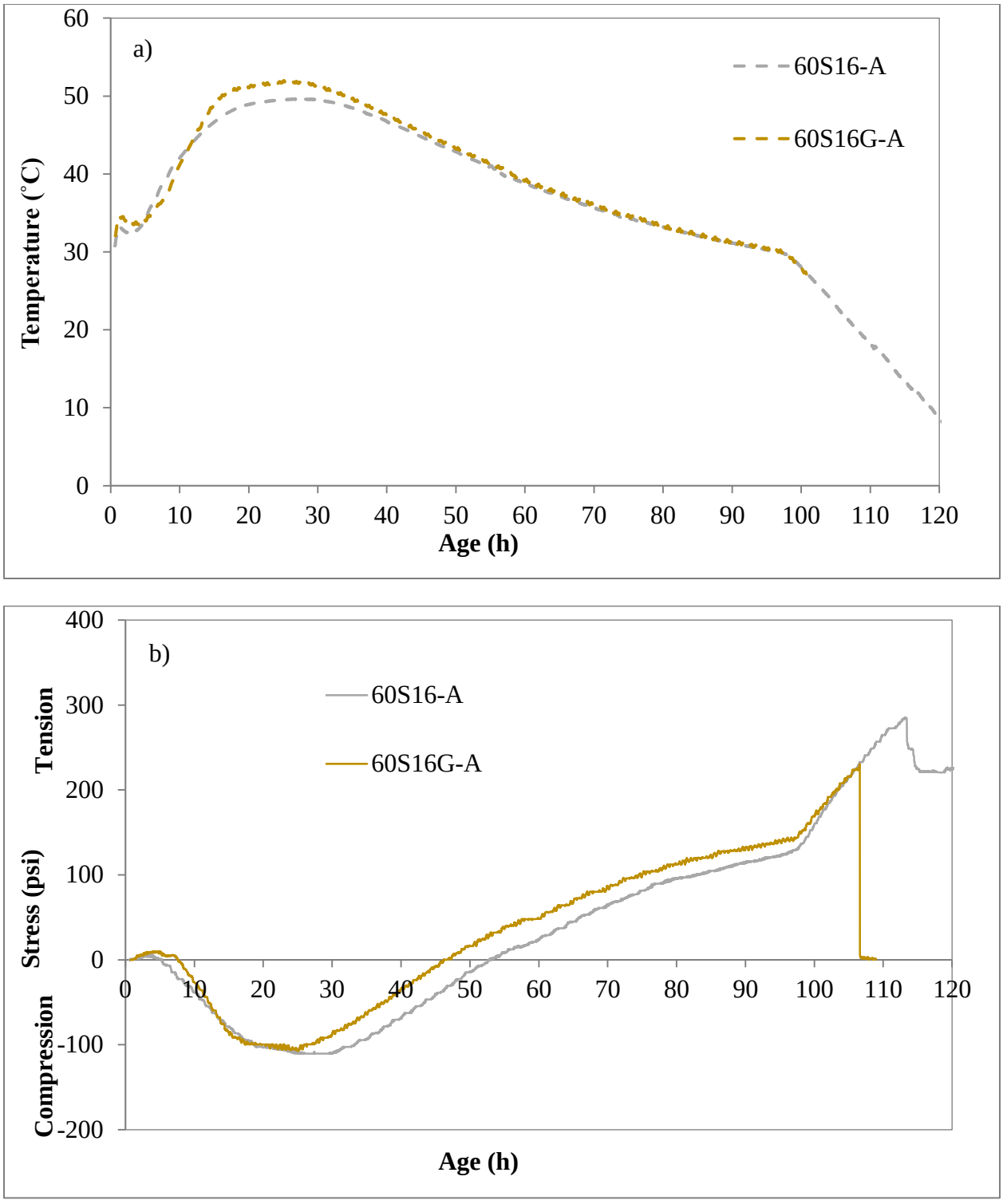

Figure 5-6: a) Temperature and b) stress development in the RCF for 60S16-A and 60S16G-A mixes

5.3.2 Mechanical Property Testing

Mechanical property testing revealed cement replacement with slag resulted in lower elastic moduli of the slag mixes at 1 day, with the exception of 60S14-A, compared to Control A (Figure 5-7). The elastic modulus of 60S14-A was notably higher at 1 day, which indicates that this mixture would be expected to have lower creep at this age. While lower modulus and increased creep are beneficial in reducing concrete stresses, all the slag mixes were still experiencing compressive stresses at 24 hours, which are beneficial in reducing subsequent tensile stress development. After 1 day, the use of slag did not have a significant effect on the elastic modulus. While there is no agreement on the effect of slag on elastic modulus in the current literature, most studies report either no effect or a decrease at early ages [20]–[24], which is in line with the results of this study.

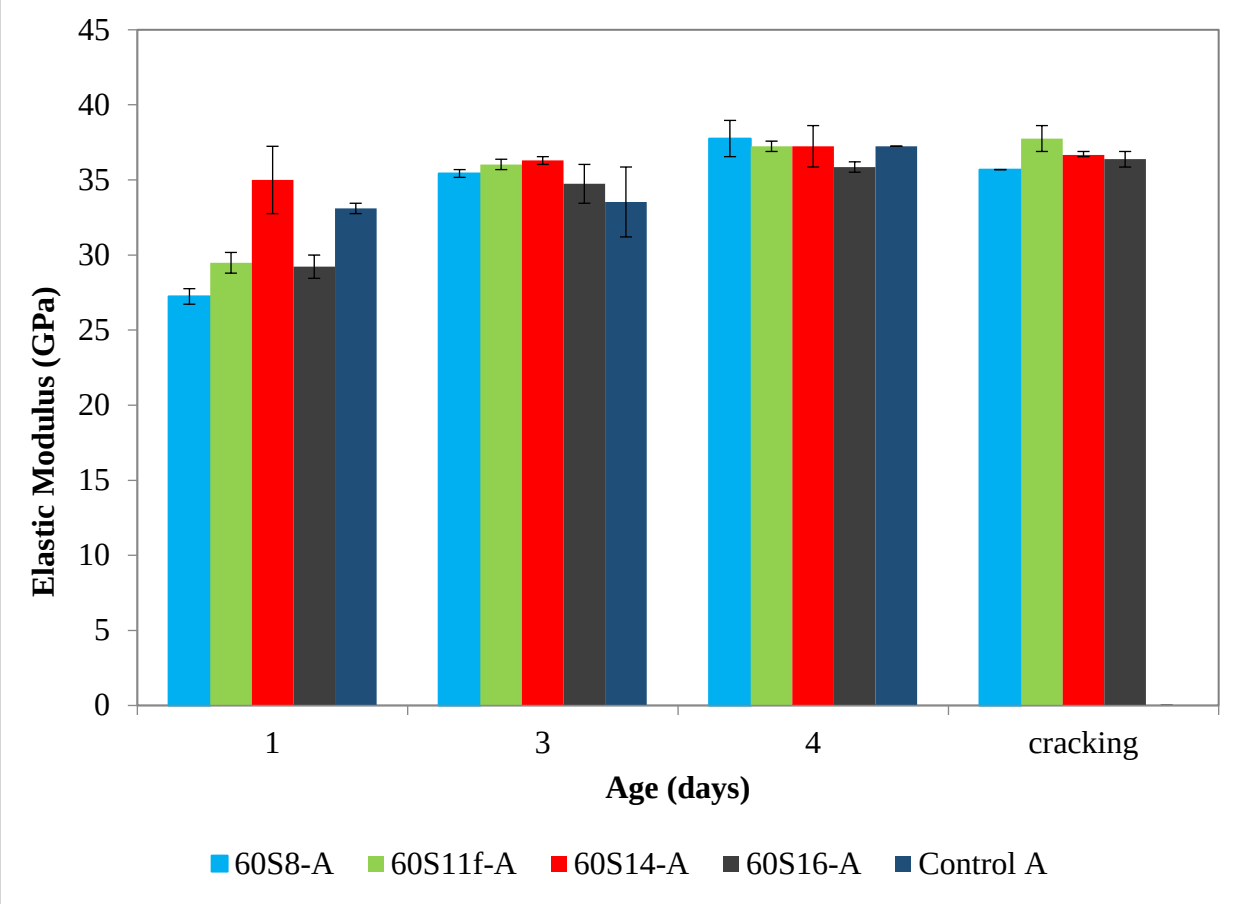

Figure 5-7: Elastic modulus for concrete mixtures

Tensile strengths of the slag mixes were also lower compared to Control A (Figure 5-8), but this did not have a negative effect on cracking resistance as the slag mixes were still in the pre-compression stage. After 1 day, tensile strengths of all the mixes were similar.

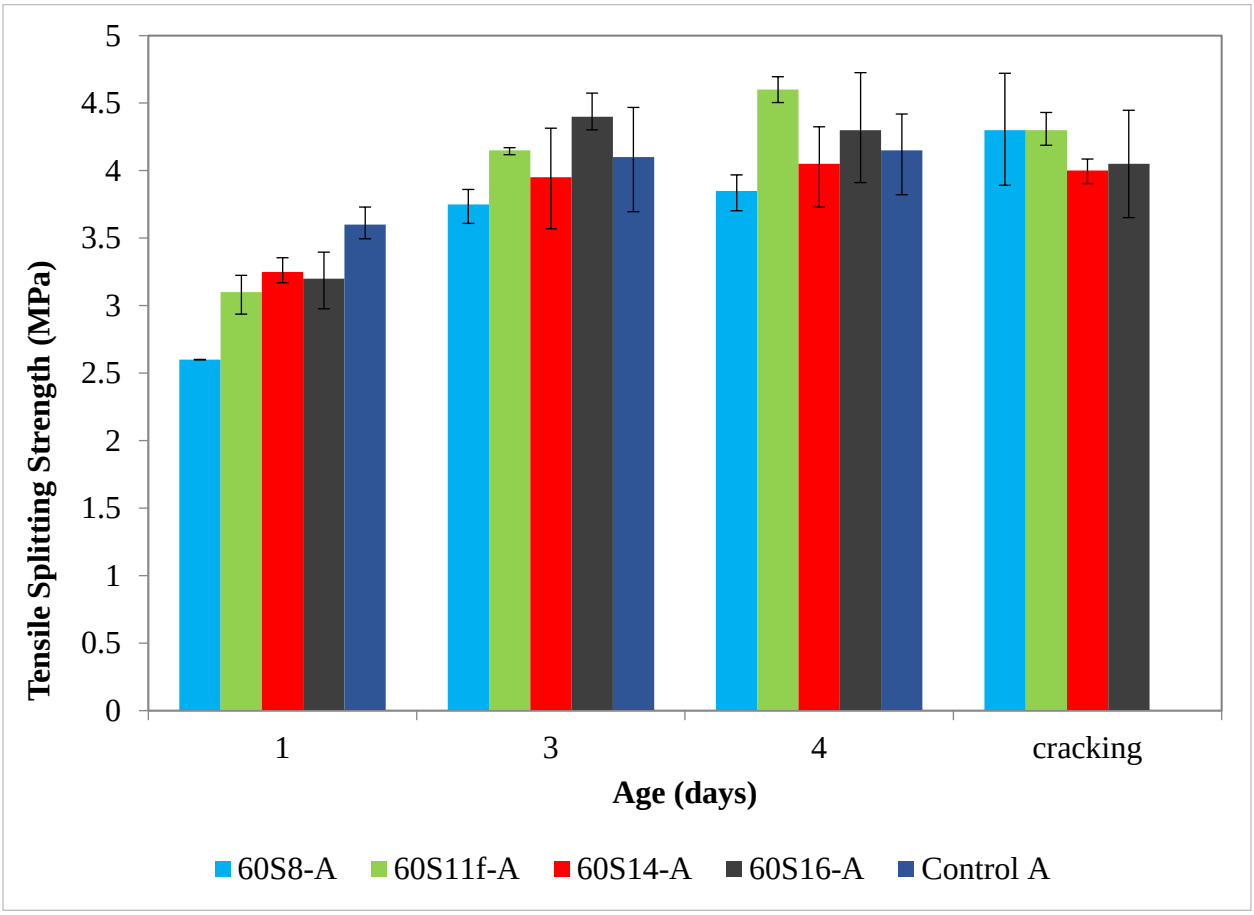

Figure 5-8: Splitting tensile strength for concrete mixtures

5.3.3 Relationship between Cracking Indices and Slag Characteristics

Based on semi-adiabatic temperature profiles, RCF testing, and mechanical property measurements, it is clear that MgO and Al_2O_3 contents of slag have an important effect on reactivity, creep, stress development, and ultimately cracking probability. While MgO or Al_2O_3 content alone did not correlate well with RCF cracking indices listed in Table 5-3, an increasing MgO/Al_2O_3 ratio appears to decrease the 2nd Zero-Stress Temperature for mixtures with both cements (Figure 5-9). A decrease in 2nd Zero-Stress Temperature indicates a lower probability of cracking since any drop in temperature below the 2nd Zero-Stress Temperature results in tensile

stress development. A linear relationship was also observed between the MgO/Al_2O_3 (M/A) ratio and 2nd Zero-Stress Time, as well as tensile stress at 96 hours (Figure 5-10 and Figure 5-11). An increasing MgO/Al_2O_3 ratio increased the time to 2nd Zero-Stress and decreased tensile stresses at initiation of cooling. The relationship between cracking temperature (T_{cr}) and MgO/Al_2O_3 ratio had a low R^2 value when the ground S16G-A slag was included for Cement A (Figure 5-12a); however, plotting cracking temperatures only for the as-received slags improved the coefficient of determination (Figure 5-12c). Since the MPS of S16G was significantly lower than that of commercially available slags, the 60S16G-A mixture may have experienced significantly higher autogenous shrinkage compared to the other slag mixes, which could explain the low coefficient of determination in Figure 5-12a. Expectedly, when the M/A ratio is scaled by the MPS (Mean Particle Size), such that the product of MPS and MgO/Al_2O_3 ratio is used as the parameter indicating early-age cracking sensitivity of slag at the same replacement level, the R^2 for the linear relationship cracking temperature (T_{cr}) and parameter improves from 0.52 to 0.86 for mixtures tested with Cement A (Figure 5-13), with a noticeable decrease in scatter, emphasizing the role of particle fineness of slag on autogenous shrinkage and consequently early-age cracking tendency indicated in Figure 5-4 through Figure 5-6.

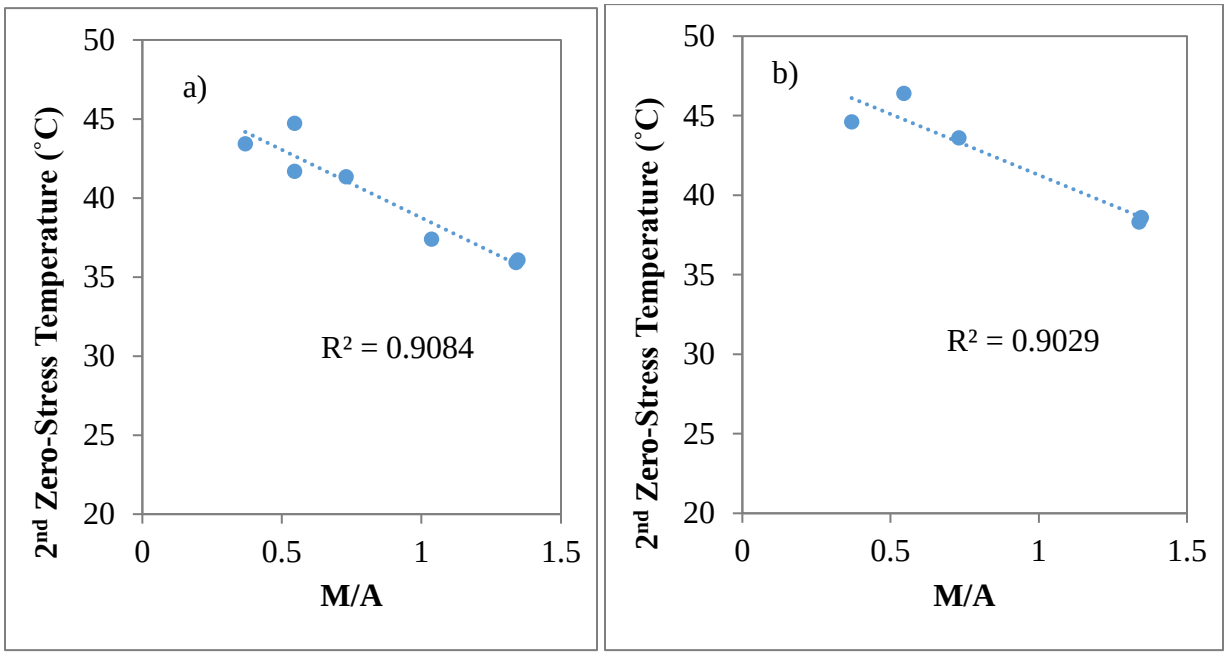

Figure 5-9: 2nd Zero-Stress Temperature vs MgO/Al_2O_3 ratio for OPC-Slag Mixtures Tested with a) Cement A and b) Cement B

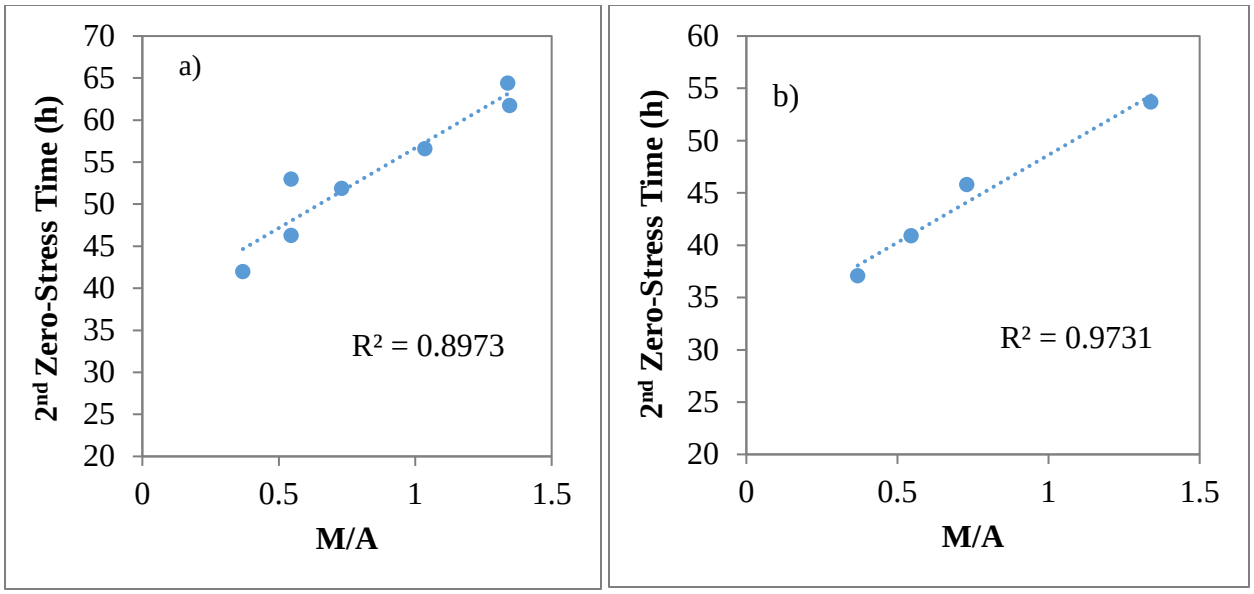

Figure 5-10: 2nd Zero-Stress Time vs MgO/Al_2O_3 ratio for OPC-Slag Mixtures Tested with a) Cement A and b) Cement B

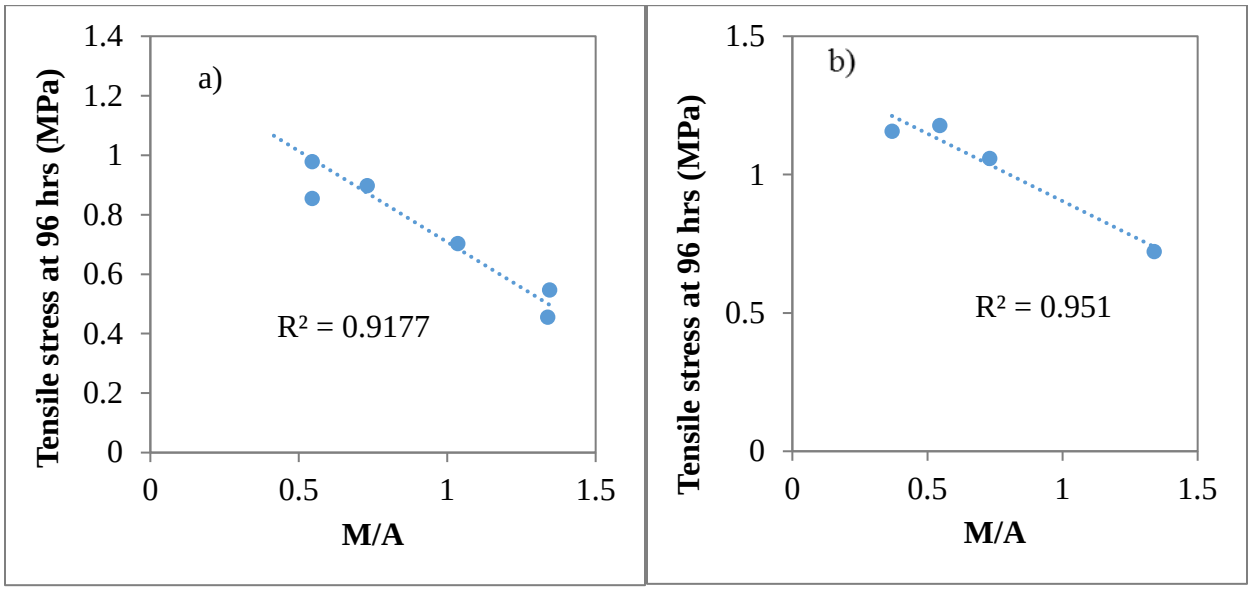

Figure 5-11: Tensile Stress at 96 hrs. vs MgO/Al_2O_3 ratio for OPC-Slag Mixtures Tested with a) Cement A and b) Cement B

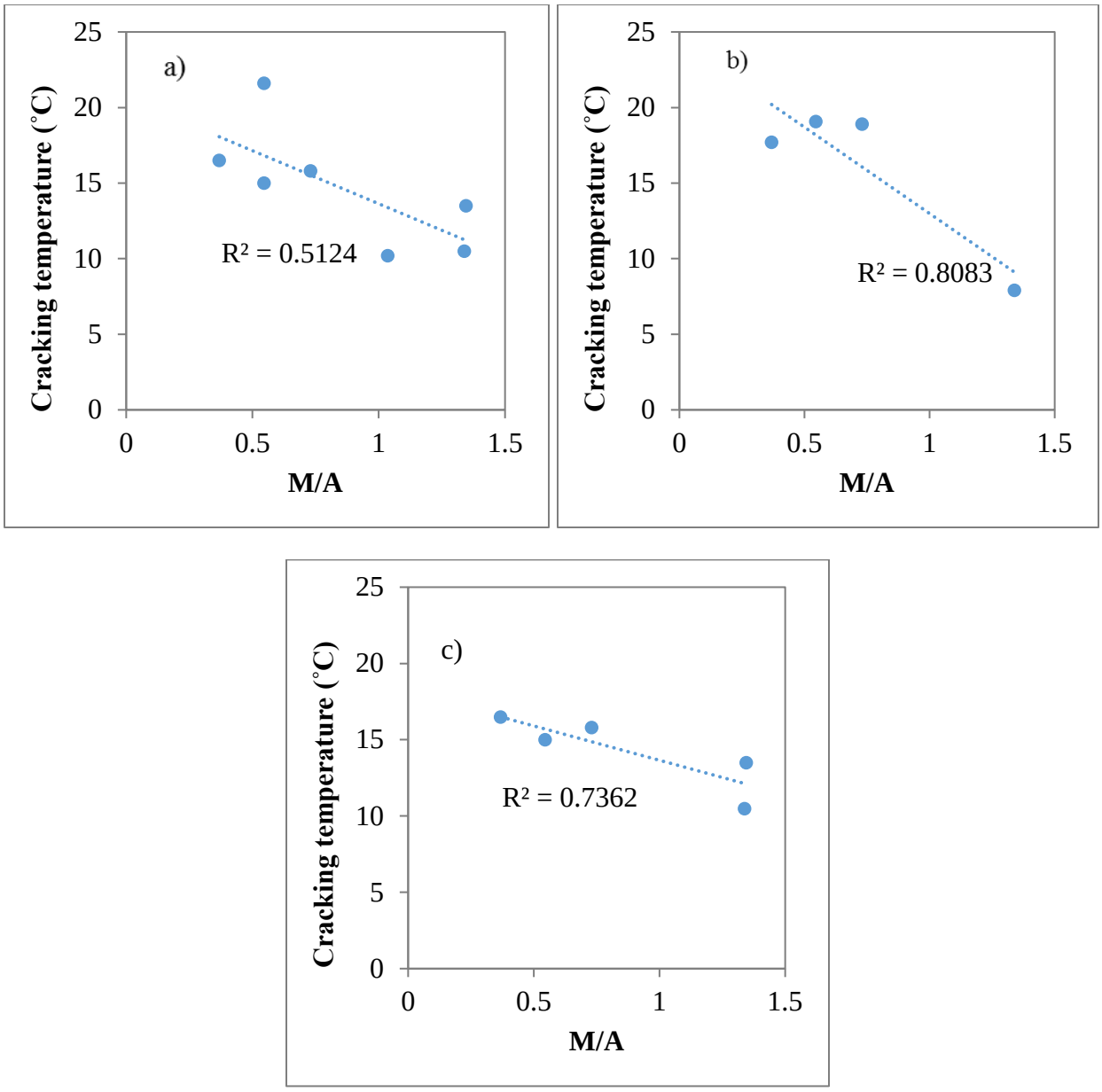

Figure 5-12: Cracking Temperature vs MgO/Al_2O_3 ratio for OPC-Slag Mixtures Tested with a) Cement A, b) Cement B, and c) Cement A mixtures including only as-received slags

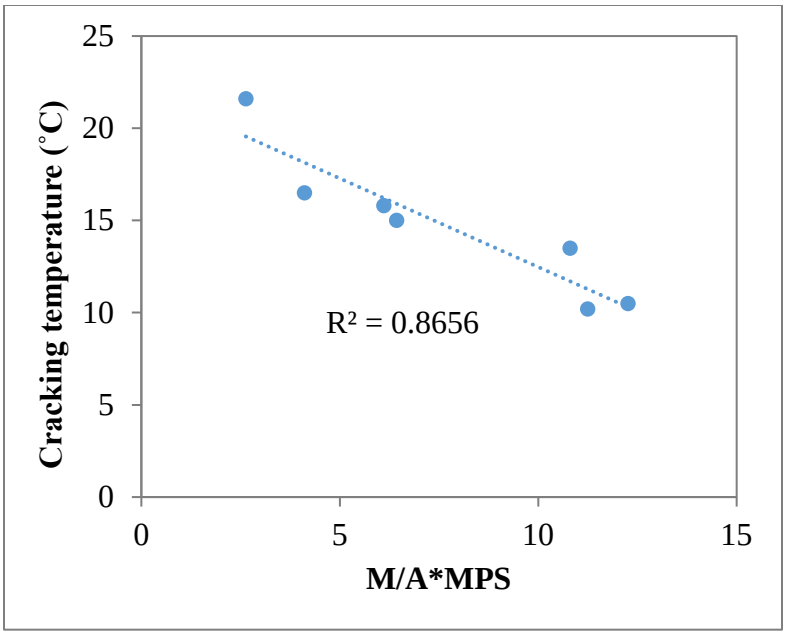

Figure 5-13: Cracking Temperature vs (MgO/Al_2O_3·MPS) for OPC-Slag Mixtures Tested with Cement A

5.4 Conclusions

Combinations of two cements with variable C_3A content and slags with variable Al_2O_3 and variable fineness were evaluated in terms of their early-age cracking potential. In all cases, semi-adiabatic calorimetry and rigid cracking frame results showed that 60% cement replacement with slag reduced concrete temperature rise and improved cracking resistance compared to the plain concrete mixtures. However, an increase in the maximum concrete temperature was observed with increase in alumina content from 8 to 16%. Stress development also increased with increasing alumina content, with exception of the 60S14-A mix. Although this mix did not have the highest temperature profile, it showed the highest tensile stress development throughout the testing period. This was attributed to the low MgO content of slag S14. The propensity of slag with similar chemical composition to S14 to produce higher autogenous shrinkage, reported in earlier investigations ([20], [25], [26]), is likely a contributing factor. Linear relationships between various cracking indices (2^{nd} Zero-Stress Temperature, 2^{nd} Zero-Stress Time, Tensile Stress at 96 hrs. and Cracking Temperature) and the MgO/Al_2O_3 ratio of slag were indicated by the results as previously noted in [27].

Increase in slag fineness, at the same alumina content, also had an effect on stress development, particularly on the time and temperature of cracking. Increasing slag fineness resulted in an earlier cracking time and a higher cracking temperature, indicating an increased risk of early-age cracking. This was reflected in the reduction of scatter when the mean particle size was included in the parameter characterizing early-age cracking tendency of slag used against the cracking temperature (Figure 5-12a and Figure 5-13) for mixtures tested with Cement A.

5.5 References

[1] ACI committee 207, “ACI 207.2R-07 Report on Thermal and Volume Change Effects on Cracking of Mass Concrete,” American Concrete Institute, Farmington Hills, MI, 2007.

[2] P. Z. Wang, R. Trettin, V. Rudert, and T. Spaniol, “Influence of Al_2O_3 content on hydraulic reactivity of granulated blast-furnace slag, and the interaction between Al_2O_3 and CaO,” *Adv. Cem. Res.*, vol. 16, no. 1, pp. 1–7, 2004.

[3] M. Whittaker, M. Zajac, M. Ben Haha, F. Bullerjahn, and L. Black, “The role of the alumina content of slag, plus the presence of additional sulfate on the hydration and microstructure of Portland cement-slag blends,” *Cem. Concr. Res.*, vol. 66, pp. 91–101, Dec. 2014.

[4] X. Wu, D. Roy, and C. Langton, “Early stage hydration of slag-cement,” *Cem. Concr. Res.*, vol. 13, no. 2, pp. 277–286, 1983.

[5] Y. Ballim and P. C. Graham, “The effects of supplementary cementing materials in modifying the heat of hydration of concrete,” *Mater. Struct.*, vol. 42, no. 6, pp. 803–811, 2009.

[6] M. Ben Haha, B. Lothenbach, G. Le Saout, and F. Winnefeld, “Influence of slag chemistry on the hydration of alkali-activated blast-furnace slag — Part II: Effect of Al2O3,” *Cem. Concr. Res.*, vol. 42, no. 1, pp. 74–83, 2012.

[7] M. Ben Haha, B. Lothenbach, G. Le Saout, and F. Winnefeld, “Influence of slag chemistry on the hydration of alkali-activated blast-furnace slag — Part I: Effect of MgO,” *Cem. Concr. Res.*, vol. 41, no. 9, pp. 955–963, 2011.

[8] ASTM C192/192M-07, “Standard Practice for Making and Curing Concrete Test Specimens in the Laboratory,” West Conshohocken, PA: ASTM International, 2010.

[9] RILEM Technical Committee 119-TCE, “RILEM TCE1 : Adiabatic and semi-adiabatic calorimetry to determine the temperature increase in concrete due to hydration heat of the cement,” *Mater. Struct.*, vol. 30, no. 10, pp. 451–464, 1998.

[10] Ø. Bjøntegård, “Interaction between thermal dilation and autogenous deformation in high performance concrete,” *Mater. Struct.*, vol. 34, no. 239, pp. 266–272, 2001.

[11] A. Williams, A. Markandeya, Y. Stetsko, K. Riding, and A. Zayed, “Cracking potential and temperature sensitivity of metakaolin concrete,” *Constr. Build. Mater.*, vol. 120, no. 2016,

pp. 172–180, 2016.

[12] A. Zayed, K. Riding, C. C. Ferraro, A. Bien-Aime, N. Shanahan, D. Buidens, T. Meagher, V. Tran, J. D. Henika, J. M. Paris, C. M. Tibbetts, and B. E. Watts, “FDOT Report BDV25-977-01: Long-Life Slab Replacement Concrete,” no. March, p. 306, 2015.

[13] D. Buidens, “Effects of Mix Design Using Chloride-Based Accelerator on Concrete Pavement Cracking Potential,” 2014.

[14] Ø. Bjøntegaard and E. J. Sellevold, “The Temperature-stress Testing Machine (TSTM): Capabilities and limitations,” *Int. RILEM Symp. Concr. Sci. Eng. A Tribut. to Arnon Bentur*, pp. 1–21, 2004.

[15] R. Springenschmid and R. Breitenbücher, “Influence of Constituents mix proportions and temperature on cracking sensitivity of concrete,” in *RILEM Report 15: Prevention of Thermal Cracking in Concrete at Early Ages*, R. Springenschmid, Ed. New York, NY: E & FN Spon, 1998, pp. 40–50.

[16] ASTM International, “ASTM C496/C496M-11-Standard Test Method for Splitting Tensile Strength of Cylindrical Concrete Specimens,” *ASTM Stand.*, vol. 04.02, 2011.

[17] “ASTM C469 / C469M - 14 Standard Test Method for Static Modulus of Elasticity and Poisson’s Ratio of Concrete in Compression,” West Conshohocken, PA: ASTM International, 2014.

[18] Y. Wei and W. Hansen, “Early-age strain-stress relationship and cracking behavior of slag cement mixtures subject to constant uniaxial restraint,” *Constr. Build. Mater.*, vol. 49, pp. 635–642, 2013.

[19] E. Berodier and K. Scrivener, “Understanding the filler effect on the nucleation and growth of C-S-H,” *J. Am. Ceram. Soc.*, vol. 97, no. 12, pp. 3764–3773, 2014.

[20] T. Kanda, H. Momose, and K. Imamoto, “Shrinkage Cracking Resistance of Blast Furnace Slag Blended Cement Concrete - Influencing Factors and Enhancing Measures,” *J. Adv. Concr. Technol.*, vol. 13, no. 1, pp. 1–14, 2015.

[21] M. A. Megat Johari, J. J. Brooks, S. Kabir, and P. Rivard, “Influence of supplementary cementitious materials on engineering properties of high strength concrete,” *Constr. Build. Mater.*, vol. 25, no. 5, pp. 2639–2648, 2011.

[22] X. Jin and Z. Li, “Effects of Mineral Admixture on Properties of Young Concrete,” *J. Mater.*

Civ. Eng. ASCE, vol. 15, no. October, pp. 435–442, 2003.

[23] J. M. Khatib and J. J. Hibbert, “Selected engineering properties of concrete incorporating slag and metakaolin,” *Constr. Build. Mater.*, vol. 19, no. 6, pp. 460–472, 2005.

[24] A. Darquennes, S. Staquet, M.-P. Delplancke-Ogletree, and B. Espion, “Effect of autogenous deformation on the cracking risk of slag cement concretes,” *Cem. Concr. Compos.*, vol. 33, no. 3, pp. 368–379, Mar. 2011.

[25] H. Tsuruta, H. Matsushita, K. Harada, and T. Goto, “Effect of Gypsum Content in Cement on Autogenous Shrinkage of Portland Blast-Furnace Slag Cement Concrete.”

[26] T. Kanda, H. Momose, K. Ishizeki, K. Imamoto, and C. Kiyohara, “Impacts of Trace Additives and Early-Stage Curing Conditions on the Shrinkage Cracking Resistance of Blast-Furnace Slag Cement Concrete,” *J. Adv. Concr. Technol.*, vol. 14, no. 8, pp. 475–488, 2016.

[27] A. Markandeya, N. Shanahan, D. Mapa, K. A. Riding, and A. Zayed, “Influence of slag composition on cracking potential of slag-portland cement concrete,” *Constr. Build. Mater.*, vol. 164, pp. 820–829, 2018.

Chapter 6 Summary, Conclusions and Recommendations

6.1 Summary and Conclusions

An extensive experimental matrix was designed to assess the durability of slag-blended cementitious systems. The initial testing matrix included 2 cements and 3 slags but had to be expanded to 4 cements and 8 slags. The cements selected here reflect the effects of variation in tricalcium silicate, tricalcium aluminate, alkalis and sulfates, while slags primarily had differences in their alumina and magnesia contents in addition to considering sulfate optimization in one slag of high alumina content. Additionally, slag fineness and particle size distribution effects were also considered in the test matrix design. The as-received cementitious materials were evaluated with methods including X-ray fluorescence, X-ray diffraction, laser particle size analysis, Blaine fineness and specific gravity. The aggregates were also characterized for their grading, bulk specific gravity, and adsorption capacity. Sulfate durability was assessed using ASTM C1012-18 with a constant w/cm ratio. In assessing the effects of the slag alumina content, the slag-portland cement mixtures were prepared at three replacement levels (30%, 50% and 70%) in addition to their control. The exposure solution was 5% sodium sulfate for all sulfate durability tests. Specimens were examined visually, and X-ray diffraction coupled with Rietveld refinement was used to identify phase assemblages at 12 months. Phase assemblage studies, using thermodynamic modeling, were also implemented for specific mixtures in addition to mercury intrusion porosimetry. The findings from external sulfate durability testing of slag-portland cement mixtures can be summarized as follows:

1. Higher cement tricalcium aluminate contents resulted in greater expansions.
2. Higher cement tricalcium silicate and aluminate contents decreased external sulfate durability.
3. Comparison of Type I and Type II(MH)cements indicates that higher tricalcium aluminate, tricalcium silicate, and alkali contents in the as-received cements decreased external sulfate durability.

4. The durability of slag-blended systems, when exposed to an external source of sulfate, depends on the chemical and mineralogical composition of the cement as well as the chemical, mineralogical and physical characteristics of the GGBFS.
    a. For a Type II(MH) cement, incorporation of slags with alumina content of 8%, A/M ratio of 0.75, and Blaine fineness 640 m^2/kg at replacement levels of 30%, 50% and 70% are recommended for "Class S3" exposure (ACI 201.2R-16 Table 6.1.4.1b).
    b. For a Type II(MH) cement, incorporation of slag with alumina content of 11%, A/M ratio of 0.95, and fineness 590 m^2/kg satisfied "Class S2" exposure at all replacement levels. The bars were predominately intact after 18 months except at 30% replacement where some bars showed cracking after 15 months. Only the 70% replacement was in compliance with "Class S3" expansion requirements.
    c. For a Type II(MH) cement, incorporation of slag with alumina content of 16% (S16) satisfied Class S2 exposure only at 70% replacement. Mortar bars prepared at lower replacement levels of 30% and 50% disintegrated between 4 months and 6 months. The control mixture performed better than the lower replacement levels of 30% and 50% for S16.
    d. For Type I cements, incorporation of slags with 8% alumina, A/M = 0.75 and Blaine fineness of 640 m^2/kg, improved the sulfate resistance substantially. At 50 and 70% replacement, the blended system was in compliance with "Class S3" criteria while 30% replacement was in compliance with "Class S2" exposure but not "Class S3" exposure.
    e. For Type I cement, incorporation of slag of alumina content of 11%, A/M = 0.95, and Blaine fineness of 589 m^2/kg satisfied "Class S3" exposure expansion requirements at 70% replacement. The 30% and 50% replacement satisfied the "Class S2" expansion limit. However, 30% mixture bars cracked following 12-month measurements and the test had to be discontinued.
    f. For Type I cement with the 16% alumina slag, all bars disintegrated prior to the 18-month measurements for all replacement levels reported here. However, the

70% blended mixture passed “Class S2” expansion limits but disintegrated beyond 15 months.

g. Slag Blaine fineness was found to have a significant role on performance of the slag-blended mixtures exposed to an external sulfate source. Testing two slag Grades (Grade 100 with Blaine fineness of 589 m^2/kg and Grade 120 of Blaine fineness of 680 m^2/kg) with alumina content of 11% (but different M/A ratios) at 70% replacement level showed that “Class S3” performance designation cannot be assigned to the higher fineness slag of alumina content of 11% (and lower M/A).
h. Considering the effect of sulfate optimization on a slag of an alumina content of 14%, the findings indicate that sulfate optimization varies with the parent cement alkali content, sulfate content, fineness and slag replacement level. Testing limited to 12 months is not adequate to reveal performance trends especially for replacement levels between 30% and 70%.

The second part of the study focused on assessing the effects of slag chemical, physical and mineralogical characteristics on the temperature rise and cracking potential of slag-blended concrete mixtures. Thirteen concrete mixtures were designed at cement factor of 666 lbs/yd^3. The w/cm ratio was maintained constant at 0.385. Two types of cements were used; namely, Type I and Type II(MH). The cement replacement level was maintained at 60%, which is a typical replacement level for mixtures used in the state of Florida for mass concrete. Twenty-six concrete mixtures were prepared to assess the temperature rise, under semi-adiabatic conditions, and the cracking potential using a rigid cracking frame operated under the temperature profile collected from semiadiabatic testing. The following are the conclusions based on the experimental findings:

1. Combinations of two cements with different C_3A contents and slags with different Al_2O_3 contents, M/A, and fineness were evaluated in terms of their early-age cracking potential. In all cases, semi-adiabatic calorimetry and rigid cracking frame results showed that 60% cement replacement with slag reduced concrete temperature rise and improved cracking resistance compared to the plain concrete mixtures.

2. An increase in the maximum concrete temperature attained was observed with increase in alumina content of the slag from 8 to 16%.
3. Tensile stress development also increased with increasing alumina content, with the exception of the 60S14-A mix. Although this mixture did not have the highest temperature profile, it showed the highest tensile stress development throughout the testing period. This was attributed to the low MgO content of slag S14. The propensity of slag, with similar chemical composition to S14, to produce higher autogenous shrinkage, as reported in earlier investigations ([1]–[3]), is likely a contributing factor.
4. A linear relationship between various cracking indices (2^{nd} Zero-Stress Temperature, 2^{nd} Zero-Stress Time, tensile stress at 96 hrs. and cracking temperature) and the MgO/Al_2O_3 ratio of slag was established [4]. The linear relationship improved when the slag fineness was also included in the relationship.

6.2 Recommendations

Based on the findings of this study, the following recommendations can be made:

1. The Florida Department of Transportation should implement modifications to slag specifications to include Blaine fineness (BF) grade limits [5].
2. Slag Mill Certificate should identify if the slag is produced by blending granules and/or blending of slags produced from different blast furnaces. If GGBFS granules are blended, the source of the blends should not be changed without additional reapproval.
3. For applications where temperature rise of a structural element is of concern, cementitious content, cement fineness, slag alumina content and fineness must be considered. Adiabatic temperature rise should be determined experimentally using the same materials (including chemical admixtures) and proportions as used in the mixture design of the structural element. The measured adiabatic temperature must be used in the analysis performed to develop the thermal control plan for the structural element. Testing for adiabatic temperature rise should be conducted in an approved laboratory facility.

4. The cementitious materials characteristics such as Blaine fineness, complete chemical oxide composition, mineralogy, limestone additions to slag, calcium sulfate additions to slag, and processing additions used in cement production must be attached to the testing results and should match what is proposed to be used in an approved mixture design. Variation of a cement source or a slag source should be accompanied by retesting and reapproval.
5. It is recommended that when a concrete mixture design is submitted to the State Materials Office for approval, where temperature rise or sulfate durability is of concern, the submitter should identify alternative cementitious materials sources in the event there is a shortage of supply in the cementitious materials submitted for mixture approval. In this event, the submitter must provide the same testing data for the alternative material as that used on the original mixture design.
6. It is recommended that the minimum amount of slag that can render a structural element durable should be used due to the higher shrinkage and higher carbonation in concrete elements prepared with high slag replacement levels (above 50%) [6], [7]. The effect is more pronounced in thin reinforced sections [6].
7. For external sulfate durability, testing was conducted for a limited period of 18 months using ASTM C1012 while maintaining a constant w/cm ratio of 0.485 for control and slag-blended mortars. The following recommendations are provided for slag-blended cementitious systems with Type II(MH) OPC (ASTM C150-16) according to ACI 201.2R-16 class of exposure criteria:
    a. **Type II (MH)-Ground Granulated Blast Furnace Slag in Class S3 Exposure** (SO_4^{2-} > 10,000 ppm in water or water-soluble SO_4^{2-} > 20,000 ppm in soil):
        i. For slag cements with alumina contents ≤ 8%, the following are recommended:
            1) Alumina-to-magnesia ratio (A/M) ≤ 0.75,

2) Blaine fineness of ≤ 640 m^2/kg, and
3) Replacement of portland cement with 30% - 70% slag.

ii. For slag cements with alumina contents of greater than 8% and less than or equal to 11%, the following are recommended:
1) A/M ≤ 0.95,
2) Blaine fineness of ≤ 590 m^2/kg, and
3) Replacement of portland cement with 70% slag.

iii. Slag cements with alumina contents greater than 11% must be tested according to ASTM C1012 using a constant w/cm ratio of 0.485. The expansion for the specific portland cement-slag cement combination must be less than 0.1% at 18 months to be used in a structural element subjected to S3 exposure conditions. If the expansion criterion is met, the approval for use is only for the specific combination of portland cement and slag cement at the specific replacement percentage used in the ASTM C1012 testing.

b. **Type II(MH) - Ground Granulated Blast Furnace Slag in Class S2 Exposure** (SO_4^{2-} content 1,500 - 10,000 ppm in water or water-soluble SO_4^{2-} content 2,000 - 20,000 ppm in soil):

i. For slag cements with alumina contents ≤ 8%, the following are recommended:
1) A/M ≤ 0.75,
2) Blaine fineness of ≤ 640 m^2/kg, and
3) Replacement of portland cement with 30% - 70% slag.

ii. For slag cements with alumina contents of greater than 8% and less than or equal to 11%, the following are recommended:
1) A/M ≤ 0.95,
2) Blaine fineness of ≤ 590 m^2/kg, and
3) Replacement of portland cement with 30% - 70% slag.

Slag cements with alumina contents greater than 11% must be tested according to ASTM C1012 using a constant w/cm ratio of 0.485. The expansion for the specific portland cement-slag cement combination must be less than 0.1% at 12 months to be used in a structural element subjected to S2 exposure conditions. If the expansion criterion is met, the approval for use is only for the specific combination of portland cement and slag cement at the specific replacement percentage used in the ASTM C1012 testing.

8. For external sulfate durability, the following recommendations are provided for slag-blended cementitious systems with Type I OPC (ASTM C150-16 and ASTM C150-18):
    a. **Type I - Ground Granulated Blast Furnace Slag in Class S3 Exposure**:
        i. For slag cements with alumina contents ≤ 8%, the following are recommended:
            1) A/M ≤ 0.75,
            2) Blaine fineness of ≤ 640 m^2/kg, and
            3) Replacement of portland cement with 50% - 70% slag.
        ii. For slags with alumina contents of 8% to 11%:
            1) A/M ≤ 0.95,
            2) Blaine fineness of ≤ 590 m^2/kg, and
            3) Replacement of portland cement with 70% slag.
        iii. Slag cements with alumina contents greater than 11% must be tested according to ASTM C1012 using a constant w/cm ratio of 0.485. The expansion for the specific portland cement-slag cement combination must be less than 0.1% at 18 months to be used in a structural element subjected to S3 exposure conditions. If the expansion criterion is met, the approval for use is only for the specific combination of portland cement and slag cement at the specific replacement percentage used in the ASTM C1012 testing.

b. **Type I - Ground Granulated Blast Furnace Slag in Class S2 Exposure**:

i. For slag cements with alumina contents of ≤ 8%, the following are recommended:

1) A/M ≤ 0.75,

2) Blaine fineness of ≤ 640 m^2/kg, and

3) Replacement of portland cement with 30% to 70% slag.

ii. For slag cements with alumina contents from 8% to 11% :

1) A/M ≤ 0.95,

2) Blaine fineness of ≤ 590 m^2/kg, and

3) Replacement of portland cement with 50% to 70% slag.

iii. Slag cements with alumina contents greater than 11% must be tested according to ASTM C1012 using a constant w/cm ratio of 0.485. The expansion for the specific portland cement-slag cement combination must be less than 0.1% at 12 months to be used in a structural element subjected to S2 exposure conditions. If the expansion criterion is met, the approval for use is only for the specific combination of portland cement and slag cement at the specific replacement percentage used in the ASTM C1012 testing.

It is recognized that the recommendations listed under item 7 and 8 can be modified if the GGBFS Blaine fineness is decreased or if calcium sulfate/limestone additions are blended with GGBFS. Since it is also recognized that performance of slag-blended cementitious systems is influenced by the cement source and not just the slag, approval under testing provision should be only issued for specific cement-slag combinations. The GGBFS source should provide:

1) A detailed elemental oxide composition of the slag cement,
2) The Blaine fineness,
3) The amount and chemical composition of each calcium sulfate addition,
4) The amount and chemical composition (must show percent of $CaCO_3$) of limestone, if added,

5) Identify any blending of granules from different blast furnaces. If blended, the slag supplier should identify the granule source of each slag in the blend, supply complete oxide compositions of each slag granule source and immediately notify the State Materials Office of any changes to the blend,
6) Any changes to the types or quantities of additions to the slag cement, or to the granule proportions if blended, will require additional testing and reapproval.

It is also recognized that Blaine fineness of slag can affect the slag designated grade. The findings of the current study indicate that slags of similar chemical composition but ground to higher fineness have a negative effect on temperature rise, cracking indices and sulfate durability. The construction industry and regulating agencies should consider emphasizing durability and strength when designing structural concrete elements rather than strength alone.

6.3 Suggestions for Future Work

Based on the findings of this study, the following is recommended;

1. Initiate a study on the effect of slag fineness, alumina content and A/M ratio on the measured adiabatic temperature rise in slag-blended concrete.
2. Initiate a study to assess sulfate optimization of higher-alumina slags in blended cementitious systems and their effect on the slag-blended systems durability. This will help minimize any potential shortage in the availability of quality slag cement needed for durable structural concrete in the state of Florida.

6.4 References

[1] H. Tsuruta, H. Matsushita, K. Harada, and T. Goto, “Effect of Gypsum Content in Cement on Autogenous Shrinkage of Portland Blast-Furnace Slag Cement Concrete.”

[2] T. Kanda, H. Momose, K. Ishizeki, K. Imamoto, and C. Kiyohara, “Impacts of Trace Additives and Early-Stage Curing Conditions on the Shrinkage Cracking Resistance of Blast-Furnace Slag Cement Concrete,” *J. Adv. Concr. Technol.*, vol. 14, no. 8, pp. 475–488, 2016.

[3] T. Kanda, H. Momose, and K. Imamoto, “Shrinkage Cracking Resistance of Blast Furnace Slag Blended Cement Concrete - Influencing Factors and Enhancing Measures,” *J. Adv. Concr. Technol.*, vol. 13, no. 1, pp. 1–14, 2015.

[4] A. Markandeya, N. Shanahan, D. Mapa, K. A. Riding, and A. Zayed, “Influence of slag composition on cracking potential of slag-portland cement concrete,” *Constr. Build. Mater.*, vol. 164, pp. 820–829, 2018.

[5] JIS A 6206, “Ground granulated blast-furnace slag for concrete,” in *Japanese Industrial Standard*, Tokyo, Japan: Japanese Standard Association, 2013.

[6] G. J. Osborne, “Durability of Portland blast-furnace slag cement concrete,” *Cem. Concr. Compos.*, vol. 21, pp. 11–21, 1999.

[7] T. A. Bier, “Influence of type of cement and curing on carbonation progress and pore structure of hydrated cement paste,” *Mater. Res. Soc.*, vol. 85, pp. 123–234, 1987.